University of Stavanger

FACULTY OF SCIENCE AND TECHNOLOGY

MASTER'S THESIS

Study program/ Specialization: Offshore Technology / Marine and Subsea Technology	Spring semester, 2013 Open / ~~Restricted access~~
Writer: Rauan Zhamangarin	..... (Writer's signature)

Faculty supervisor: Prof. Arnfinn Nergaard Ph.D (University of Stavanger)

External supervisor(s): Jens-Olav Rundsag (Statoil, Stavanger, Norway)

Title of thesis:

Analytical Model for J-Tube Pull-in

Credits (ECTS): 30

Key words: J-Tube, Subsea, Tie-ins, Local Buckling, pipeline bending, pull-in head, pipeline installation, plastic bending, relaxation of the pipeline, Calculation tool	Pages: .....79..... + enclosure: .....I..... **Stavanger, 14th June 2013**

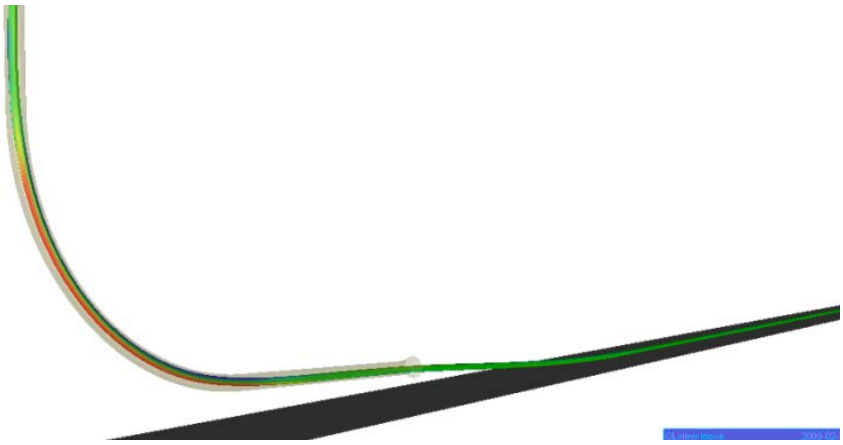

Analytical Model for J-Tube Pull-in

Rauan Zhamangarin

University of Stavanger

June 2013

Acknowledgement

This thesis is part of the study curriculum to fulfill master degree in Marine and Subsea Technology, at the University of Stavanger in the department Mechanical and Structural Engineering and Material Science. This thesis was done in cooperation with Statoil Company, where I was also provided with office facilities. The department of Pipeline Engineering and Construction also supported me with technical information through all time.

First of all, I would like to use the opportunity to thank the God and my parents, who brought up me in best way and still supporting me with their love. I would like to also thank my brother and my fiancé for their existence, by having them I have always reason to be happy.

I also would like to thank my external supervisor Jens-Olav Rundsag for his trust in me for this thesis, for his supervision during this spring. Moreover, I am very grateful for his encouragement and organizing brainstorming meetings inside the company with experts.

I would like to give my special gratitude to my internal supervisor Arnfinn Nergaard, I would like to thank him for his positiveness and support, I strongly believe that Mr. Arnfinn is the kind of person from whom we can learn many things not only in aspect of subsea technology, but also in many aspects of life.

At the end, I would like to take this opportunity to thank my friends for being together all this time.

I would like to give my big thanks for my country “Kazakhstan” who give me big opportunities all my life.

Stavanger June, 2013

Rauan Zhamangarin

Executive Summary

In the Oil & Gas industry pipelines are used to connect one facility to another facility. Connecting new facilities to existing facilities represent improved economic potential of the field development. J-tube pull-in method is one of the preferable methods for new pipeline tie-ins. Advantages of the J-tube pull-in method from other alternative methods are minimal subsea connections, less installation time, low installation and pre-installation costs, low and medium operational and installation risks and topside connection. Moreover pre-installed J-tubes can allow connecting pipeline at any time during operational life.

As long as J-tubes are installed during the platform installation, only minor thing can be changed after installation. The method implies pulling the pipeline through J-shaped tubes (J-tube). In spite of the all the advantages mentioned before, the method requires design analysis in term of required pulling force, riser integrity and J-tube integrity. There are mainly two ways for design analysis; Finite Element analysis and Analytical method. First approach is time consuming and costly, meanwhile it provides accurate and versatile result. The latter would be good guidance at initial phases of the project.

In this project the analytical method was established to examine riser integrity and to determine required winch pulling capacity. Riser integrity was analyzed in accordance with DNV-OS-F101 for local buckling. The winch's pulling capacity is calculated using the Capstan equation, beam theory for plastic deformation and the energy method. The method calculates tension force on winch during different stage of J-tube pull-in installation by taking into account the riser's dimensions, material properties and the J-tube's geometry.

The paper also consist sensitivity analysis for the calculation model and comparison of the results obtained from the established model to FEA results. The Excel tool is attached to the Master thesis and principles of working shown in the appendix.

Table of Contents

List of Figures

List of Abbreviations and Symbols

Abbreviations

DNV	Det Norske Veritas
CoF	Coefficient of friction
DC condition	Displacement Controlled condition
FEA	Finite Element Analysis
LC condition	Load Controlled condition
HSE	Health, Safety, Environment
PP	Polypropylene
ROV	Remote Operated Vehicle
SV	Support Vessel
SMYS	Specified Minimum Yield Strength
SMTS	Specified Minimum Tensile Strength

Latin Symbols

A	Ramber-Osgood moment to curvature coefficient
Ai	Area of incremental part of pipe's cross section
Apipe	Cross sectional area of pipeline
B	Ramber-Osgood moment to curvature coefficient
C_1	Coefficient for determining to distance between touch points
C_2	Coefficient for determining to distance between touch points
C_{1pp}	Coefficient C_1 including effect of coating
C_{2pp}	Coefficient C_2 including effect of coating
D	Inner diameter of J-tube
d	Outer diameter of riser
dmax	Maximum out roundness diameter
dmin	Minimum out roundness diameter
d_m	mean diameter of riser
E	Young's modulus
f_o	Initial ovality
f_o'	Ovality after bending
f_y	Yield stress to be used in design

$f_{y,temp}$	Derating on yield stress to be used in design
F	Applied force, Force required to pull the riser inside J-tube
F_N	Normal force in scraping
$F_{friction.cable}$	Cable's friction force to J-tube
$F_{friction.pipe}$	Pipe's friction force to J-tube in horizontal section
g	Gravity acceleration
I	Second moment of inertia
k	Curvature
k_o	Yielding curvature
k1	Coefficient for determining scrapping force
k2	Coefficient for determining scrapping force
L	Length of beam or Distance between lower touch points riser to J-rube
L1	Length of horizontal section of J-tube
L_{ph}	Length of pullhead
l_1	Distance between touch points inside bended section of J-tube
l_2	Distance between touch points just outside bended section of J-tube
l_3	Distance between touch points when riser reversely touches the J-tube
M	Moment of bending
Mo	Yield initiating moment
Moval	Moment of bending for oval pipes
Mp	Fully plastic moment
$\bar{M}$	Moment on fixed end of beam
N	Normal reaction force
No	Pullhead to J-tube normal force
P	Lateral force acting on beam
Pb	Pressure containment resistance
Pc	Characteristic collapse pressure
Pe	External pressure
Pel	Elastic collapse pressure
Pmin	Internal pressure
Pp	Plastic collapse pressure
P_1	Maximum pull-in force in stage-I
P_2	Maximum pull-in force in stage-II
P_3	Maximum pull-in force in stage-III

P_4	Maximum pull-in force in stage-IV
P_5	Maximum pull-in force in stage-V
P_6	Maximum pull-in force in stage-VI
R_N	Scraping objects scraping area
R	J-tube's radius of bending
Re	Elastic bending radius
Rp	Plastic bending radius
S	Cross section area of pipeline
t	Wall thickness of pipeline
tpp	Wall thickness of polypropylene coating
T_1	Tension on lower section of pulling wire or riser in bended section
T_2	Tension on upper section of pulling wire or riser in bended section
T_3	Tension on lower section of pulling wire when pipe and wire in bended section
$T_{back.tension}$	Backtension form the bellmouth
T_{max}	Maximum tension force in pipe's cross section
U	Internal energy
V	Volume
W	Weight of riser per length
Wr	Weight of riser in vertical segment of J-tube

Greek symbols

α	Ramberg-Osgood coefficient stress-strain coefficient
$\alpha\left(\frac{M}{M_0}\right)$	Coefficient of deflection
$\alpha_{ph}\left(\frac{M}{M_0}\right)$	Coefficient of deflection including pullhead effect
α_1	Angle of inclination of the J-tube's horizontal segment
α_2	Angle of inclination of the J-tube's vertical segment
α_u	Material strength factor
α_h	Strain hardening
α_{gw}	Girth weld factor
α_{fab}	Fabrication factor
β	Ramberg-Osgood stress-strain coefficient
$\beta(\frac{M}{M_0})$	Coefficient of rotation

$\beta_{ph}(\frac{M}{M_0})$	Coefficient of rotation including pullhead effect
β_2	Angle between pipe's upper touch point and horizontal axis
β_1	Angle between pipe's lower touch point and horizontal axis
ε	Strain
ε_A	Accidental load strain
ε_c	Characteristic bending strain resistance
ε_E	Environmental load strain
ε_F	Functional load strain
ε_I	Interferential load strain
ε_O	Yielding strain
ε_{sd}	Design compressive strain
γ_A	Load effect factor for accidental load
γ_c	Condition load effect factor
γ_{SC}	Safety class resistance factor
γ_ε	Resistance factor, strain resistance
γ_E	Load effect factor for environmental load
γ_F	Load effect factor for functional load
γ_m	Material resistance factor
γ_2	Angle between lower touch point of pulling wire and horizontal axis
γ_1	Angle between upper touch point of pulling wire and horizontal axis
μ_c	Coefficient of friction between J-tube and pulling wire
μ_p	Coefficient of friction between J-tube and pipe
μ_{ph}	Coefficient of friction between J-tube and pullhead
θ	Angle between riser's lower touch point and vertical axis
θo	Angle between pullhead and pulling wire's touch point
ρ_w	Density of water
ρ_p	Density of pipe material
ρ_{pp}	Density of coating material
σ	Stress
σ_o	Yielding stress
ν	Poisson ratio
τ	Angle between pullhead and riser's touchpoint

φ	Any angle
Φ	Supplementary value in order to solve cubic equation
ω	Angle of plasticity in pipe's cross section
Δ	Deflection

1. Introduction

1.1. Background

The demand for hydrocarbons in the 21st century requires searching the oil and gas beyond onshore and go further to offshore. Unlike onshore, any operation committed on the sea is challenging due to the environment conditions and environmental limitations and requires a lot of effort. Not only building platforms and drilling on offshore is a challenge, but also transporting the hydrocarbons, designing and laying pipelines and approaching them to the platforms possesses high operational challenges as well.

Generally, any pipeline has at least two tie-ins, and can be tied between a subsea well to the platform, the subsea well to a production line or between two platforms. There are many ways on tie-in techniques how to connect the pipeline to the platform such as spool piece, lateral pull, j-tube pulling-in and reverse pulling methods.

J-tube riser installation method is suitable for installation of small diameter pipeline or flexible cables or risers for offshore platforms. It has both technical and commercial merits compared over other methods:

- Minimal subsea riser to pipeline connections
- Effective lay-away time for the barge
- Initially installed J-tube can provide accommodation for riser at any time in production life.
- Low operational and installation risk
- Low pre-installation and installation cost etc.

The installation method involves passing a pulling wire from a top-side winch through J-tube down to and out to a pipeline lay vessel, connecting it with pullhead on leading part of pipeline, then by activating winch pipe pulled-up from the lay vessel through J-tube inner section to platform's top-side. Then lay vessel starts to lay-away the pipe from the vessel.

J-tube is designed and installed before the lunching platform. As long as platform is set, there is not so much things can be done if tube is too small or has small bending radius etc. That is why proper methods of analysis needed in order to obtain required winch pull-in force,

possible pipeline size and integrity of J-tube itself. Generally Finite Element Analysis is used for solving a number of problems which were mentioned previously.

Although FE analysis can provide with more detailed and accurate results for all process, the analysis can be not preferred due to cost and time consuming. Consequently there is a need for a tool in early stage of the project in order to determine suitable pipeline size solution, required pull-in force, strain on pipeline and contact force between J-tube with fairly good accuracy. The tool must be able to give the results instantly and be cost-effective. Some analytical approaches have been developed before, but many factors like: effect of pullhead and effect of polypropylene coating were not included in it.

The main aim of this paper is to develop new analytical approach for J-tube pull-in method, which will be adequate analysis method in early stage of the project, compare new proposed approach with FE Analysis results and as-built data to show accuracy of the tool in determining results. Reliance on FE Analysis tools can leads design engineers to lose practical ability to assess the correctness of the results. Thereby developed method can be a guideline for inspection of any certain parameters during designing.

1.2. Purpose and Scope

Despite the fact that many literatures in pipeline engineering have many descriptions regarding pipeline design and installations, there are still limited information about J-tube pull-in method and its mechanics. Main difficulties in understanding mechanics of pull-in process are understanding mechanics and behavior of the pipe in J-tubes' bended section.

The allowable dimensions of pipeline are mainly governed by dimension of the J-tube, whereas magnitude of maximum pulling force can be determined from following parameters:

- Submerged weight of pipe per unit length.
- Friction coefficient between pulling wire and J-tube.
- Friction coefficient between pipeline and J-tube.
- Friction coefficient between pullhead and J-tube.
- Backtension on the pipeline from the tension force on laying vessel.
- Strain-stress characteristics of pipe material.
- J-tube dimensions.
- Pipeline dimensions.
- Pullhead dimensions.
- Coating Properties.

The ability of assessing the possible pipe dimension solutions and maximum allowable pulling force without any expenditure in early stage of the project can be very crucial, and can give significant impact in decision making.

Therefore, the objective of the thesis is to:

- develop equations which enable to:
    - check for pipeline integrity
    - determine maximum allowable pulling force
    - determine pullhead and J-tube contact force
- Adopt developed formulas and equations to EXCEL spread sheet and make calculation tool.
- Comparison with calculated results against FE Analysis results.
- Discuss the result and make recommendation for further study.

1.3. Limitations

Developed equations in this thesis have some limitations, and for that reason some assumptions was proposed. The list of the limitations is given in this chapter, whereas key assumptions are mentioned in the following subchapter. The limitations inherent in this paper are:

- Imperfection of riser's wall thickness.
- Imperfection of riser's diameter.
- Imperfection of coating's thickness.
- Risers motion complexity inside J-tube.
- Welding effect on pipe mechanics.
- Uncertainties regarding mean yielding stress.
- Complexity of pipe's yielding behavior.
- Complexity of bending pipe under combined axial and lateral loading.
- Complexity of J-tube to pullhead interaction.
- Deformation of J-tube.
- Deformation of J-tube supports.
- Complexity of pipeline to seabed interaction.
- Effect of pipeline coating to bending stiffness.
- Shrinkage of pipeline coating due to pipeline to J-tube contact.

1.4. Key Assumptions

Some assumptions need to be made in order to eliminate limitations listed above and to be able to continue calculation. The assumptions proposed by the author are:

- PP coating of the riser doesn't give any effect for bending stiffness of the riser.
- PP coating doesn't shrink due to riser to J-tube interaction.
- Coefficient of friction between riser and J-tube is constant along the J-tube
- Coefficient of friction between pulling cable and J-tube is constant along the J-tube
- Change in bending stiffness due to axial load is negligible
- Pullhead will be considered as completely stiff part of pipeline.
- J-tube and it's supports is completely stiff and doesn't deform during installation
- Riser material has uniform yielding stress along the length.
- Weight of the pulling wire is negligible.

2. Pipelines and Tie-in methods

This chapter gives information about pipeline laying methods and platform approach methods in order to give an idea for non-specialists. The chapter also includes more detailed information about J-tube pull-in method and installation procedures.

2.1. Introduction to pipelines

Pipelines in Oil & Gas business can be defined as tubular arrangement or pipe conduit designed for transportation of crude or refined hydrocarbons from storage, wellhead or refinery to customers or other facilities.

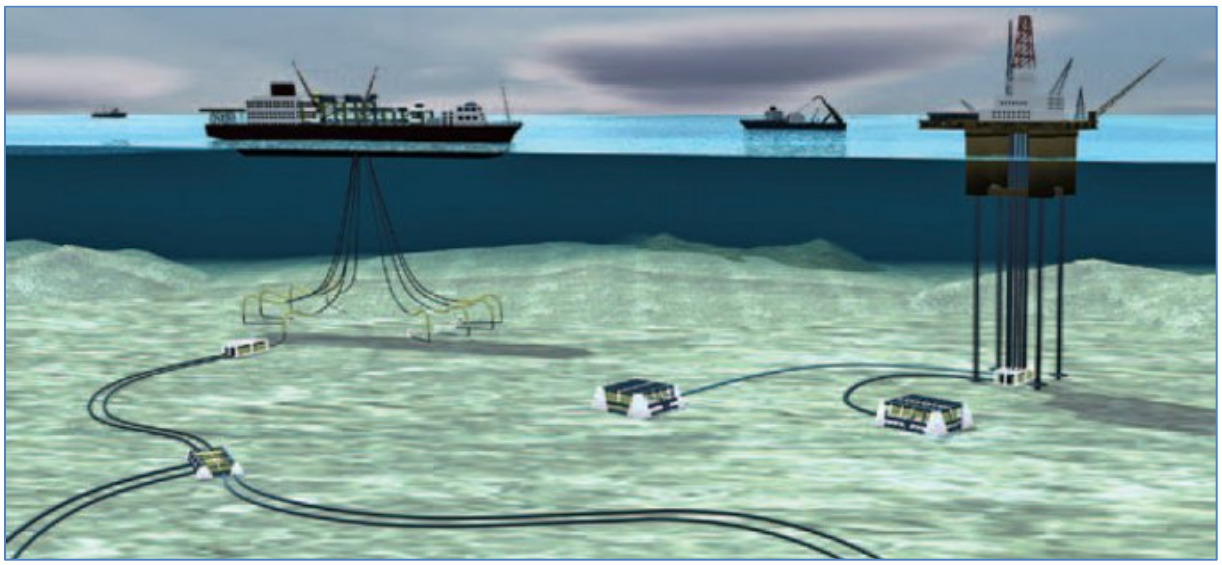

Figure 2-1 Offshore Pipelines **(ISOVER, 2012)**

Usually offshore field development concept consist infield and export flowlines (Boyun Guo, 2005). Whereas for infield pipelines are flowlines transporting hydrocarbons from subsea satellites to subsea manifold, flowlines between subsea manifolds and platforms with production facilities for production transportation or for water/chemical injections. (Young Bai, 2005)

The design of pipelines primarily governed by parameters like: reservoir performance, oceanographic and metrological data, fluid and water compositions etc. That is why any individual field has individual approach and different pipeline solution. Pipeline diameters usually vary between 10-30 inches in diameter, and depending on field remoteness and flow rate magnitude and the length also can vary significantly. For instance gas transportation pipeline from Ormen Lange field in Norway to Easington in United Kingdom, by having 44

inches diameter and 1166 km length known as the longest subsea pipeline in the world. (Gjertveit, 2013)

2.2. Pipeline installation methods

Pipeline installation regarding on suspended pipe shape during installation can be classified into methods like S-lay or J-lay. Where pipe joints delivered to lay barge by supply vessel in the form of fabricated, coated and provided with anodes pipes, then pipeline is produced on barge by joining them together and laying them back to the seafloor. Some pipelines with smaller diameter may be produced onshore and reeled on to a spool. Afterwards this spool installed in to the laying barge and pipe laying process performed by reeling out the pipe from the spool, this method is called reel lay method.

In S-lay method the pipelines welded together on lay barge and installed on place, the barge there might have several welding points, and in this manner the installation process can be accelerated. The S-lay barges need only minimum modification in order to install pipelines with different dimension. Upper bend of S-curve is called overbend and controlled by the stinger whereas lower bend called sagbend and this curvature controlled by tensioner in the barge. Typical configuration of S-lay method is shown in the Figure 2-1.

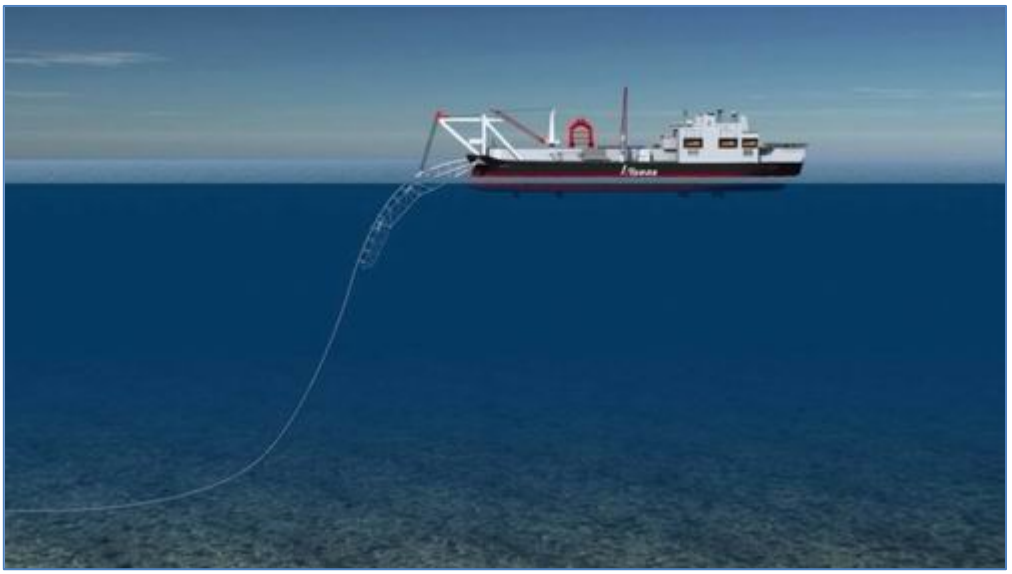

Figure 2-2 Typical S-lay configuration **(Allsea, 2013)**

S-lay method is suitable in water depth up to 700 m, due to increase submerged weight of the pipe, allowable maintainable overbend force in deeper waters will be increased, and J-lay is the preferred option in deeper waters. The name J-lay comes from pipe's installation shape, the pipe will leave the barge in vertical direction and will bend later on seafloor and forms J-

shape. Because pipe joining performed in vertical direction, the vessel may have only one welding point on board, so that it is very prudent to use double or triple pipe joints together in order to accelerate installation. It is feasible to install pipelines in waters over than 2000 m depth, but dynamic positioning can be only option for station keeping in this situations. Owing to vertical entrance to water some vessels equipped with moon pool, or some of them has vertical stinger at the end of the barge. Typical configuration of J-lay method is shown in the Figure 2-3.

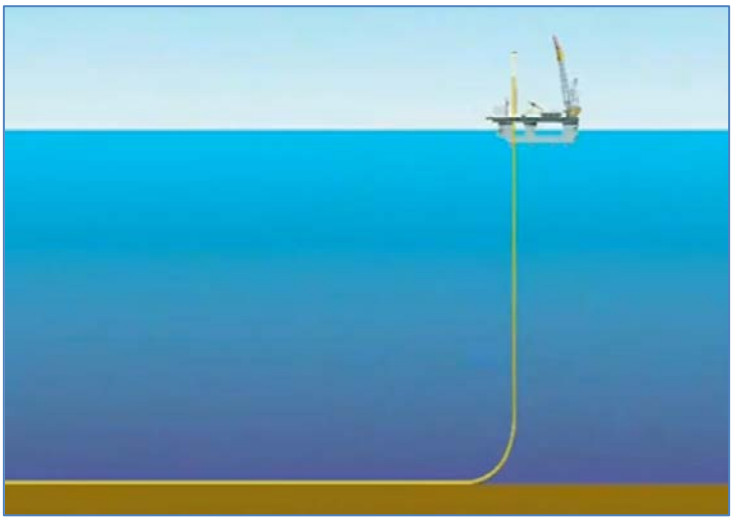

Figure 2-3 Typical J-lay configuration **(Huisman, 2008)**

Reel-lay vessel resembles cable-lay vessel or umbilical-lay vessel. Reel-lay vessel has a spool with up to 30 m diameter where pipe pulled out and straightened and leaves the vessel from the stern. The sagbend controlled from the topside, by adjusting tension on the reel. Main disadvantage of this method is: the pipe dimensions is very limited and can be used to installed pipelines with maximum 16 inches diameter and the pipes cannot be assembled with concrete coatings where on bottom stability must be ensured solely by pipe's wall thickness. The method can be suitable for very deep waters because of pipe's small diameter and thick wall thickness. In the Figure 2-4 is shown vessel for reel-lay installation.

Figure 2-4 Reel-lay vessel **(Huisman, 2008)**

Towing method is another option for pipeline installation, where pipeline produced onshore and towed to location, given the fact that it is quick way of installation, the method very susceptible for weather conditions. (Mikael W.B, 2005)

2.3. Pipeline tie-in methods

There are many ways how to tie the pipe to the platform like spool piece, lateral pull, j-tube pulling-in and reverse pulling method. All of them have pros and cons related to installation processes and connection difficulties. This subchapter describes tie-in methods in individually and highlights their pros and cons. (Young Bai, 2005)

A tie-in spool installation method is the most common tie-in method. The spools are special pipe arrangement, which is fabricated after installation of the pipeline end terminal (PLET) by measuring dimensions. It has to satisfy number of criteria regarding safe product transportation while it has subjected some loads like axial force due to thermal expansions etc. In order to avoid leakage in flanges, the sealing of the connectors is very important. To ensure good sealing capability the loads on flanges and connectors need to be reduced, with an eye to reduce loads, spools designed with some bend, which can absorb some forces. The bends give some flexibility regarding to misalignments and some inaccuracies in the installation. The typical tie-in spool is illustrated in the Figure 2-5. (Young Bai, 2005)

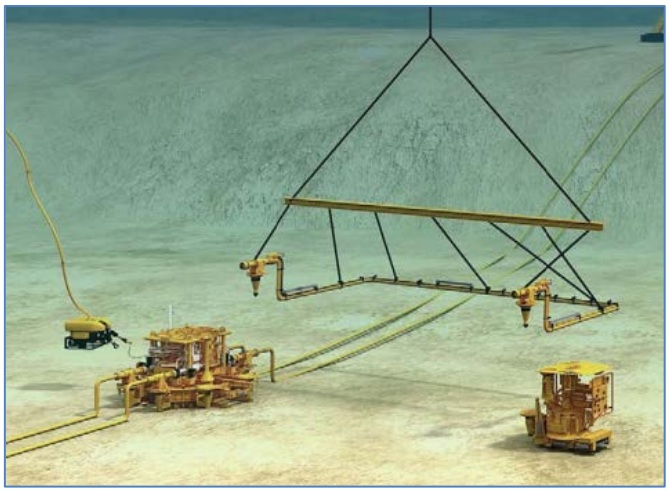

Figure 2-5 Horizontal Tie-in Spool **(Young Bai, 2010)**

Other tie-in method is lateral pull method. The method involves locating one end of the pipe in one side of the platform or manifold and pulling it in lateral direction into target point. It has some drawbacks compared to other method, like: need for a clear area in one side of the platform or manifold and reaching alignment during pulling etc. In order to eliminate remedial work the vertical deflection method was developed, where pipe end will be suspended by buoys and pulling will be performed by wires or system of wires.

In order to reach accuracy in alignment the single wire or system of wires can be used for the pulling, and with an eye to reduce friction force between seabed and give more flexibility to installation buoys can be used for deflecting the part of pipeline.

The method is feasible when direct pulling method cannot be done, because when you are laying away the flowline it is easier to pull it directly to the target point (e.g. J-tube pull-in method), rather than laying down to the point. The lateral pull method is illustrated in the Figure 2-6 (Young Bai, 2005).

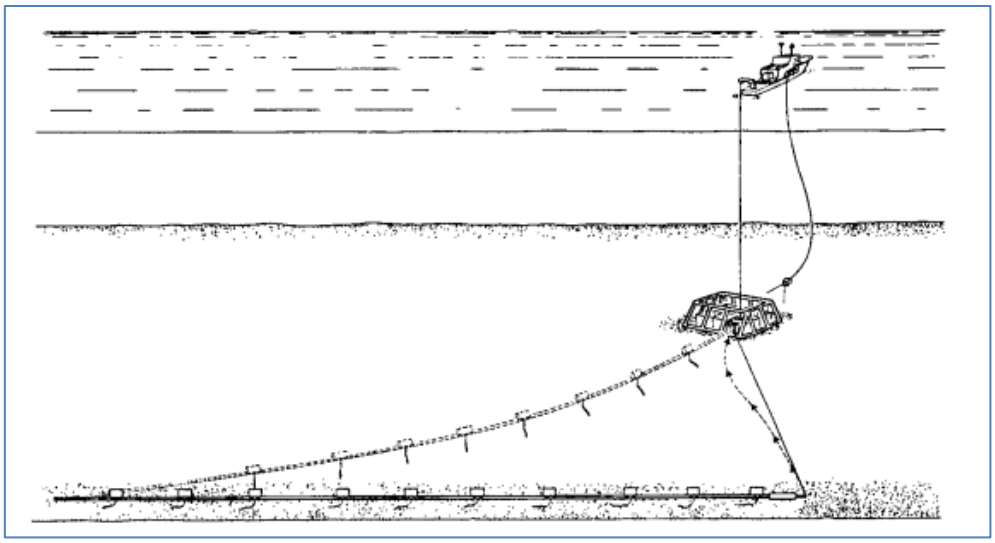

Figure 2-6 Lateral Pull method **(Bruton D.A.S, 1989)**

Connect and lay away method is similar to direct pull in method, but the connection is done subsea. The method can be used in deep waters where using divers intervention is not feasible, despite this advantages, implementation of the method is quite costly because of complex mechanics of connection tools. Due to pipeline expansion, the flanges can be subjected to high axial loads during operational phase. The typical connection system from FMC is shown in Figure 2-7.

Figure 2-7 Connection system **(FMC, 2012)**

Stalk-on method is another method to tie-in, where barge lay-down a flow line to the platform with its adjoining riser. The platform riser will be lifted on barge and welded to the pipe there, and afterwards the pipe and riser will be lowered to the seabed and riser will be connected to the platform. Main advantage of this method is that the same vessel can complete whole operation, but the method is depth restricted and can be used in water depth up to 40 m. On operational phase due to the pipe expansion the pipe can be subjected to axial loads. The typical illustration of Stalk –on method is shown on the Figure 2-8. (Young Bai, 2005)

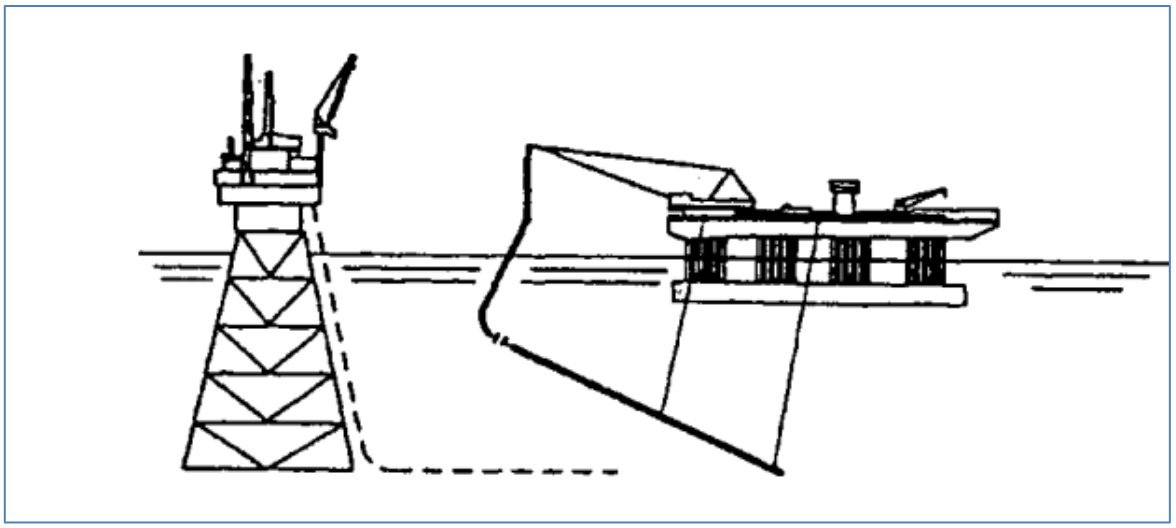

Figure 2-8 Stalk-on method **(Young Bai, 2005)**

J-tube riser installation method is suitable for installation of small diameter pipeline or flexible cables or risers for offshore platforms. It has both technical and commercial advantages compared to other methods:

- Minimal subsea riser to pipeline connections.
- Lay-away time can be used more effectively for the barge.
- Initially installed J-tube can provide accommodation for riser at any time in production life.
- Low operational and installation risk.
- Low pre-installation and installation cost etc.

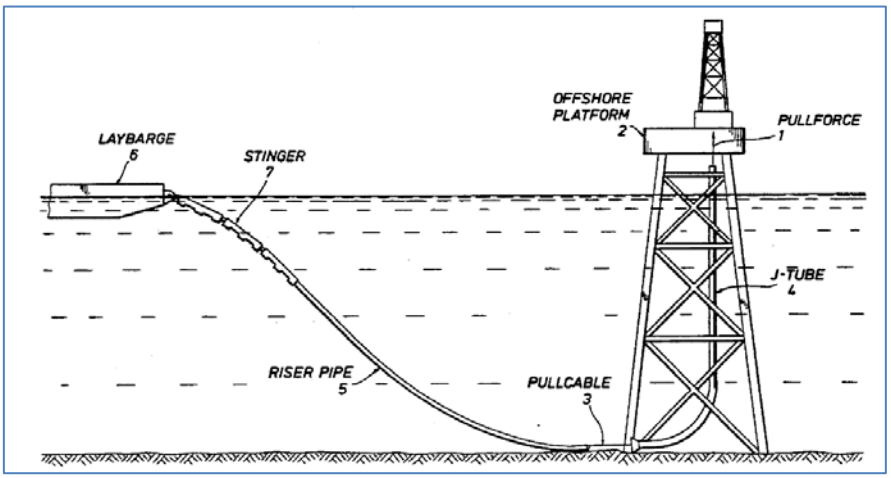

Figure 2-9 J-Tube Pull-In Method **(Titus, 1992)**

Since the paper presents the analytical solution for J-tube pull-in method, detailed description of J-tube pull-in method will be given in the following paragraph.

2.4. J-tube pull-in process

J-tube's usually installed during platform installation for future tie-in. The name J-tube comes from its shape, the tube has mainly three segments: vertical, bended part and horizontal one. Some of J-tubes have several bended parts and the vertical and horizontal segments can be slightly inclined. In order to conduct installation, pull-in winch need to be installed on the platform. Winches can vary on its pulling range, and it is important to know the required pulling force for particular riser before winch selection. Pullhead need to be deployed on leading head of pipeline, in order to ensure pulling wire connection and for riser integrity during installation.

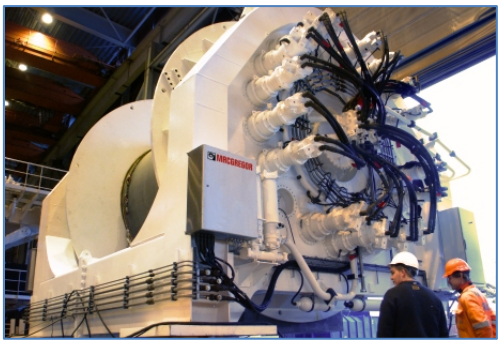

Figure 2-10 Offshore Winch **(MacGregor, 2013)**

The installation sequence of J-tube pull-in method is given below.

- Removing of a bellmouth plug.
  - SV approaches the platform.
  - ROV removes the plug.
  - ROV inspects condition of the belmouth and inside of J-tube.
- Recovery of a pulling wire on SV board.
  - SV will lower recovery wire on the ROV.
  - The ROV connects recovery wire to the pulling wire.
  - SV by spooling recovery wire receives the pulling wire.
  - During spooling of recovery wire, the winch will layout pulling cable.
- Recovery of the pulling wire onboard of pipe lay barge.
  - Pipelay vessel will approach SV with its stinger.
  - The pulling wire will passed to pipelay vessel.
  - Pulling cable will be connected to pullhead.
- Pipe pulling process.

- Winch will be activated and it will start to pull the pipe.
- Pipe will be welded and coated and send further form pipelay vessel.
- Pipeline will be pulled through J-tube.
- When pullhead is received on the top-side it will be hanged off.
- Pipelay process continues…

As in other offshore installation processes the safety in J-tube pull-in process is utmost important. In order to eliminate upsets and inefficient operations the following recommended practices should be considered.

- Familiarize with HSE regulation and safety rules all personnel.
- Certify and test all equipment and vessel prior to operation.
- Assess weather window by taking into account uncertainty factor (alfa factor) for current location.
- The weather window needs to encompass time from pulling wire recovery to pipeline hang off on the platform topside.
- Assess contingency time within weather window, or activities can be divided into some sub-activities, so all process can be fitted into several weather windows.
- Establish proper communication channel between lay barge and SV, and with winch operator on the platform.
- Establish spare communication action as a contingency action
- Positioning of the vessel and anchoring of it must be handled with communication meaning as well
- Winch need to be deactivated when sealing reaches on bellmouth and be placed.
- Replace permanent hang-off with permanent one, when laid pipeline length exceeds designed value. During sealing installation pipeline buckling control must be utmost important in order to avoid buckling and pipe replacement.
- Prepare emergency evacuation plan and contingency plan for any sort of contingency actions and all personnel need to be competent with appropriate certificate and knowledge.
- Verify J-tube dimensions by gauging pigs against drawings and specifications before riser installation.
- Conduct pipe pulling test in order to check for pullhead jamming.
- Monitor pullhead entrance into bellmouth by ROV

- Monitor pulling force on the winch by load cells or gauges in order to avoid exceeding allowable pull-in force (DNV, 2010).

3. Theoretical part

Determining pulling force in J-tube pull-in process can be obtained by understanding behavior of the riser inside J-tube and understanding interaction force between them. Riser's strain during bending will exceed elasticity range and will deform plastically. Due to residual strain after bending, pipe will have residual curvature and will have extra contact force to the J-tube's vertical wall. The pullhead will be considered as infinitively stiff part of the pipeline, which will not deflect or rotate. It is expected to get maximum pull-in force in preliminary bending, secondary bending or on final stage of installation due to suspended weight of the riser (Eriksen G, 1989). Number of tests has been done (Tan H, 1981) in 1981 and result expected by Eriksen G was obtained.

The maximum pull-in force during installation can be governed by following factors:

- Riser's and J-tube's geometry.
- Pullhead geometry.
- Bending behavior riser due to external forces.
- Backtension on riser due to tension on pipelay vessel.
- Coefficient of friction between the riser and J-tube, J-tube to pulling wire and the pullhead to J-tube.
- Submerged weight of the riser in seawater per unit length etc.

The analytical approach in this paper will take into account all above mentioned issues by using simple mechanical and geometrical formulations. Some estimations regarding to pipe bending behavior will be referred from other works. During developing analytical tool, in order to simplify formulation whole process of pulling was divided into six individual stages:

- Riser at the bellmouth entrance.
- Riser just before J-tube's bended section.
- Riser at J-tube's bended section.
- Riser at J-tube's bended section exit.
- Pullhead touches other side of J-tube due to residual bending.
- Pipe at topside level.

All of these stages have been demonstrated on the Figure 3-22 and formulations regarding each stage have been developed and presented in the chapter 3.7.

3.1. Moment to curvature relationship for the riser

In order to get moment to curvature relationship for the riser bending characteristics it is important to know the stress-strain relationship of material behavior. It was assumed that material has elastic-perfectly plastic stress-strain relationship. Cross section of the bended pipe shown on the Figure 3-1, the pattern part in the drawing shows plastic part of bending in the given quadrant. The angle ω shows the half angle encompassing plastic part of bending, d_m is the mean diameter of the pipe. Due to stress difference in elastic and plastic parts the total moment of bending can be sum of them.

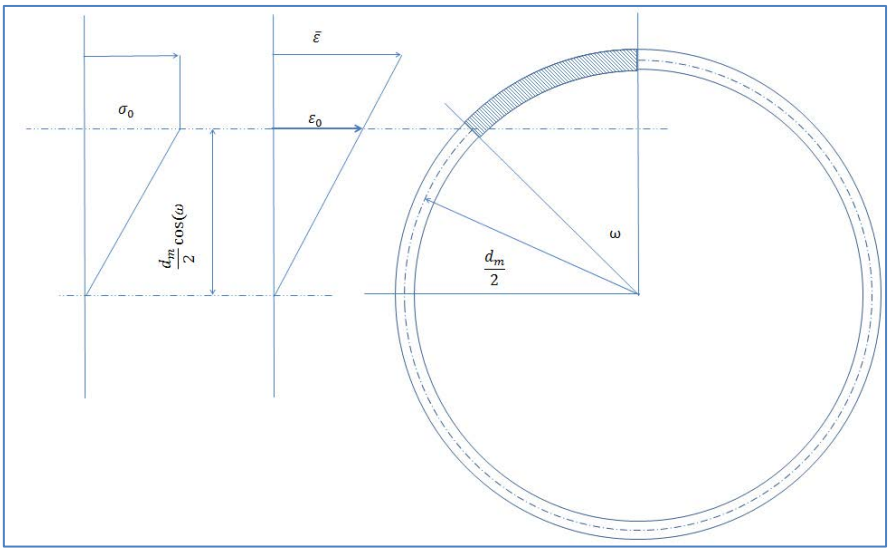

Figure 3-1 Pipe's cross section

The bending moment can be calculated as sum of the moments from plastically and elastically deformed section (Arthur P, 2003).

$$M = M_e + M_p = \int \sigma \cdot y \cdot dA + \int \sigma_0 \cdot y \cdot dA$$

So the following integration gives values of the total moment of bending for the pipe's cross section shown in the Figure 3-1.

$$M = 4 \cdot \left(\overbrace{\int_0^{\omega} \sigma_0 \frac{d_m}{2} \cos(\varphi)\, t \frac{d_m}{2} d\varphi}^{\text{Elastic part}} + \overbrace{\int_{\omega}^{\frac{\pi}{2}} \sigma_0 \frac{\cos(\varphi)}{\cos(\omega)} \frac{d_m}{2} \cos(\varphi)\, t \frac{d_m}{2} d\varphi}^{\text{Plastic part}} \right)$$

By solving the integration above, plasticity angle to moment relationship equation can be obtained, and this equation will have following form:

$$M = \sigma_0 d_m^2 t \left(\sin(\omega) + \frac{1}{\cos(\omega)}\left(\frac{\pi}{2} - \omega - \cos(\omega)\sin(\omega)\right)\cdot\frac{1}{2}\right) \quad (1)$$

Whereas:

ω: Angle of plasticity (Figure 3-1).

σ_0: Yielding stress of material.

d_m: Mean diameter of pipeline.

t: Wall thickness of pipeline.

Yielding moment will occur when the stress on the outer edge of pipe will be equal to yielding stress of the pipe material. So the yielding moment or fully elastic bending occurs when $\omega = 0$ and takes following form:

$$M_o = \frac{\pi}{4}\sigma_0 d_m^2 t$$

The fully plastic moment of bending will occur when the whole cross section of the pipe will have yielding stress, whereas $\omega = \frac{\pi}{2}$, and by substituting it to the equation (1) the equation for fully plastic moment can be obtained and takes following form:

$$M_p = \sigma_0 d_m^2 t$$

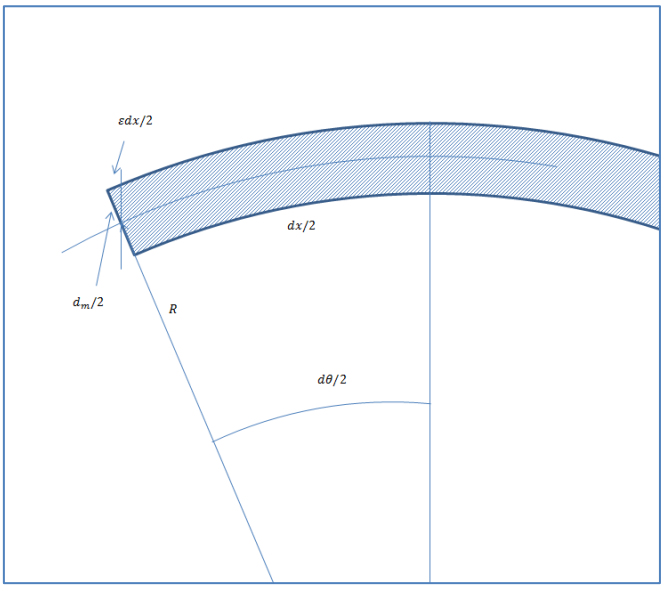

Figure 3-2 Lateral deflection of bended pipe

The Figure 3-2 shows the lateral section of bended pipe and where the angle of deflection in pipe can be found by the next equation.

$$\frac{d\theta}{2} = \frac{\varepsilon dx}{d_m} = \frac{dx}{2R} \tag{2}$$

Elimination of terms dx in equation (2) will give equation for determining maximum strain in pipe's cross section:

$$\varepsilon = \frac{d_m}{2R} \tag{3}$$

The yielding strain can be found from yielding stress and elasticity module:

$$\varepsilon_0 = \frac{\sigma_0}{E}$$

The equation (3) shows that strain has inverse relationship to radius of bending and so has linear relationship to curvature of bending, and provided that statement $\frac{\varepsilon}{\varepsilon_0} = \frac{k}{k_0}$ is true.

By substituting all the values developed before, the dimensionless form of moment to angle equation is obtained and it has following form:

$$\frac{M}{M_0} = \frac{4}{\pi}\left(\sqrt{1-\left(\frac{\varepsilon_0}{\varepsilon}\right)^2} + \frac{\varepsilon}{\varepsilon_0}\left(\frac{\pi}{2} - \operatorname{acos}\left(\frac{\varepsilon_0}{\varepsilon}\right) - \frac{\varepsilon_0}{\varepsilon}\sqrt{1-\left(\frac{\varepsilon_0}{\varepsilon}\right)^2}\right)\cdot\frac{1}{2}\right) \tag{4}$$

The graphical form of the equation (4) shown in the Figure 3-3. When maximum strain is less than yielding stress of material, the relationship will have linear dependence afterwards dependence will take nonlinear form. Any bending will led to pipe ovalization, ovality of pipe has tendency to reduce bending moment, and in practice this reduction is almost neglectable for small bending (Jirsa .J.O, 1972). In the equation (4) the effect of ovality of the pipe is not taken into account, but in chapters later we will include if ovality for the moment of bending.

By knowing moment to curvature relationship, it is possible to find curvature to moment relationship as well. The curvature to moment relationship equation suggested taking following form as in equation (5), whereas in industry some industrial software like OFFPIPE based on this equation (Assitant, 2013)

$$\frac{E}{\varepsilon_0} = \frac{M}{M_0} + A\left(\frac{M}{M_0}\right)^B \tag{5}$$

Whereas A and B are coefficients of Ramberg-Osgood moment to curvature relationship.

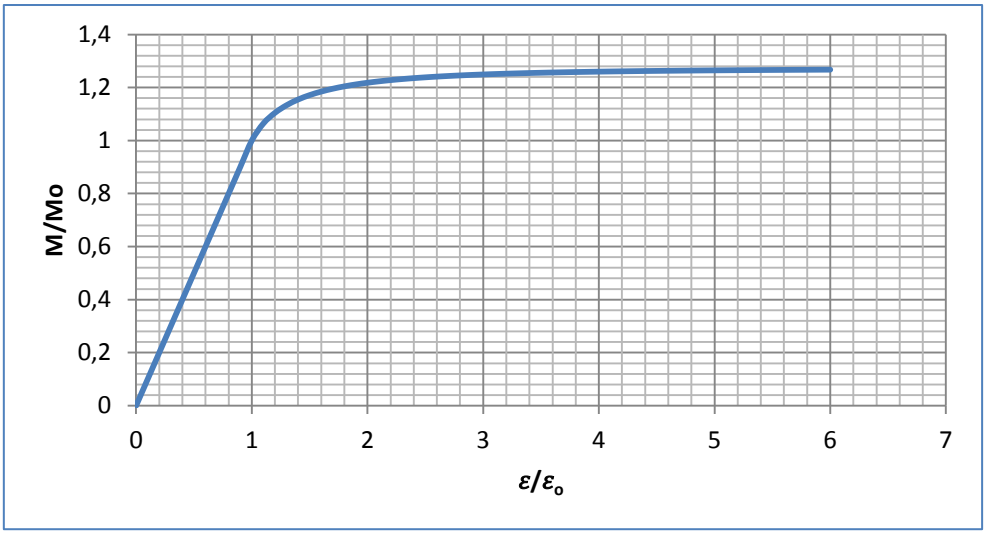

Figure 3-3 Moment to curvature relationship

By knowing the two points of this relationship the unknowns A and B can be found from system of equations. System of equations for two points will have next form.

$$\frac{\varepsilon_1}{\varepsilon_0} = \frac{M_1}{M_0} + A\left(\frac{M_1}{M_0}\right)^B$$

$$\frac{\varepsilon_2}{\varepsilon_0} = \frac{M_2}{M_0} + A\left(\frac{M_2}{M_0}\right)^B$$

Value of B for both cases takes next form:

$$B = \log_{\frac{M_1}{M_0}} \frac{\frac{\varepsilon_1}{\varepsilon_0} - \frac{M_1}{M_0}}{A} = \log_{\frac{M_2}{M_0}} \frac{\frac{\varepsilon_2}{\varepsilon_0} - \frac{M_2}{M_0}}{A}$$

By changing logarithmic form of the equation above into natural logarithmic form the following equation can be obtained:

$$\frac{\ln\left(\frac{\varepsilon_1}{\varepsilon_0} - \frac{M_1}{M_0}\right) - \ln A}{\ln\frac{M_1}{M_0}} = \frac{\ln\left(\frac{\varepsilon_2}{\varepsilon_0} - \frac{M_2}{M_0}\right) - \ln A}{\ln\frac{M_2}{M_0}}$$

Solution of the equation above gives following values for coefficients A and B:

$$A = e^{\frac{\ln\left(\frac{\varepsilon_1}{\varepsilon_0} - \frac{M_1}{M_0}\right)\ln\frac{M_2}{M_0} - \ln\left(\frac{\varepsilon_2}{\varepsilon_0} - \frac{M_2}{M_0}\right)\ln\frac{M_1}{M_0}}{\ln\frac{M_2}{M_0} - \ln\frac{M_1}{M_0}}}$$

$$B = \log_{\frac{M_1}{M_0}} \frac{\frac{\varepsilon_1}{\varepsilon_0} - \frac{M_1}{M_0}}{A} = \frac{\ln\left(\frac{\varepsilon_1}{\varepsilon_0} - \frac{M_1}{M_0}\right) - \ln(A)}{\ln\frac{M_1}{M_0}}$$

By substituting values of relative strain and relative moment, the values of A and B is obtained:

$$A = 3.4 \cdot 10^{-5}$$

B=50

In the Figure 3-4 is shown the approximated graph of moment to curvature relationship from the equation (5) and the moment to curvature graph of the equation (4). Both graphs have very close values, so it can be claimed that approximation equation is good.

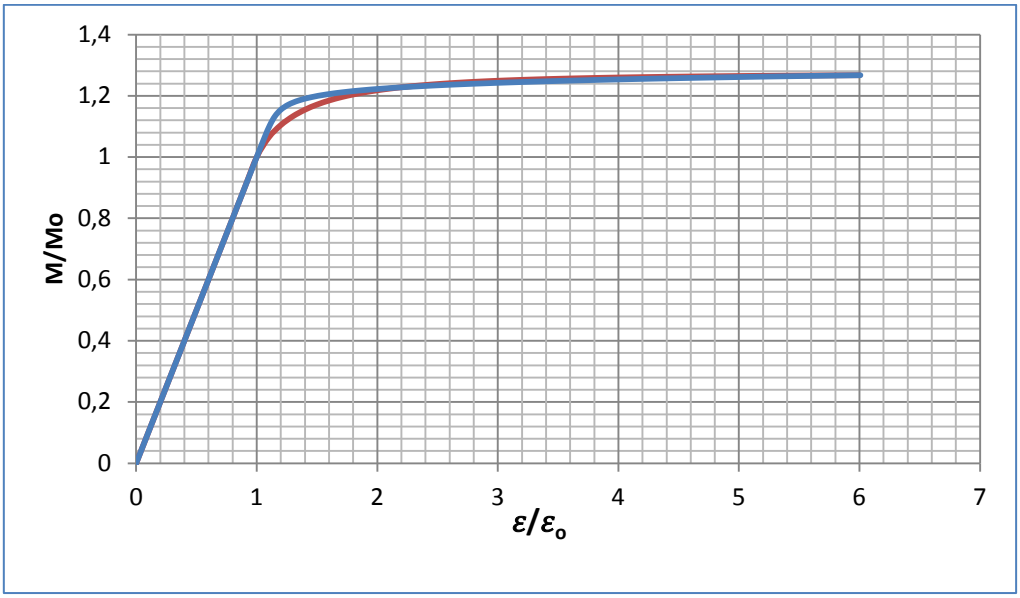

Figure 3-4 Approximated moment to curvature relationship

The both graphs show linear dependence in elastic range when $\frac{\varepsilon}{\varepsilon_0} < 1$ and non-linear in plastic range. The final equation for moment to curvature relationship will take next form:

$$\frac{\varepsilon}{\varepsilon_0} = \frac{M}{M_0} + 3.4 \cdot 10^{-5} \left(\frac{M}{M_0}\right)^{50}$$

It should be noted that the equation is done for the strain range: $6 > \frac{\varepsilon}{\varepsilon_0} > 1$

The stress – strain relationship is not always linear as it was described before. A Ramberg-Osgood relationship shows non-linear stress-strain relationship with smooth elastic to plastic transition (Ramberg W, 1943). In the Figure 3-5 (Wisnom, 1994) is shown an experimental data regarding shear stress-strain relationship and fitted Ramberg-Osgood relationship, whereas both graphs are identical to each other.

Generally Ramberg-Osgood relationship has following form:

$$\frac{\varepsilon}{\varepsilon_o} = \frac{\sigma}{\sigma_o} + \alpha\left(\frac{\sigma}{\sigma_o}\right)^{\beta}$$

Whereas α and β constants depending material characteristics.

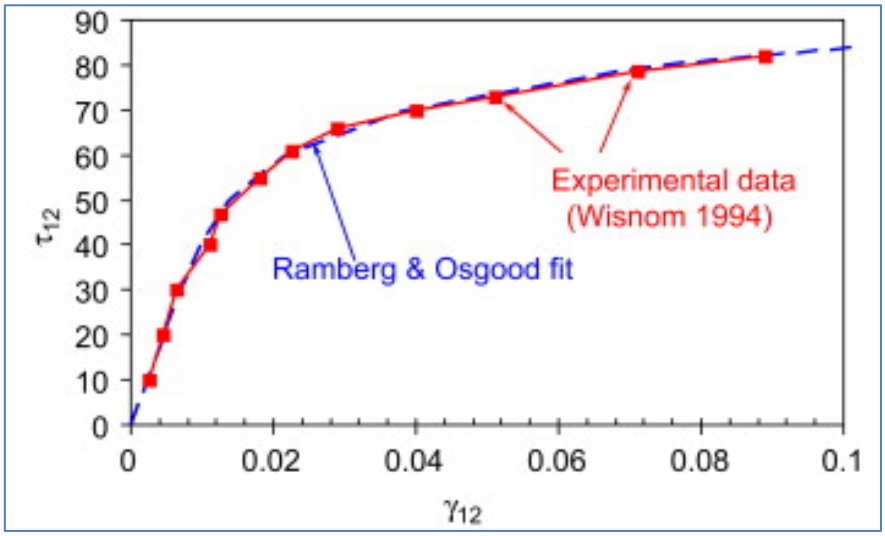

Figure 3-5 Shear stress-strain relationship **(Wisnom, 1994)**

For individual coefficients α and β particular moment to curvature coefficients A and B exists. There is some commercial software for calculating values of A and B, these values mainly depends on Ramberg-Osgood properties and pipe dimensions.

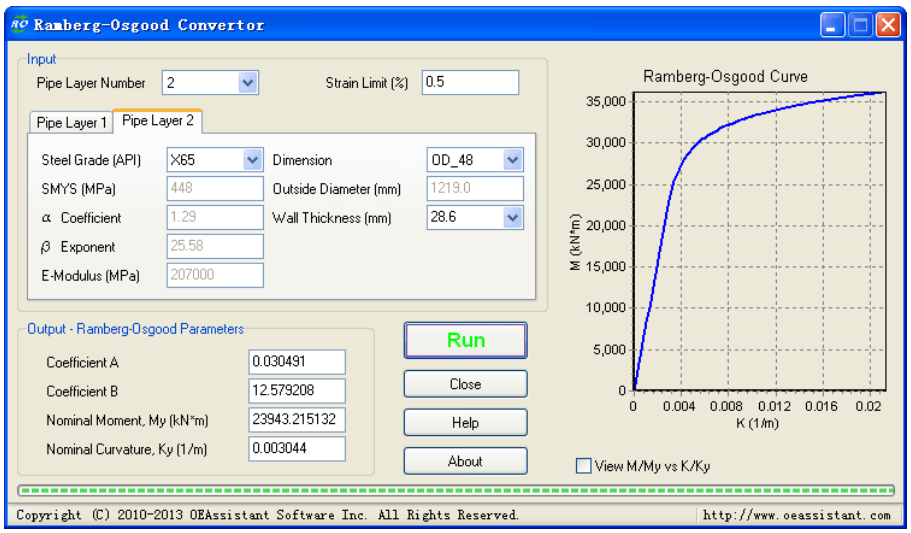

Figure 3-6 Software for calculating coefficients A and B **(Assitant, 2013)**

In the Figure 3-6 (Assitant, 2013) is shown the interface of commercial software "Ramberg-Osgood Converter" for determining Ramberg-Osgood coefficients for API 5L X65 pipeline with outer diameter 48" and 28.6 mm wall thickness.

3.2. Bending characteristics of pipeline

Distance between riser's touch points into J-tube's wall can be used in order to find contact forces between riser and J-tube. There is need for finding the risers end deflection to moment, and risers leading end rotation to moment relationship in order to find the distance between touch points. A riser section between touch points can be considered as simple cantilever beam. There is already developed formulations for the beam deflection and beam rotation for the elastic bending (S. S. Bhavikatti, 1998). The deflection and rotation can be found by next formulas:

$$\Delta = \frac{PL^3}{3EI} \tag{6}$$

$$\theta = \frac{PL^2}{2EI} \tag{7}$$

As long as the bending exceeds elastic range, the deflection and rotation of the free end of the cantilever beam will take different form and the equations given above are not valid. The rotation of the end of the cantilever beam θ can be found as sum of rotation angle in plastic-electric part and in elastic part. Same with deflection of the end of the beam "Δ", total deflection can be calculated as a sum of the deflection of the beam with elastic part and elastic-plastic part (Figure 3-7).

The beam is considered to be fixed at one end and restricted for any kind of deflection, whereas another end of the beam absolutely free.

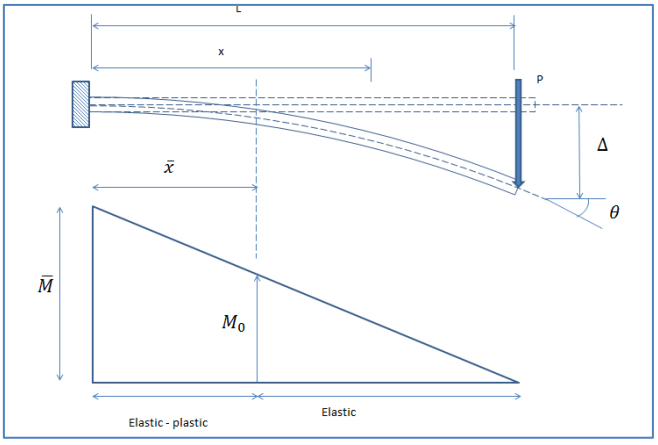

Figure 3-7 Deflection of the beam

The pullhead has an effect of reducing deflection and rotation of the leading end of the riser, the reason for that: pullhead has higher stiffness than riser itself and it will not deflect. In

order to simplify calculation, first bending of the riser without pullhead was considered and in the following chapter the effect of pullhead will be included.

The incremental rotation of the incremental part of the beam can be calculated form the equation (2) and will take a form of equation (8). So the rotation will depend on the strain of the beam and thickness of it.

$$d\theta = \frac{2\varepsilon dx}{d_m} \tag{8}$$

The integration of the equation (8) along the length of the beam will give the equation for total rotation:

$$\theta = \frac{2\varepsilon_0}{d_m}\int_0^L \frac{\varepsilon}{\varepsilon_0}dx \tag{9}$$

By substituting equation (5) to the equation (9), the following integration can be obtained.

$$\theta = \frac{2\varepsilon_0}{d_m}\int_0^L \frac{\varepsilon}{\varepsilon_0}dx = \frac{2\varepsilon_0}{d_m}\int_0^L \left(\frac{M}{M_0} + A\left(\frac{M}{M_0}\right)^B\right)dx \tag{10}$$

Bending moment on the beam's cross section located at distance x from the fixed end (Figure 3-7) can be found in the following way:

$$M = P(L-x) = \frac{\bar{M}}{L}(L-x) \tag{11}$$

Whereas:

L: Total length of the beam

$\bar{M}$: Moment of bending at fixed end.

From the equation (11), incremental distance can be expressed on the following way:

$$dx = -\frac{L}{\bar{M}}dM \tag{12}$$

By substituting the equations (12) and (5) to the equation (10), the following integration can be obtained.

$$\theta = \frac{2\varepsilon_0}{d_m}\int_0^L \frac{\varepsilon}{\varepsilon_0}dx = \frac{2\varepsilon_0}{d_m}\frac{L}{\bar{M}}\int_0^{\bar{M}} \left(\frac{M}{M_0} + A\left(\frac{M}{M_0}\right)^B\right)dM$$

The solution of the integration above will give final formulation for the rotation of the beams end.

$$\theta = \frac{\varepsilon_0 L}{d_m}\left(\frac{\bar{M}}{M_0} + \frac{2A}{B+1}\left(\frac{\bar{M}}{M_0}\right)^B\right)$$

The equation of rotation can be reduced to the next form:

$$\theta = \frac{L\varepsilon_0}{d_m}\beta\left(\frac{M}{M_0}\right)$$

Whereas $\beta(\frac{M}{M_0})$ is coefficient of rotation, which depends on $\frac{M}{M_0}$, and equal to:

$$\beta\left(\frac{M}{M_0}\right) = \left(\frac{\bar{M}}{M_0} + \frac{2A}{B+1}\left(\frac{\bar{M}}{M_0}\right)^B\right)$$

In the case when bending does not exceed the plastic range the coefficient of rotation can be approximated in following way:

$$\beta\left(\frac{M}{M_0}\right) \approx \frac{\bar{M}}{M_0} \tag{13}$$

Because A has negligible value and B is too high. So the total rotation in elastic bending can be rewritten in the following form:

$$\theta = \frac{L\varepsilon_0}{d_m}\left(\frac{M}{M_0}\right) = \frac{L\varepsilon_0}{d_m}\left(\frac{PL}{\frac{\pi}{4}\sigma_0 d_m^2 t}\right) = \frac{PL^2}{\frac{\pi}{4}Ed_m^3 t} \approx \frac{PL^2}{\frac{\pi}{32}E(d^4-(d-2t)^4)}$$
$$= \frac{PL^2}{2EI}$$

Whereas: P is the lateral load acting on free end of the beam Figure 3-7.

The equation above is identical to the equation (7), so it is solid evidence for correctness of the formulation developed.

In the same manner the deflection of the riser's end can be found. By knowing angle of rotation the deflection can be found by the formula below.

$$\Delta = \int_0^L \theta dx = \int_0^L \left(\frac{2\varepsilon_0}{d_m}\frac{L}{\bar{M}}\int_M^{\bar{M}}\left(\frac{M}{M_0} + A\left(\frac{M}{M_0}\right)^B\right)dM\right)dx \tag{14}$$

By taking constant part out of the integration, and by inserting equation (12) to the equation (14), the formulation for the deflection can be rewritten in next form.

$$\Delta = \frac{2L\varepsilon_0}{d_m}\left(\frac{\bar{M}}{M_0}\right)^{-2}\int_0^{\bar{M}}\left(\left(\frac{1}{2}\left(\left(\frac{\bar{M}}{M_0}\right)^2-\left(\frac{M}{M_0}\right)^2\right)\right.\right.$$

$$\left.\left.+\frac{A}{B+1}\left(\left(\frac{\bar{M}}{M_0}\right)^{B+1}-\left(\frac{M}{M_0}\right)^{B+1}\right)\right)\right)d\frac{M}{M_0}$$

Solution for the integration above will be:

$$\Delta = \frac{L^2\varepsilon_0}{d_m}\left(\frac{2}{3}\left(\frac{\bar{M}}{M_0}\right)+\frac{2A}{B+2}\left(\frac{\bar{M}}{M_0}\right)^B\right)$$

As in case of the elastic bending the equation for deflection can be approximated as:

$$\Delta = \frac{2L^2\varepsilon_0}{3d_m}\left(\frac{\bar{M}}{M_0}\right)$$

The last equation can be modified in a same manner as in equation (15), and the result in the equation (15) absolutely identical to the equation (6), which gives good argument to claim that formulation developed was correct.

$$\Delta_e = \frac{2L^2\varepsilon_0}{3d_m}\frac{FL}{\frac{\pi}{4}\sigma_0 d_m^2 t} = \frac{2FL^3}{\frac{3\pi}{32}E(d^4-(d-2t)^4)} = \frac{FL^3}{3EI} \qquad (15)$$

The equation for the deflection can be simplified in the following way:

$$\Delta = \frac{L^2\varepsilon_0}{d_m}\alpha\left(\frac{M}{M_0}\right) \qquad (16)$$

Whereas $\alpha\left(\frac{M}{M_0}\right)$ is coefficient of deflection, which depends on $\frac{M}{M_0}$, and equal to:

$$\alpha\left(\frac{M}{M_0}\right) = \frac{2}{3}\left(\frac{\bar{M}}{M_0}\right)+\frac{2A}{B+2}\left(\frac{\bar{M}}{M_0}\right)^B$$

In case of elastic bending the coefficient of deflection can be approximated in the next form by eliminating second part of the equation:

$$\alpha\left(\frac{M}{M_0}\right) \approx \frac{2\bar{M}}{3M_0}$$

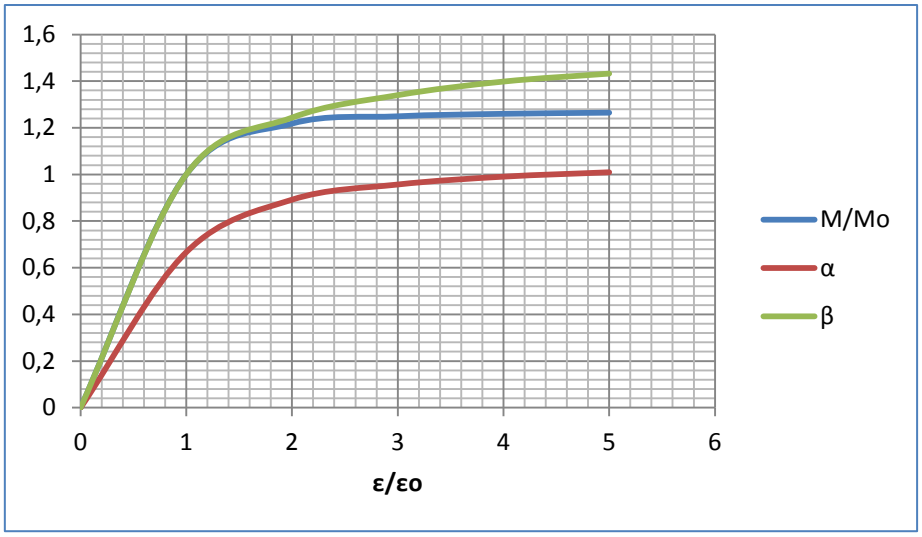

Figure 3-8 Relationship between coefficients of bending and strain

In the Figure 3-8 is shown dependence between coefficient of deflection and rotation from the relative curvature. The graph shows linear relationship between moment and coefficients when bending does not exceed elastisity range, but when it exceeds the elastisity limit the strain in the fixed edge of the beam will increase much progressively than the deflection and the rotation on other end.

In the Figure 3-9 is shown relationships between coefficients α and β and moment induced. It is clearly seen from the graph that the deflection will increase in higher rate than increase of moment in plastisity range and has linear dependance in elasticity range, which is very reasonable in practice. (During bending any beam after it start to bend plastically it will not require much force increse)

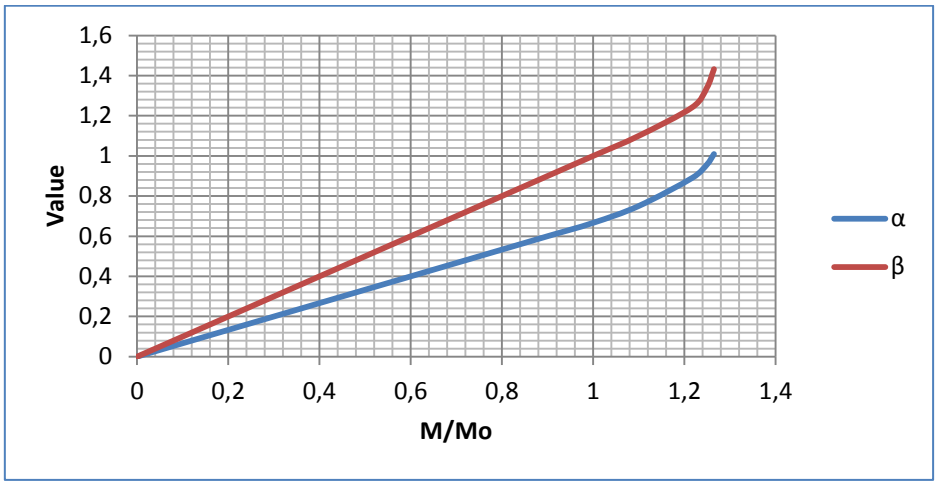

Figure 3-9 Moment to deflection coefficients relationship

3.3. Pullheads effect on pipeline's bending

In this paper the pullhead is considered as part of the riser with infinitive bending stiffness. So the pullhead by itself will not have any deflection and rotation, in practice the pullhead is solid pipe without any hole or thicker wall, so the assumption about the stiffness of the pullhead should be reasonable.

Illustration of the pullhead shown in the Figure 3-10, the pullhead is shown in blue color and has length L_{ph}, the distance L is the distance between touch points.

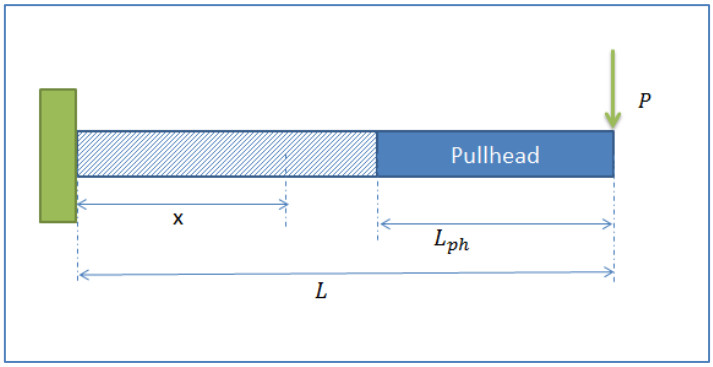

Figure 3-10 Pullhead

In order to find rotation of the pipe with pullhead the equation (9) can be used for rotation but rotation of the pullhead (bending of pullhead) will not be taken into account. So the equation (9) will take next form.

$$\theta = \frac{2\varepsilon_0}{d_m}\int_0^{L-L_{ph}}\left(\frac{\tilde{\varepsilon}}{\varepsilon_0}\right)dx = \frac{2\varepsilon_0}{d_m}\frac{L}{\bar{M}}\left(\int_{\bar{M}L_{ph}/L}^{\bar{M}}\left(\frac{M}{M_0}+A\left(\frac{M}{M_0}\right)^B\right)dM\right)$$

Formulation for the rotation obtained by solving integration above and it has following form:

$$\theta = \frac{\varepsilon_0 L}{d_m}\left(\frac{\bar{M}}{M_0}\left(1-\left(\frac{L_{ph}}{L}\right)^2\right)+\frac{2A}{B+1}\left(1-\left(\frac{L_{ph}}{L}\right)^{B+1}\right)\left(\frac{\bar{M}}{M_0}\right)^B\right)$$

The equation of rotation with pullhead can be rewritten in terms of coefficient of rotation as it was done in the previous chapter.

$$\theta = \frac{L\varepsilon_0}{d_m}\beta_{ph}\left(\frac{M}{M_0}\right)$$

Whereas the coefficient of rotation takes next form:

$$\beta_{ph}\left(\frac{M}{M_0}\right)=\left(\frac{\bar{M}}{M_0}\left(1-\left(\frac{L_{ph}}{L}\right)^2\right)+\frac{2A}{B+1}\left(1-\left(\frac{L_{ph}}{L}\right)^{B+1}\right)\left(\frac{\bar{M}}{M_0}\right)^B\right)$$

The formulation above shows that rotation of the riser is depend on the induced moment and pullhead's length. The graphical form of this relationship is given in the Figure 3-11. Rotation will increase by increasing moment on fixed end and will decrease for increase of pullhead length.

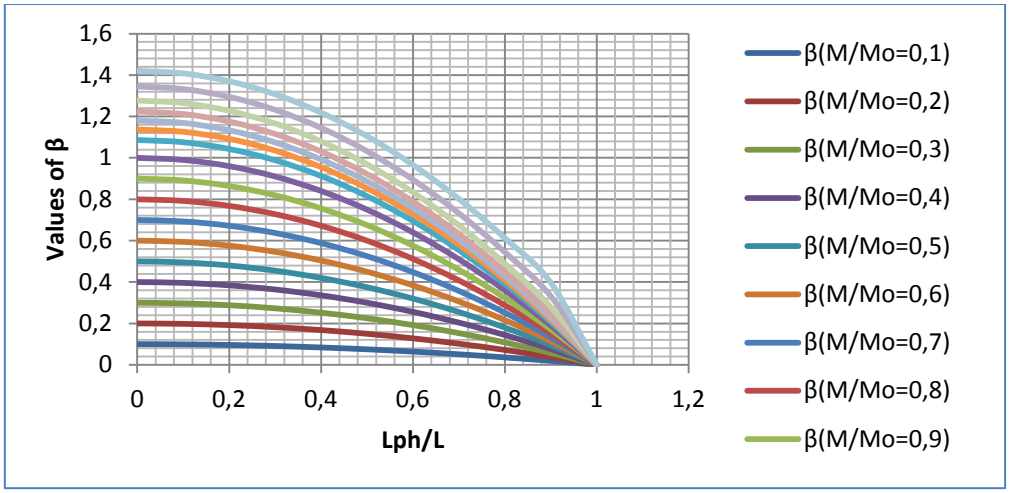

Figure 3-11 Coefficient of rotation's relationship from pullhead length

It is obvious that pullhead will decrease the deflection of the total riser due to its stiffness, and in the Figure 3-12 illustrated bending of the riser with and without pullhead. Differences in deflection for the risers with and without pullhead are equal to deflection of the part of the riser with length equal to the pullhead length and with pipeline's stiffness.

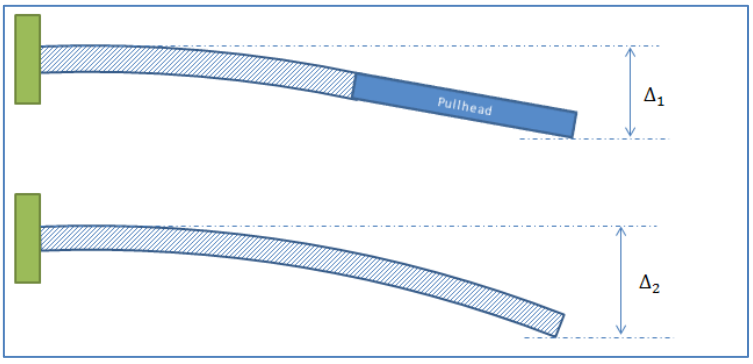

Figure 3-12 Riser deflections with and without pullhead

The equation below is based on the statement given above and valid given that pullhead will not deflect at all (infinitely stiff).

$$\Delta_2 - \Delta_1 = \frac{{L_{ph}}^2 \varepsilon_0}{d_m} \alpha\left(\frac{M(L_{ph}/L)}{M_0}\right)$$

By substituting equations (16) to the equation above, the following equation can be taken:

$$\frac{L^2 \varepsilon_0}{d_m} \alpha\left(\frac{M}{M_0}\right) - \frac{L^2 \varepsilon_0}{d_m} \alpha_{ph}\left(\frac{M}{M_0}\right) = \frac{{L_{ph}}^2 \varepsilon_0}{d_m} \alpha\left(\frac{M(L_{ph}/L)}{M_0}\right)$$

Coefficient of deflection for the riser with pullhead can be found by solving equation above, and takes following form:

$$\alpha_{ph}\left(\frac{M}{M_0}\right) = \alpha\left(\frac{M}{M_0}\right) - \frac{{L_{ph}}^2}{L^2} \alpha\left(\frac{M(L_{ph}/L)}{M_0}\right) \quad (17)$$

As in case of the coefficient of rotation with pullhead effect, the coefficient of deflection with pullhead effect also depends on moment on fixed end of the riser and length of the pullhead. The graphical form of this relationship is shown in the Figure 3-13. It is clearly seen from the graph that increase of pullhead length will decrease the deflection and increase of moment on fixed end will led to increase of deflection.

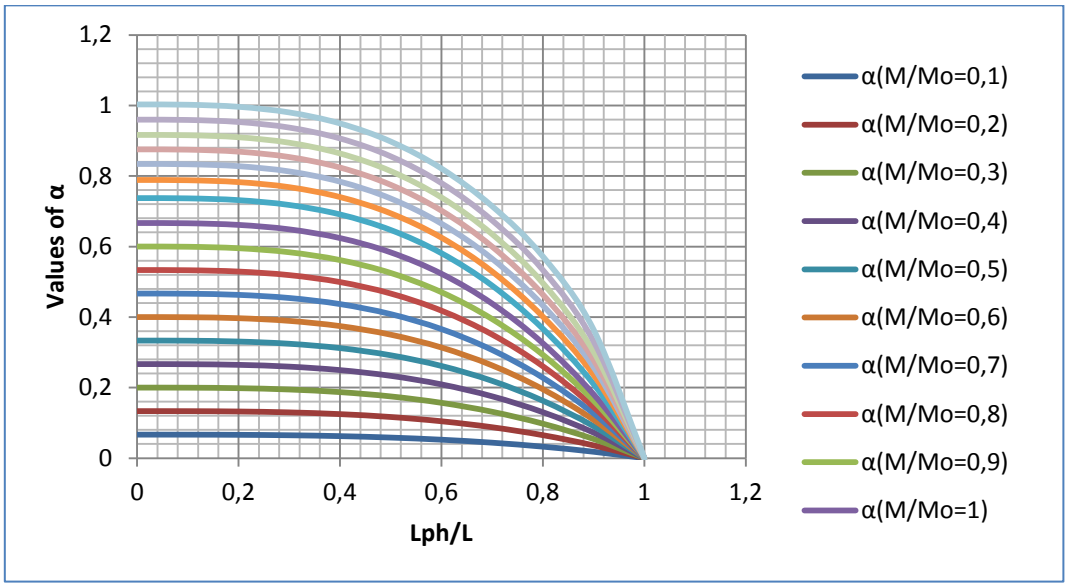

Figure 3-13 Coefficient of deflection relationship to pullhead length

In the Figure 3-14 relationship between moment and deflections is shown. The relationship on the graph is linear when moment on the fixed end is less than plasticity moment and has nonlinear relationship with deflection rate is much higher than moment rate otherwise. Again by comparing Figure 3-14 with Figure 3-9 it can be seen that riser with pullhead has lower coefficient of deflection rather than riser without pullhead.

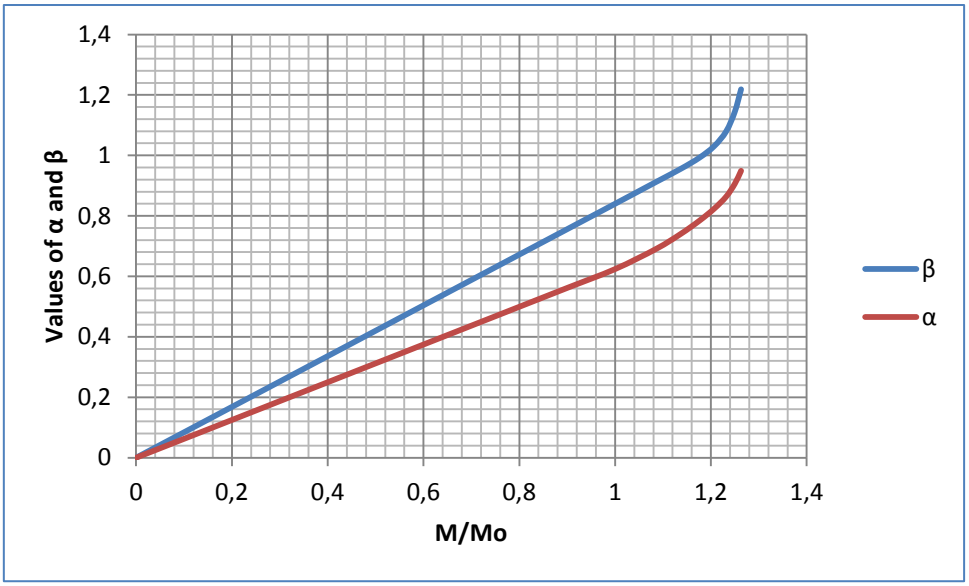

Figure 3-14 Deflection coefficient to moment relationship

3.4. Coefficient of friction between pullhead and J-tube.

From elementary physics it is known that friction force obey to Coulomb and Amontons' friction law (Kazimi, 2006). Whereas friction force is proportional to reaction force from the surface and coefficient friction does not depend from the reaction force. But in practice a high reaction force to small contact area can cause to scratching or digging into surface, which will increase the coefficient of friction. In the Figure 3-15 is shown scratching effect on surface. Improper pullhead design and high reaction force between pullhead and J-tube's inner side can result in scratching and respectively increases of coefficient of friction.

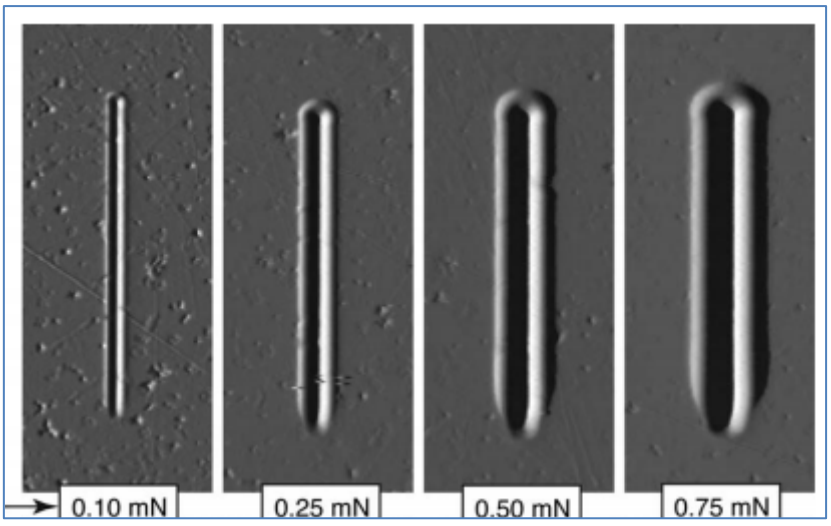

Figure 3-15 Scratching of PMMA with different reaction force **(Shane E. Flores, 2008)**

The following analytical approach for determining coefficient of friction was suggested by Shane E (2008). Whereas coefficient of friction depends on a normal coefficient of friction when digging does not occur and from the reaction force, which induce yielding of subjected material.

$$\mu_{new} = \mu + k_1(1 + \mu \cdot k_2)\sqrt{\frac{F_N}{{R_N}^2 \sigma_y}}$$

Whereas coefficients $k_1 = 0.184$ and $k_2 = 1.75$.

In the Figure 3-16 is shown how coefficient of friction increases by increasing normal force and by reducing contact area.

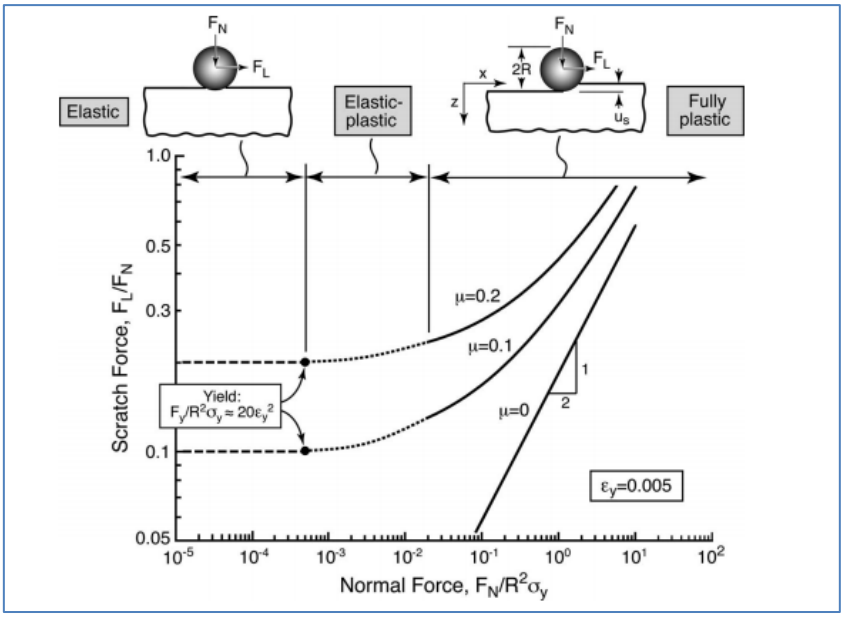

Figure 3-16 Illustration of increase of CoF from reaction force **(Shane E. Flores, 2008)**

In the Figure 3-17 the note μ=10 stands for coefficient of friction when radius shape of interacting object is equal to 10 mm, and notes μ=20, μ=30 when interacting object has edge radius 20 and 30 mm respectively. The Figure 3-17 shows how increase in interacting object's radius leads to decrease in coefficient of friction.

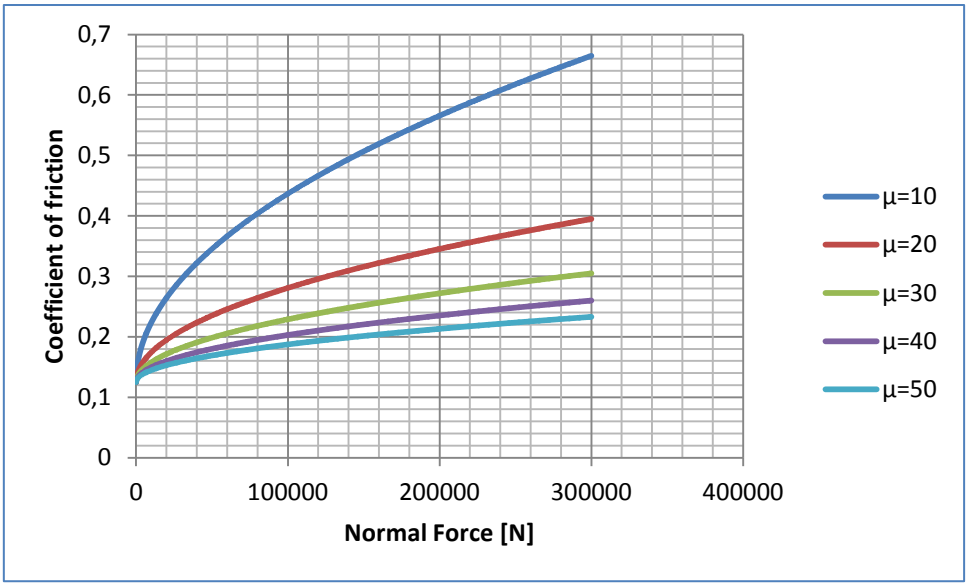

Figure 3-17 Coefficient of Friction to Normal force relationship

3.5. Moment to ovality relationship

In the Figure 3-18 illustrated pipe's moment to curvature relationship. During pipe bending, pipe's ovality will increase and it may local buckling. Ovalization of pipe happens due to increase in curvature and it has unique relationship for individual pipe, depending on material and geometrical properties of pipe (Jirsa .J.O, 1972).

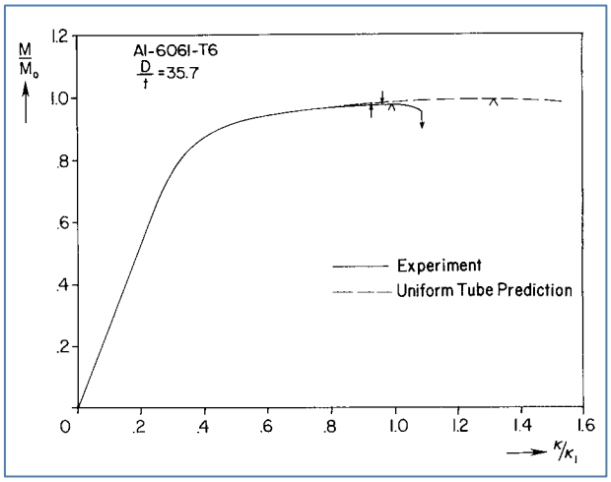

Figure 3-18 Pipe's moment to curvature relationship with ovalization effect **(Stelios K, 2007)**

Ovalization will cause decrease of dimensions of pipe in one direction, and consequently decrease of dimensions will cause to decrease of arm of moment (Mousselli, 1979).

In DNV-OS-F 101 the following formulation is suggested for finding ovality of pipe:

$$f_o = \frac{d_{max} - d_{min}}{d}$$

Then formulation for bending moment will be reduced due to reduction of force arm, and equation to determine moment of bending can be modified into following form:

$$M_{oval} = \int \sigma \left(\frac{d_{min}}{d}\right) y dA = \frac{d_{min}}{d} \int \sigma y dA = \frac{d_{min}}{d} M$$

$$M_{oval} = \frac{d_{min}}{d} M = \frac{d - \frac{d_{max} - d_{min}}{2}}{d} M = \left(1 - \frac{f_o}{2}\right) M$$

The equation above shows how increase in ovality will decrease the moment of bending, this relationship valid only for small ovalization, because when increase in ovality will result in pipe's cross section will not possess elliptical shape.

The ovality of the bended pipeline can be calculated by the formula suggested on DNV-OS-F101.

$$\acute{f}_o = \frac{f_o + \left[0.030\left(1 + \frac{d}{120t}\right)\left(2\varepsilon_c \frac{d}{t}\right)^2\right]}{1 - \frac{p_e}{p_c}}$$

The parameters on the equation above will be explained in detail in the chapter 3.8.

3.6. Effect of the axial force on bending moment

Axial force will reduce bending moment of the pipe due to initial axial strain. In the Figure 3-19 is shown the stress distribution in pipe's cross section. Stress strain relationship in this figure can be approximated as ideally plastic deformation. Søren Hauch and Young Bai,2000 developed formula of moment of bending for the case of axial force and ideally plastic bending.

$$M = \sigma_0 d_m^2 t \cdot \sin(\varphi)$$

Whereas φ is angle of compression part, but in reality it is not always possible to have ideal plastic bending and the bending of pipe is not always perfectly plastic.

In order to obtain real moment of bending for the elastic-plastic bending case, tool has been developed in Excel. Tool consists integration model for both bending moments, with and without of axial effect.

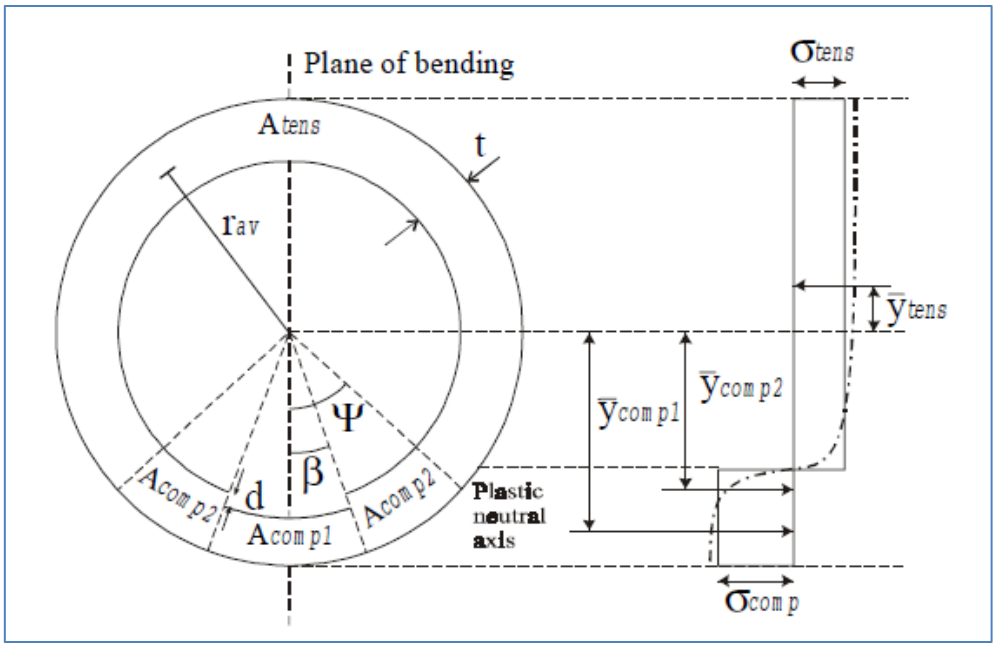

Figure 3-19 stress distribution in pipe's cross section **(Hauch Søren, 2000)**

Material type on the tool was assumed to be elastic perfectly plastic because it is more closely simulates reality. The maximum strain due to bending can be calculated from the J-tube's and pipe's dimension and the maximum strain due to axial force can be calculated by knowing magnitude of axial tension force and cross section area of the pipe. Maximum axial tension supposed to be on the vertical part of pipe bend inside J-tube, because it is leading edge of pipe and has higher axial force than elsewhere. Ratio of moments due to axial effect and without can be simply calculated by the following way:

$$\frac{M_a}{M} = \frac{\sum \sigma(\varepsilon_a + \varepsilon_{bi}) \cdot y_i \cdot dA_i}{\sum \sigma(\varepsilon_{bi}) \cdot y_i \cdot dA_i}$$

Whereas upper part of equation and lower part equation on right hand side shows corresponding moments with and without axial force effect respectively.

In order to increase accuracy in calculation tool the pipe segment was divided into 4000 elements, and analysis was carried regarding to relative strains, in the Figure 3-20 is shown dependence of moment ratio from the ratio of bending strain to yielding strain, and this dependence is shown in different axial strain profile. The minimum ratio for moments can be obtained on point when bending strain is more than yielding strain for around 20%. After overcoming this region the moment ratio will decrease, and will increase by increasing axial strain. In developed calculation tool this ratio will be implemented in order to find more accurate pipe's normal forces to the wall.

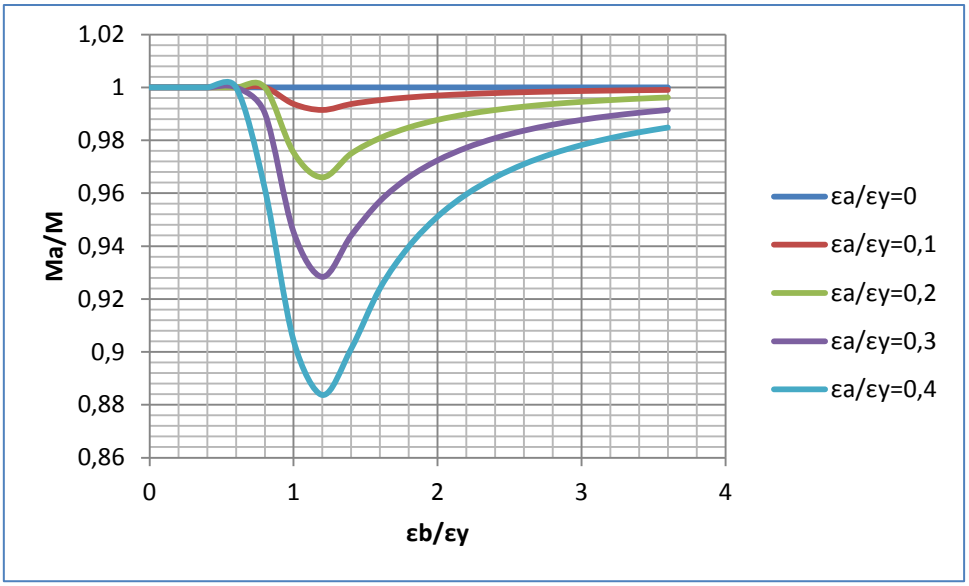

Figure 3-20 Moment ratio to bending strain relationship

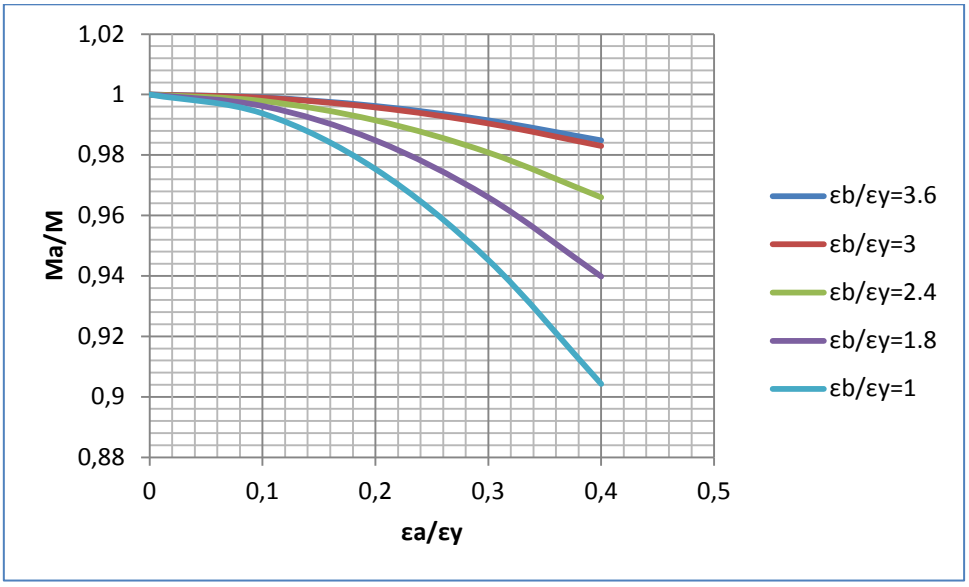

Figure 3-21 Moment ratio to axial strain relationship

The figure above is shown relationship between moment ratio to axial strain, in different bending strain profile. The relationship best fitted to trigonometric relationship which is also described in Søren Hauch and Young Bai's ,2000. paper.

3.7. Pulling mechanics

During developing analytical tool, in order to simplify formulations, whole process of pulling was divided into six individual stages as follow:

- Riser at bellmouth entrance.

- Riser just before J-tube's bended section.
- Riser at J-tube's bended section.
- Riser at J-tube's bended section exit.
- Pullhead touches other side of J-tube due to residual bending.
- Riser at topside level.

All of these stages have been demonstrated on the Figure 3-22 and formulations regarding each stage have been developed and presented in the following chapters.

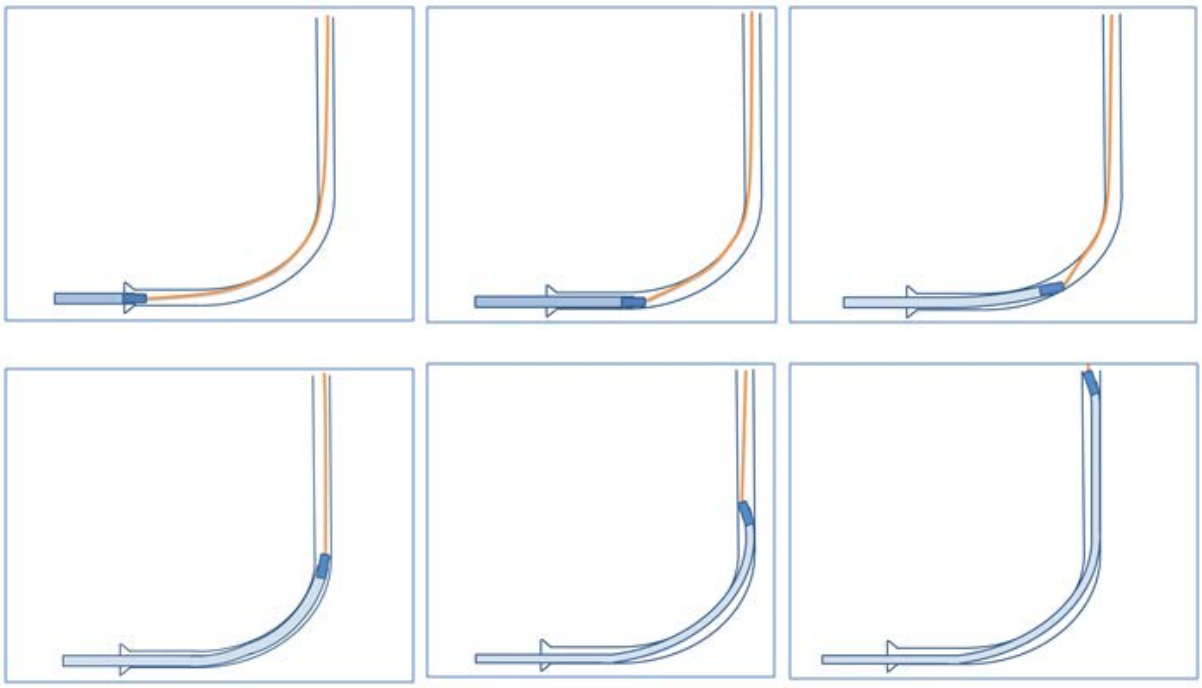

Figure 3-22 J-tube Pull-in Stages

3.7.1 Pipe at bellmouth entrance

When the riser located at the bellmouth entrance, the tension on pulling wire on pullhead will be equal to backtension on riser. The tension force on winch side can be determined by knowing the reaction force between J-tube and pulling wire, and knowing the friction force between them.

On the Figure 3-23 is shown typical illustration of tension forces on pulling wire on both sides of bent part, and incremental section of pulling wire shown in order to demonstrate the reaction and the friction forces between pulling wire.

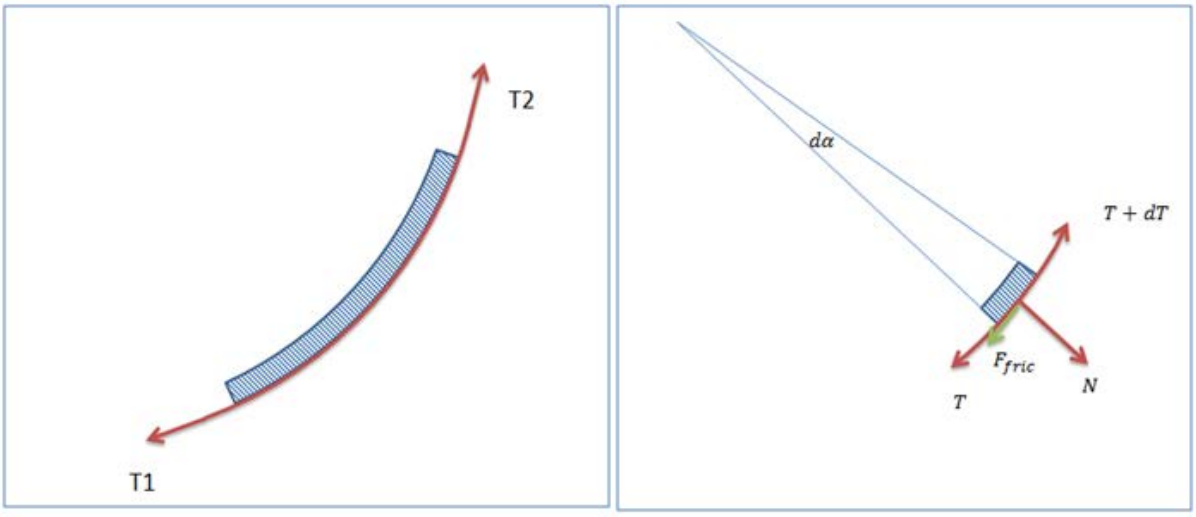

Figure 3-23 Tension forces on Pulling wire

The assumption is done regarding to pulling velocity and the pulling speed will be considered as constant or slightly accelerated, so increase of pulling force due to inertia can be eliminated. Sum of the acting forces on riser and cable can be taken as zero. By applying first law of Newton for motions for incremental part of pulling wire (right-hand side part of Figure 3-23) equation of motion for incremental part of the riser can be written in the following form (Peter Lindenfeld, 2011).

$$\overrightarrow{T + dT} + \vec{T} + \vec{N} + \overrightarrow{F_{fric}} = 0 \qquad (18)$$

By taking projection of the equation (18) in the direction of the normal force $\vec{N}$, the following equation can be obtained:

$$T\frac{d\alpha}{2} + (T + dT)\frac{d\alpha}{2} - N = 0$$

Elimination of terms of tension on the equation above results on finding J-tube to pulling cable reaction force.

$$N = Td\alpha \qquad (19)$$

By taking projection of the equation (18) in direction of $\vec{T}$, the following equation can be obtained:

$$T + dT - T = dT = F_{fric}$$

By substitution of the equation (19) to the equation above, will result in next equation:

$$dT = N\mu = \mu T d\alpha \qquad (20)$$

the differential equation (20) can be solved by integrating both sides of equation. The obtained equation called Capstan equation (Attaway, 1999).

$$\int \frac{dT}{T} = \int \mu d\alpha$$

$$T_2 = T_1 e^{\mu_c(\alpha_2 - \alpha_1)} \quad (21)$$

Whereas last term was obtained by implementing boundary conditions and T_2 stands for tension on upper side of the pulling cable, T_1 – tension on lower side of the pulling cable.

Whereas tension force on lower side of the pulling cable is equal to backtension on pipe at bellmouth:

$$T_1 = T_{back.tension} \quad (22)$$

Finally by substituting equation (21) to the equation (22) general formula for determining Pull-in force in stage-I can be calculated, and it has following form:

$$P_1 = T_2 = T_{back.tension} e^{\mu(\alpha_2 - \alpha_1)} \quad (23)$$

Whereas α_1 and α_2 are angles of inclination of vertical and horizontal part of J-tube from vertical axis. In the Figure 3-24 the angles mentioned above is illustrated on J-tube's profile.

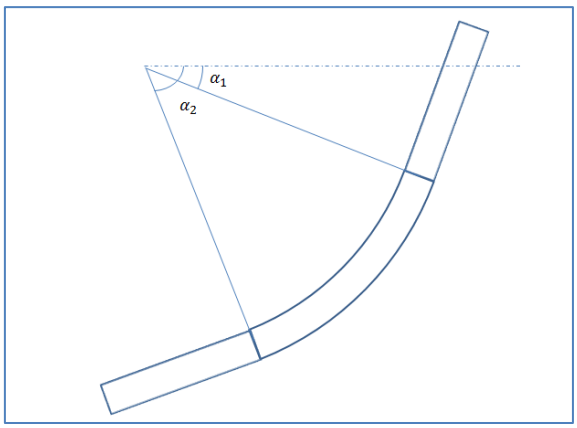

Figure 3-24 J-tube segments inclined angles

The friction force in bent part of J-tube, can be determined by the following way.

$$F_{friction.cable} = T_2 - T_1$$

As it can be seen from the equation (20) the governing factor on pull-in force in first stage is the coefficient of friction between the pulling wire and J-tube's inner wall, and backtension on riser at bellmouth entrance.

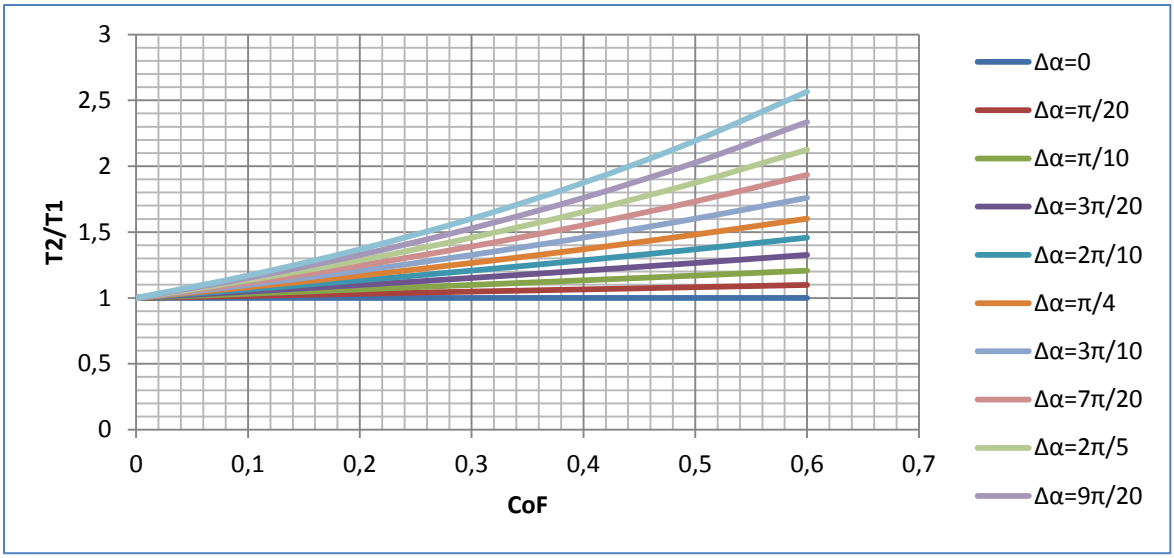

Figure 3-25 Tension difference from angle of bending and CoF

The Figure 3-25 shows the tension ratio from coefficient of friction and from angle of bending, the increase in angle of bending and increase in coefficient of friction causes increase in top tension on winch.

3.7.2 Riser just before curvature entrance

Riser, during sliding on horizontal part of J-tube (Figure 3-22 mid-upper column), it will experience friction force from J-tube's wall. The friction force induced due to riser to J-tube contact forces. The contact forces can vary a lot, but in this paper it was assumed that riser enters the J-tube smoothly that the only weight of the riser will induce reaction force on J-tube's wall. The reaction force on J-tube's wall can be illustrated on the Figure 3-26. From the first Newton's law of motion, the following equation can be obtained:

$$\overrightarrow{F_{fric}} + \vec{N} + \vec{F} + \vec{W} = 0 \qquad (24)$$

By taking projection of the equation (24) in direction of the reaction force $\vec{R}$, equation for the reaction force between J-tube and riser can be obtained and takes form shown below:

$$N = W \cdot \cos(\alpha) \qquad (25)$$

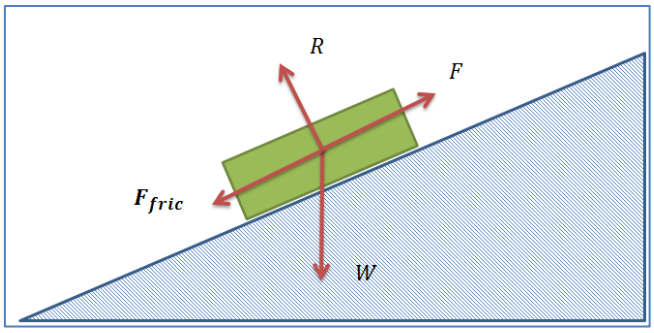

Figure 3-26 Illustration of friction force on simple brick

In this stage of pulling, the top tension force can be calculated in the same manner as it was done in the previous chapter. The only difference is the pulling wire's tension on pullhead side will be equal to sum of the backtension, the friction force between riser and J-tube and weight force if the entrance segment of J-tube deflects from horizontal axis. So equation for the tension on pullhead side is:

$$T_1 = T_{back.tension} + F_{friction.pipe} + W \cdot L_1 \cdot \sin\left(\frac{\pi}{2} - \alpha_2\right)$$

Whereas friction force between pipe and J-tube can be determined by using equation (25) and Coulomb and Amontons' friction law (Kazimi, 2006).

$$F_{friction.pipe} = \mu_p \cdot W \cdot L_1 \cdot \cos\left(\frac{\pi}{2} - \alpha_2\right)$$

So tension force on the top of the cable can be determined from the equation (23), so pulling force on this stage equal to tension on the top of the pulling wire.

$$P_1 = T_2 = \left(T_{back.tension} + \mu_p \cdot W \cdot L_1 \cdot \cos\left(\frac{\pi}{2} - \alpha_2\right) + W \cdot L_1 \cdot \sin\left(\frac{\pi}{2} - \alpha_2\right)\right) e^{\mu_c(\alpha_2 - \alpha_1)} \quad (26)$$

3.7.3 Riser at curvature entrance

In the first two stages the riser was straight by entering the curved part of the J-tube it will undergo bending (Figure 3-22 Right-top column). J-tube's bend radius, the J-tube's inner diameter and the riser's outer diameter will govern the bending characteristics of the riser. In J-tubes with higher bended radiuses the riser can experience purely elastic bending, but usually J-tube's has smaller radius compared to riser's outer diameter and so they will experience elastic-plastic bending. During bending riser experiences series of loads from the

J-tube's wall; like friction force and other contact forces. In order to determine them it is important to know the distance between contact points. The test has shown that the distances between contact points are remaining constant during pulling operation (Tan H, 1981). This observation gives good basis for pruning down the formulations in analysis. The developed formulations shows that this contact points mainly depend on J-tube's and riser's geometry, and mechanical properties of J-tube. In the paper it was assumed that friction force on pullhead and riser will obey Coulomb and Amontons' friction law, but there may be cases when pullhead to J-tube interaction has small contact area and high contact force, then the digging process can increase actual friction force. In order to reduce the digging force, increase of contact area is suggested by designing pullhead with proper geometry. So, when pipe enters the J-tube's curved section it will undergo high tension force due to the higher friction force, pullhead length and possible digging force.

The distance between contact forces can be obtained by using beam theory for elastic-plastic bending, whereas pipe segment is considered as a cantilever beam. In the chapters 3.1, 3.2 and 3.3 formulation for the effect of bending of beam in elastic-plastic region was developed by taking into account Ramberg-Osgood stress-strain material relationship.

Bending characteristics of the riser allows finding distance between touch points of riser inside the J-tube. Deflection of the riser or beam Δ is illustrated in the Figure 3-27, whereas L is distance between second and third touch points (touch points on the bottom and with mid of the J-tube), and φ angle of rotation.

In the Figure 3-27 is illustrated the deflection of the riser inside J-tube, and it is clearly seen that the deflection can be found by the equation below:

$$\Delta = L\phi - \frac{R+D}{2}\phi^2 - (D-d) \tag{27}$$

Whereas L is distance between touch points on the bottom of J-tube and the expression $\frac{R+D}{2}\phi^2$ comes from deflection of the riser in vertical axis.

The vertical deflection is calculated by the following equation:

$$(R+D) - (R+D)\cos(\phi) = (R+D)(1-\cos(\phi))$$

The cosine functions of the equation above can be replaced by sine functions:

$$(R+D)\left(1-\sqrt{1-sin^2(\phi)}\right) = (R+D)(1-(1-sin^2(\phi))^{1/2})$$

By using special limits for the equation above, the sin functions can be approximated as:

$$(R+D)(1-(1-sin^2(\phi))^{1/2}) \approx (R+D)(1-(1-\phi^2)^{1/2})$$

$$(R+D)\left(1-(1-\phi^2)^{\frac{1}{2}}\right) \approx (R+D)\left(1-\left(1-\left(\frac{1}{2}\right)\phi^2\right)\right) = \frac{R+D}{2}\phi^2$$

The final expression shows the deflection in vertical axis.

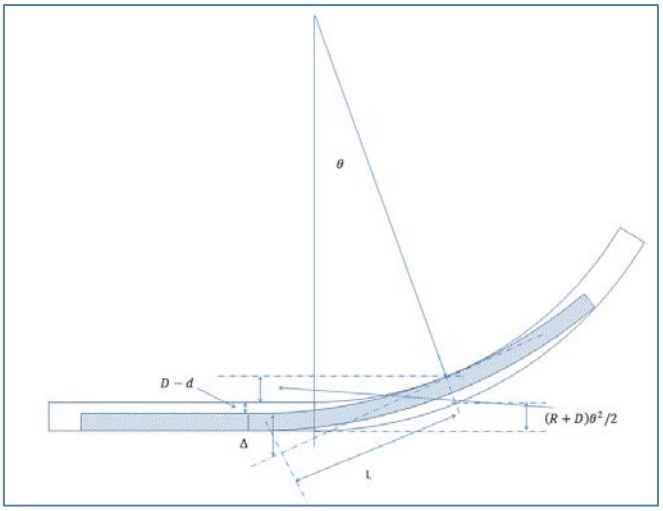

Figure 3-27 Distance between touch points

Substitution of the equation (16) to the equation (27) gives the follwing equation:

$$\frac{L^2\varepsilon_0}{d_m}\alpha\left(\frac{M}{M_0}\right) = L\frac{L\varepsilon_0}{d_m}\beta\left(\frac{M}{M_0}\right) - \frac{R+D}{2}\left(\frac{L\varepsilon_0}{d_m}\beta\left(\frac{M}{M_0}\right)\right)^2 - (D-d)$$

The equation above can be separated in terms of L and solved. Then formulation for determining distance L between touchpoints is:

$$L = \sqrt{\frac{d-D}{\frac{\varepsilon_0}{d_m}\alpha\left(\frac{M}{M_0}\right) - \frac{\varepsilon_0}{d_m}\beta\left(\frac{M}{M_0}\right) + \frac{R+D}{2}\left(\frac{\varepsilon_0}{d_m}\beta\left(\frac{M}{M_0}\right)\right)^2}}$$

Dimensionless form of the formulation is obtained by dividing both sides of the equation into pipe's outer diameter, and formulation for it takes following form:

$$\frac{L}{d} = \sqrt{\frac{1-\frac{D}{d}}{\varepsilon_0\alpha\left(\frac{M}{M_0}\right) - \varepsilon_0\beta\left(\frac{M}{M_0}\right) + \frac{\frac{R}{d}+\frac{D}{d}}{2}\left(\varepsilon_0\beta\left(\frac{M}{M_0}\right)\right)^2}}$$

The polypropylene coating will led to reduction of distance between contact points. The effect of polypropylene coating can be considered as the J-tube with smaller inner diameter, and bit higher bending radius. The effect of polypropylene coating will change she equation above into next equation:

$$\frac{L}{d} = \sqrt{\frac{1 - \frac{D - 2t_{pp}}{d}}{\varepsilon_0 \alpha(\frac{M}{M_0}) - \varepsilon_0 \beta(\frac{M}{M_0}) + \frac{\frac{R + t_{pp}}{d} + \frac{D - 2t_{pp}}{d}}{2} \left(\varepsilon_0 \beta(\frac{M}{M_0})\right)^2}}$$

The rotation of the riser (bending angle of the riser) can be calculated from the equation (13), and this is angle of touching of riser to J-tube from vertical. Illustration of the angle θ is shown in the Figure 3-27.

$$\theta = \frac{L\varepsilon_0}{d_m} \beta(\frac{M}{M_0})$$

In the Figure 3-28 is shown the relationship between distance of touch points, internal diameter of the J-tube and radius of bending of the J-tube. The relationship shows that, increase in radius of bending of the J-tube or increase in the internal diameter of the J-tube will led to increase in distance between touch points and this is reasonable.

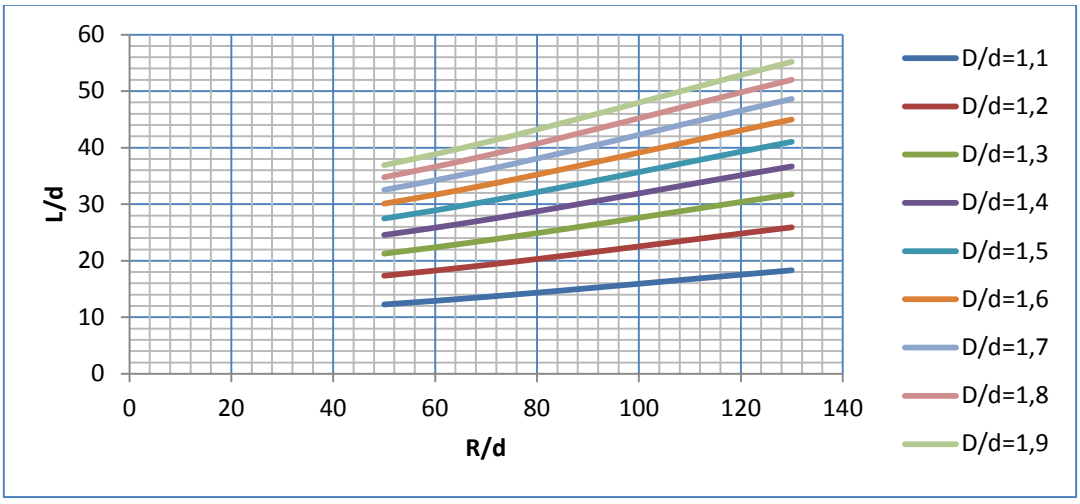

Figure 3-28 Distance between 1st and 2nd contact points

Symbol l_1 was chosen in order to illustrate the distance between second and third touch points (Figure 3-29).

Pifogor's theorem is implemented in order to find distance between touch points l_1 (Figure 3-29).

$$X = l_1^2 - \Delta^2 = (R + D)^2 - (R + d - \Delta)^2$$

The equation above can be rewritten as:

$$l_1^2 - 2(R + d)\Delta = (R + D)^2 - (R + d)^2$$

By substituting equation (16) to equation above, the following equation can be obtained:

$$l_1^2 - \frac{l_1^2 \varepsilon_0}{d_m} \alpha \left(\frac{M}{M_0}\right) \cdot 2(R + d) = (R + D)^2 - (R + d)^2$$

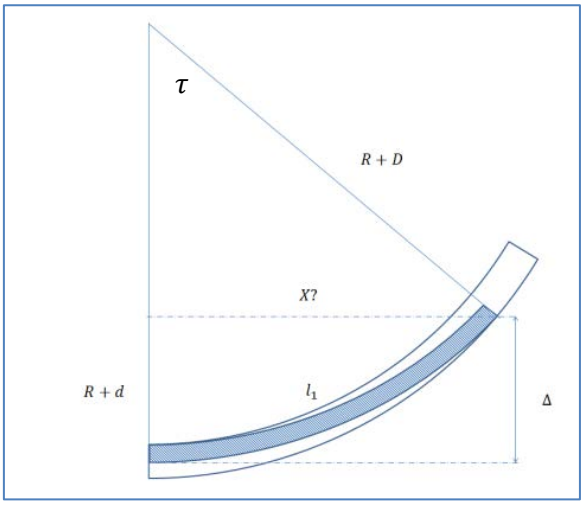

Figure 3-29 Distance from pullhead and touch point

By separating equation above in terms of l_1 and by taking square root of it, the expression for l_1 is obtained:

$$l_1 = \sqrt{\frac{(R + D)^2 - (R + d)^2}{1 - \frac{2\varepsilon_0}{d_m} \alpha \left(\frac{M}{M_0}\right)(R + d)}}$$

The equation in dimensionless form can be rewritten in next form:

$$\frac{l_1}{d} = \sqrt{\frac{\left(\frac{R}{d} + \frac{D}{d}\right)^2 - \left(\frac{R}{d} + 1\right)^2}{1 - 2\varepsilon_0 \alpha \left(\frac{M}{M_0}\right)\left(\frac{R}{d} + 1\right)}} \quad (28)$$

The equation above can be modified for the effect of polypropylene coating in the next form:

$$\frac{l_1}{d} = \sqrt{\frac{\left(\frac{R + t_{pp}}{d} + \frac{D - 2 \cdot t_{pp}}{d}\right)^2 - \left(\frac{R + t_{pp}}{d} + 1\right)^2}{1 - 2\varepsilon_0 \alpha \left(\frac{R + t_{pp}}{d} + 1\right)}}$$

In the Figure 3-30 illustrated the relationship of the distance between touch points from the internal radius of the J-tube and bending radius of the J-tube. The figure shows that increase in radius of bending and increase in inner radius of the J-tube will cause to increase in distance between J-tube.

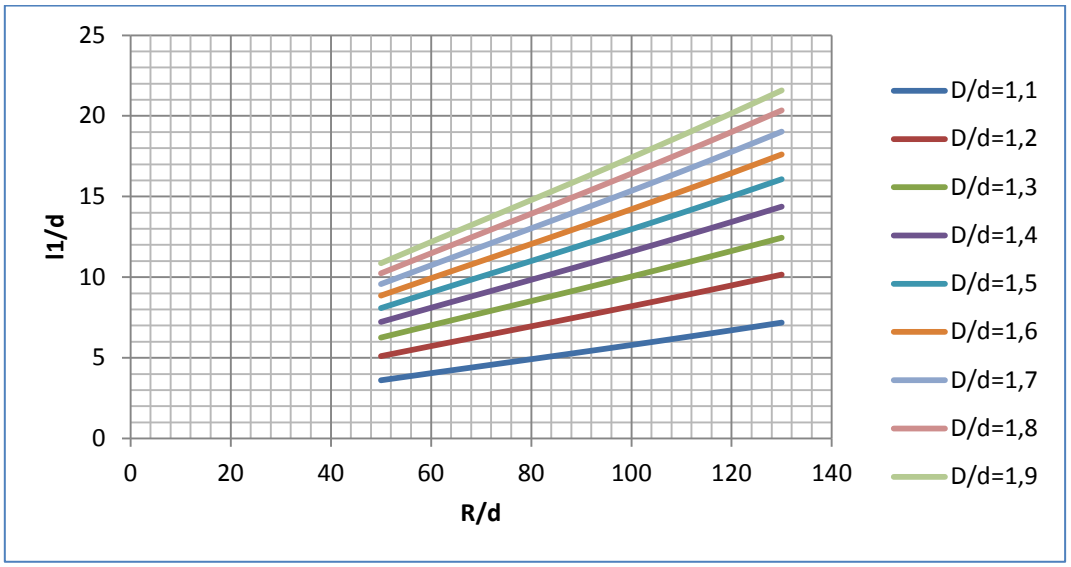

Figure 3-30 Distance between pullhead and touch point

The angle τ between pullhead and riser's touch point (Figure 3-29) can be found from the next equation:

$$\tau = \arcsin\left(\frac{l_1}{R + D - t_{pp}}\right)$$

The angle θo between pullhead and pulling cable's touch point can be found from the next equation:

$$\theta o = \arccos\left(\frac{R}{R + D - t_{pp} - d/2}\right)$$

During bending riser restricts to bend due to its bending stiffness, that is why the pulling effect requires additional force in order to pull it into J-tube, this force exist even all the coefficient of frictions is absolutely zero. The force required to pull-in riser into J-tube can be found form energy conservation law (Arthur P, 2003).

$$Fdx = dU$$

Whereas dU is change of internal energy of the riser during bending and Fdx is work done by pulling force.

Change of internal energy can be written in form of stress and strain (Arthur P, 2003).

$$dU = \varepsilon\sigma dV$$

Whereas incremental volume can be written as $= Sdx$, and the equation for the energy will take next form:

$$Fdx = \varepsilon\sigma Sdx$$

Integration of the both sides of the equation gives general formula for determining pulling force.

$$F = \varepsilon\sigma S = \int \varepsilon\sigma dS$$

By replacing stress and strain with appropriate values for plastic and elastic region (Figure 3-1), and by integration in terms of area will take next form:

$$F = 4\left(\int_0^{\omega} \sigma_0 \frac{\varepsilon_0 \cos(\varphi) d_m t}{2\cos(\omega)} d\varphi + \int_{\omega}^{\frac{\pi}{2}} \frac{\sigma_0 \cos(\varphi)}{\cos(\omega)} \frac{\varepsilon_0 \cos(\varphi) d_m t}{2\cos(\omega)} d\varphi\right)$$

Solution for this integration gives value of pulling force:

$$F = \frac{2\sigma_0 \varepsilon_0 d_m t}{\cos(\omega)}\left(\sin(\omega) + \frac{\frac{\pi}{2} - \omega - \cos(\omega)\sin(\omega)}{2\cos(\omega)}\right)$$

By dividing equation above to the equation (1) will give bending moment to force relationship on the riser.

$$\frac{M}{F} = \frac{d_m \cos(\omega)}{2\varepsilon_0} = R_e \cos(\omega) = \frac{d_m \frac{\varepsilon_0}{\varepsilon}}{2\varepsilon_0} \approx \frac{d}{2\varepsilon} = R$$

The equation for the pulling force shows that force is inversely related to the radius of curvature of the J-tube, and it means riser requires higher force in order to be pulled into sharply bended J-tubes.

J-tube to riser friction force cannot be calculated as in case of pulling wire to J-tube friction force, due to existence of weight of the riser and bending stiffness (causes additional contact forces).

It was assumed that having a bending stiffness will create couple of forces on the wall of J-tube, these additional forces basically cause an increase in friction force. In the Figure 3-34 shown additional contact forces due to pipe's bending stiffness. Due to small distance

between touch points comparatively with radius of bending, it can be assumed these forces acting on counter direction on touch points. So the total friction force will be sum of the friction force caused by this couple of forces on touch points and friction force due to riser to J-tube interaction.

In the Figure 3-31 are shown forces acting on the riser. On the left hand side shown all the forces on incremental part of the riser, and it were assumed that riser is flexible the additional forces due to stiffness was eliminated and determination of the additional friction forces will be discussed bit later in paper. Newton's law of motion for the incremental part of riser is:

$$\vec{N} + \vec{W} + \overrightarrow{T + dT} + \vec{T} + \overrightarrow{F_{fric}} = 0 \qquad (29)$$

By taking projection the equation above, in the direction of the vector $\vec{N}$, the following equation can be obtained:

$$N + WRsin(\alpha) = Td\alpha$$

By separating the term of normal force from other terms, the following equation for determining normal force can be taken:

$$N = (T - WRsin(\alpha))d\alpha$$

By taking projection of the equation (26) in the direction perpendicular to the vector $\vec{N}$, the equation (26) can be rewritten in the next form:

$$T + dT = T + N\mu + WRcos(\alpha)d\alpha$$

By eliminating tension forces in both sides of the equation, the following equation can be obtained:

$$dT = N\mu + WRcos(\alpha)d\alpha$$

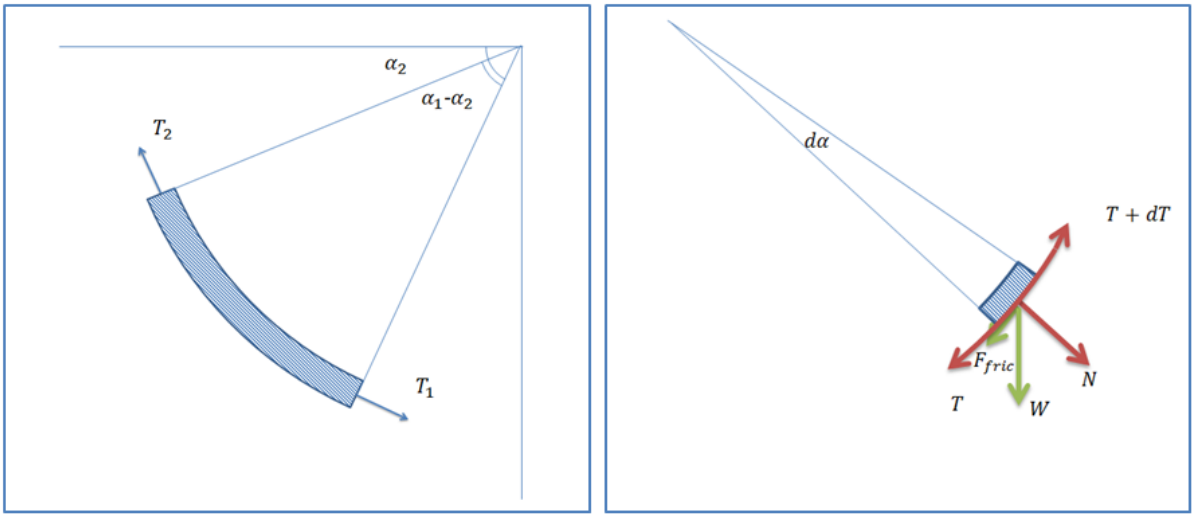

Figure 3-31 Forces on flexible riser

By substituting of the equation for the normal force to the equation above, gives next differential equation:

$$dT = \mu\big(T - WRsin(\alpha)\big)d\alpha + WRcos(\alpha)d\alpha$$

Solution of this differential equation will take following form:

$$T_2 = T_1 e^{-\mu_p(\beta_2-\beta_1)} - WR\big(\sin(\beta_2) - \sin(\beta_1)e^{-\mu(\beta_2-\beta_1)}\big) \quad (30)$$

Whereas β_1 is angle between lower touch point and horizontal axis, and can be expressed as:

$$\beta_1 = \alpha_2 - \theta$$

And $\beta_2$is angle between upper touch point and horizontal axis, and can expressed as:

$$\beta_2 = \varphi + \tau$$

The graphs in the Figure 3-32 and in the Figure 3-33 show the relationship of the top-tension on riser from the weight and from the angle of contact respectively. The increase of the angle of contact and increase of submerged weight of the riser is led to increase in top-tension on the riser.

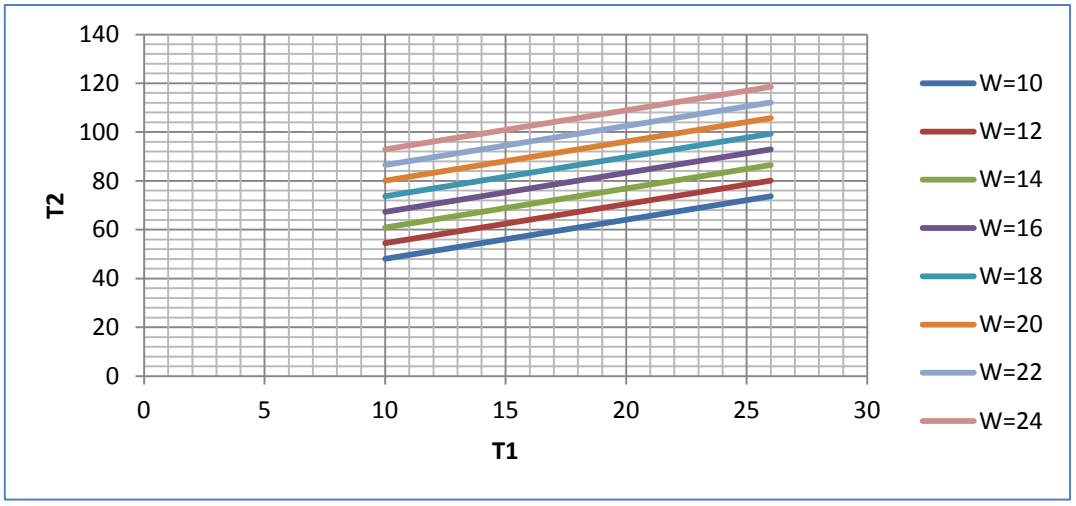

Figure 3-32 Tension to weight relationship

Tension on the lower part of riser can be found by the equation below:

$$T_1 = T_{back.tension} + F_{friction.pipe} + W \cdot L_1 \cdot \sin\left(\frac{\pi}{2} - \alpha_2\right)$$

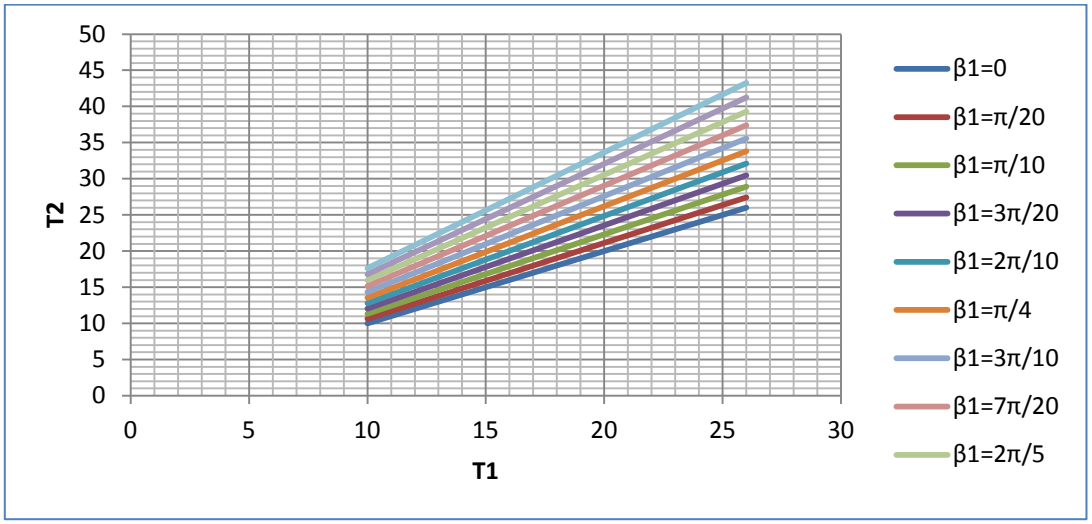

Figure 3-33 Tension to angle relationship

As it was mentioned before, bending stiffness will create couples of contact forces on the J-tube's wall. This contact forces can be found by knowing moment in touch point of the riser and distance between touch points. In the Figure 3-34 shown these contact forces and friction forces due to contact forces. The formulation for these contact forces is:

$$F_1 = M\frac{1}{L} \text{ and } F_2 = M\frac{1}{l_1}$$

Consequently friction forces

$$F_{fric1} = \mu_p M \frac{1}{L}$$

$$F_{fric.ph.2} = \mu_{ph} N_o = \mu_{ph} F_2$$

$$F_{fric2} = \mu_p N_o = \mu_p F_2$$

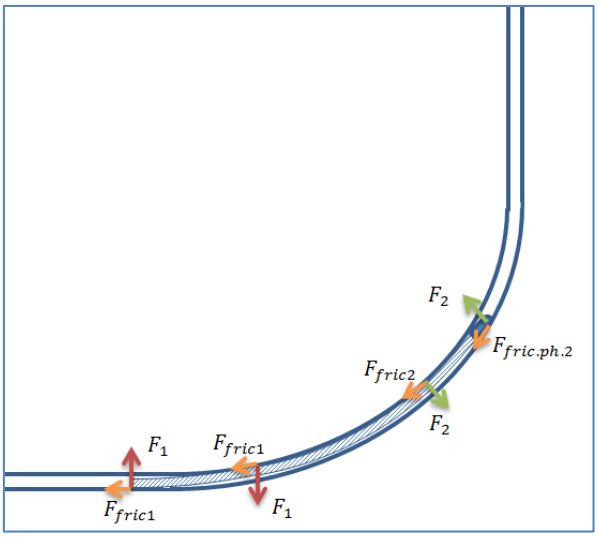

Figure 3-34 Forces acting on riser inside J-tube

It need to be noted that contact forces shown in the Figure 3-34 is for the case when no other force acts on riser, but when there are other forces acting on the riser like: tension force of pulling cable and backtension the reaction forces will have reduced values.

The total force for pulling will be sum of the friction forces on the pullhead of the riser and friction force on the body of riser and force required to pull-in the riser:

$$T_3 = \frac{M}{R} + \mu_{ph} N_o + \mu_p N_o + T_2 \quad (31)$$

Whereas T_2 can be obtained from the equation (30).

As in equation (21), the toptension in the upper part of pulling wire can be calculated as:

$$P_3 = T_3 e^{\mu(\gamma_2 - \gamma_1)}$$

γ_2 is angle between lower touch point of pulling wire with J-tube and horizontal axis:

$$\gamma_2 = \varphi - \theta o$$

φ is angle between touch point of pullhead and horizontal axis

$\gamma_1$is angle between upper touch point of pulling wire and horizontal axis:

$$\gamma_1 = \alpha_1$$

In order to find contact force between J-tube and pullhead, the magnitude of acting forces need to be known. Figure 3-35 shows forces acting on pullhead. By knowing the moment of bending in the fixed end of riser, the reaction force on pullhead's edge can be obtained.

The equation for moment of forces in fixed end is:

$$M = l_1\left(N_o\cos(\tau) + T_3\sin(\tau+\theta_o) - N_o\mu_{ph}\sin(\tau)\right)$$

By solving equation above, equation for determining normal force on the pullhead can be obtained:

$$N_o = \frac{\left(\frac{M}{l_1} - T_3\sin(\tau+\theta_o)\right)}{\cos(\tau) - \mu_{ph}\sin(\tau)}$$

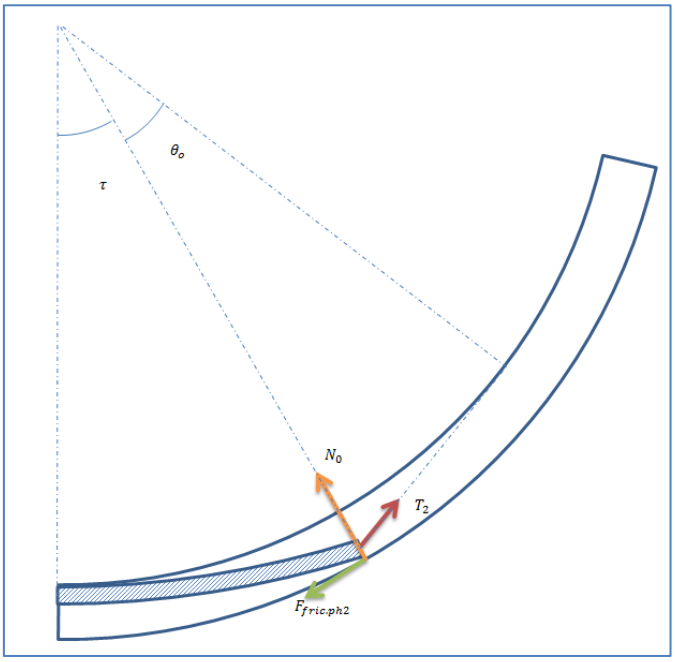

Figure 3-35 Forces acting on pullhead

The substitution of the last equation to the equation (31), gives following equation:

$$T_3 = \frac{M}{R} + \left(\mu_{ph} + \mu_p\right)\frac{\left(\frac{M}{l_1} - T_3\sin(\tau+\theta_o)\right)}{\cos(\tau) - \mu_{ph}\sin(\tau)} + T_2$$

By separating equation in terms of T_3, the final equation for pulling force on pullhead side can be obtained:

$$T_3 = \frac{\frac{M}{R} + (\mu_{ph} + \mu_p)\frac{\left(\frac{M}{l_1}\right)}{\cos(\tau) - \mu_{ph}\sin(\tau)} + T_2}{1 + (\mu_{ph} + \mu_p)\frac{\sin(\tau + \theta_o)}{\cos(\tau) - \mu_{ph}\sin(\tau)}}$$

The formulation for determining pulling force on winch for this pulling stage is determined from Capstan equation and takes following form:

$$P_3 = \left(\frac{\frac{M}{R} + (\mu_{ph} + \mu_p)\frac{\left(\frac{M}{l_1}\right)}{\cos(\tau) - \mu_{ph}\sin(\tau)} + T_2}{1 + (\mu_{ph} + \mu_p)\frac{\sin(\tau + \theta_o)}{\cos(\tau) - \mu_{ph}\sin(\tau)}} \right) e^{\mu(\gamma_2 - \gamma_1)}$$

3.7.4 Pipe at curvature exit

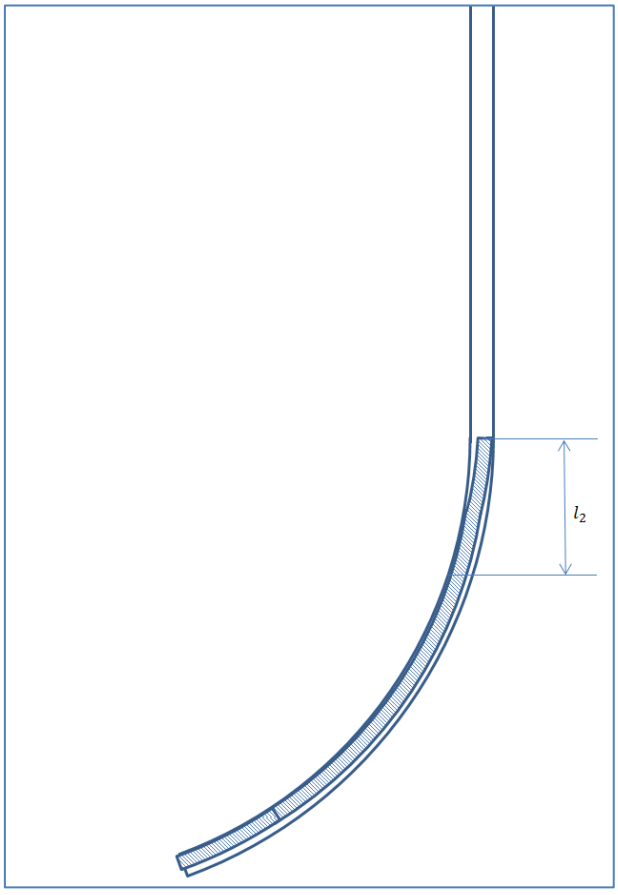

Figure 3-36 Pipeline at curvature exit

Distance between contacts points l_2 can be found by the way suggested A.C Walker (1983)

$$\frac{l_2}{d} = \left[\frac{2C_1(D/d - 1)}{(2 - C_1/C_2) - (R/d + D/d)/C_1} \right]^{1/2} \quad (32)$$

Whereas:

$$C_1 = (d/R - \sigma_0/E)^{-1} \text{ and } C_2 = (d/R - 2\sigma_0/3E)^{-1}$$

By taking into account effect of PP coating, the equation above can be modified into following equation:

$$\frac{l_2}{d} = \left[\frac{2C_{1pp}\left((D - 2t_{pp})/d - 1\right)}{\left(2 - C_{1pp}/C_{2pp}\right) - \left((R + t_{pp})/d + (D - 2t_{pp})/d\right)/C_{1pp}}\right]^{1/2}$$

Respectively

$$C_{1pp} = (d/(R + t_{pp}) - \sigma_0/E)^{-1} \text{ and } C_{2pp} = (d/(R + t_{pp}) - 2\sigma_0/3E)^{-1}$$

In the Figure 3-37 graphical form of the equation (32) is given. The graph shows that distance between touch points will increase if the inner diameter of J-tube increases, and it is clearly seen that distance between touch points has bath shape graph, which is mean some radius of curvature of the J-tube will represent for the minimum distance between touch points. The reason for that is: higher radius of bending gives higher distance between touch points, but increase of distance when the radius of bending decreases can be explained due to residual curvature of pipe, the riser after passing J-tube with lower radius of bending will inherent low residual radius of curvature which led to increase of distance between contact points.

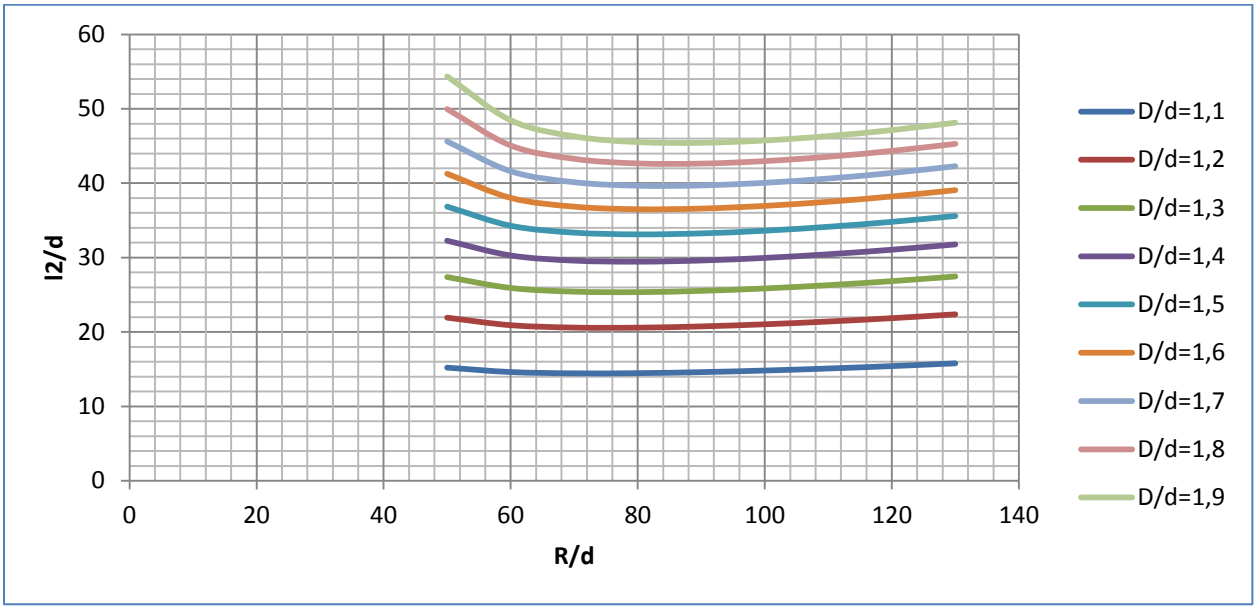

Figure 3-37 Distance between 2nd and 3rd touch points

The total pulling force for this stage of pulling can be sum of the bending force, friction force from pullhead, friction force from the riser and Capstan force due to riser to J-tube interaction, and equation takes following form:

$$P_4 = \frac{M}{R} + \mu_{ph}(M - P_4(D-d))\frac{1}{l_2} + \mu_p(M - P_4(D-d))\frac{1}{l_2} + T_2$$

By separating equation in terms of P_4 into one side, the following equation for determingin pulling force in stage-IV, can be obtained:

$$P_4 = \frac{\frac{M}{R} + \mu_{ph}M\frac{1}{l_2} + \mu_p M\frac{1}{l_2} + T_2}{1 + \frac{(\mu_{ph}+\mu_p)(D-d)}{l_2}}$$

By including effect of coating for the equation above, the equation can be modified into following form:

$$P_4 = \frac{\frac{M}{R} + \mu_{ph}M\frac{1}{l_2} + \mu_p M\frac{1}{l_2} + T_2}{1 + \frac{(\mu_{ph}+\mu_p)(D-2t_{pp}-d)}{l_2}}$$

Whereas T_2 can be found from equation (20)

It should be noted that, the angles β_1 and β_2 will be equal to angles α_2 and α_1 respectively for the reason while pullhead is on curvature exit, the whole bended section of J-tube will have contact with riser.

During pulling operation, because of residual curvature on the riser, the pullhead will experience the contactless time with J-tube. In this case the riser will be supported only by its pipeline site to the wall and that is why friction effect of pullhead can be eliminated and the equation for pulling force will become:

$$P_4 = \frac{\frac{M}{R_p} + 2\mu_p M\frac{1}{l_2} + T_2}{1 + \frac{2\mu_p(D-d)}{l_2}}$$

Including effect of PP coating the formulation above will take next form:

$$P_4 = \frac{\frac{M}{R_p} + 2\mu_p M\frac{1}{l_2} + T_2}{1 + \frac{2\mu_p(D-2t_{pp}-d)}{l_2}}$$

Whereas R_p residual radius, or plasticity radius.

The bending radius of the pipeline can be written in the form of plasticity and elasticity radiuses (Mikael W.B, 2005):

$$\frac{1}{R} = \frac{1}{R_p} + \frac{1}{R_e}$$

The radius of elasticity can be found from the equation (3) and the equation above will take next form:

$$\frac{1}{R} = \frac{1}{R_p} + \frac{2\sigma_o}{d \cdot E}$$

Then the plasticity radius can be expressed in following way:

$$R_p = \frac{d}{\frac{d}{R} - \frac{2\sigma_o}{E}}$$

3.7.5 Pullhead touches the other side of J tube.

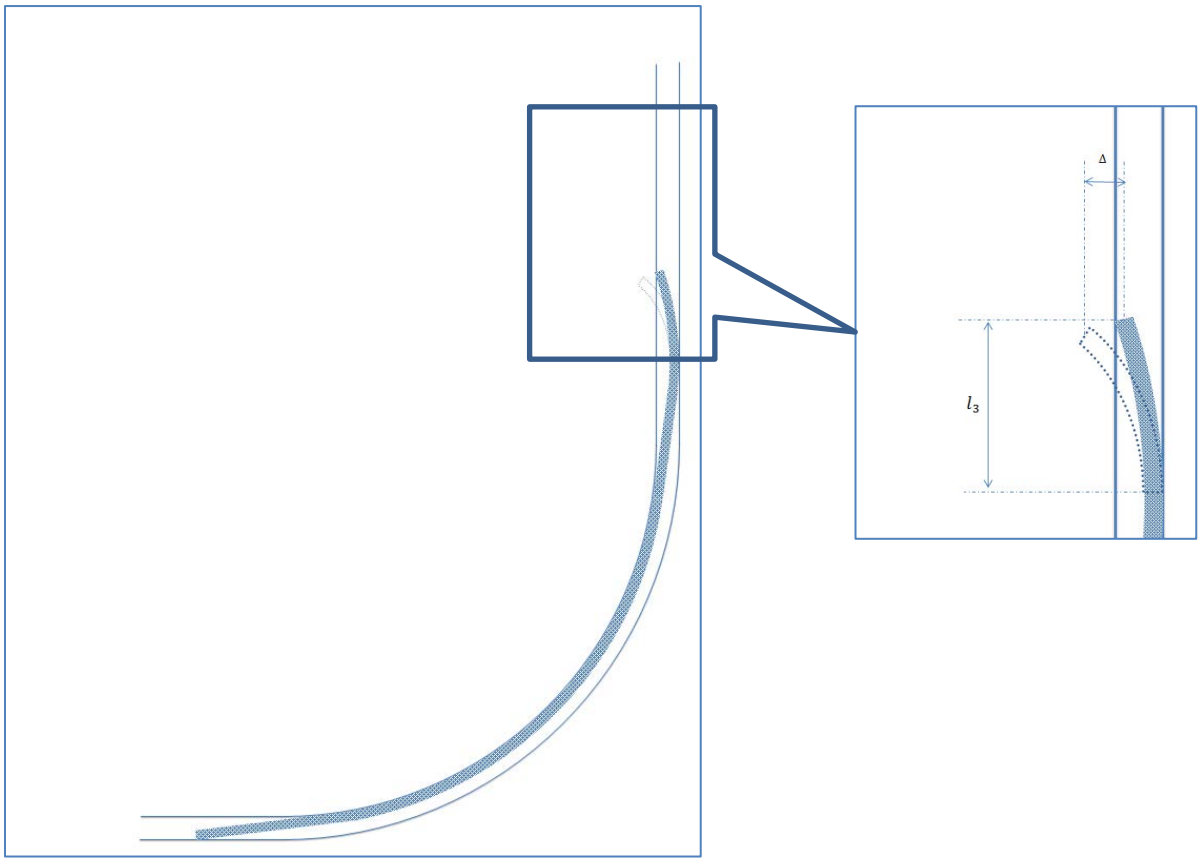

Figure 3-38 Pullhead touches other side of the J-tube

Figure 3-38 illustrated how the riser will have a contact with other side of J-tube's wall due to its residual curvature. Second touch in the wall will also have contact force between wall and pullhead. The contact force will cause additional friction force on the wall. Magnitude of the contact force is influenced by the distance of the touch points and, by the moment on the touch point. Deflection of the riser is important in order to find distance between touch points. The deflection can be found by using simple geometry formulations and can be expressed with following formulation.

$$\Delta + D - d - 2t_{pp} = \Delta_{I-part} + \Delta_{II-part} + \Delta_{III-part}$$

Part of the riser between pullhead and touch point can be divided into three parts due to its shape. Not all part of riser will have residual strain. Heading edge of the riser will not have any residual strain, afterwards from some point it starts to have some residual radius of bending, later it will start to increase up to R_p and after continues with this radius of bending. That is why it is prudent to divide riser in to three section as shown below.

- Part where residual bend has radius equal toR_p.
- Part where residual bend has radius equal to R_p on one end and on other does not have any.
- Part where pipe doesn't have any residual bend.

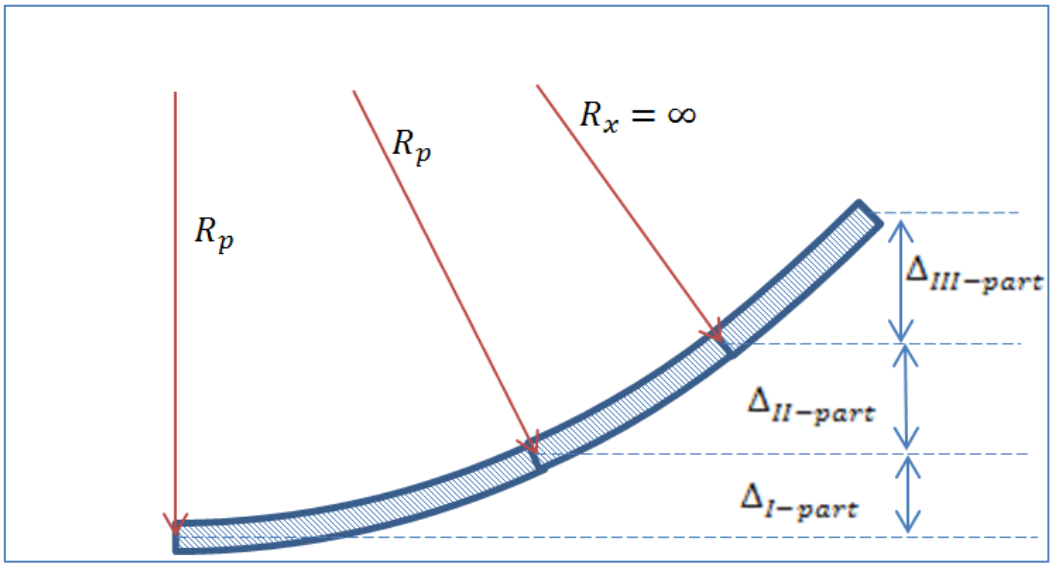

Figure 3-39 Part of the riser with different residual radiuses.

In the Figure 3-39 the different part of the riser with different residual radiuses illustrated.The deflections of each part will be calculated individually. The $l_3$denotes for the length of the

distance between the pullhead edge and touch point. Then equation for deflection for the part which has residual radius R_p can be found in the following way:

$$\Delta_{I-part} = R_p(1-\cos(\varphi)) \approx \frac{(l_3-l_1)^2}{2\cdot R_p}$$

Deflection of the second part which has residual radius R_p in one end and does not have any residual bend on other end is: $l_1 \cdot \left(1-\frac{M_0}{M}\right)$ because when the bending moment on the riser equal to yielding moment, from that point residual strain starts to build up. Deflection in this case despite to previous case will have different character. As long as residual radius decreases slowly it resembles the simple beam with loaded in the end. The formula for edge loaded simple beam $\frac{FL^3}{3EI}$, from the similarities to previous equation where deflection for simple beam is $\frac{ML^2}{2EI}$, the equation for the deflection can be obtained in the following form:

$$\Delta_{II-part} = \frac{l_1^2 \cdot \left(1-\frac{M_0}{M}\right)^2}{3\cdot R_p} + \frac{(l_3-l_1)\cdot l_1 \cdot \left(1-\frac{M_0}{M}\right)}{R_p}$$

It should be noticed that the second part of the equation was generated by taking into account the angle of deflection of the first part of the riser.

Angle of the deflection of the first part of the riser is:

$$\alpha_{I-part} = \frac{(l_3-l_1)}{R_p}$$

The third part of the riser does not have residual radius that is why the deflection generated only by the built up angle in previous two sections:

$$\Delta_{III-part} = \left(\frac{l_3-l_1}{R_p} + \frac{l_1\cdot\left(1-\frac{M_0}{M}\right)}{2R_p}\right)\cdot l_1 \cdot \frac{M_o}{M}$$

Whereas $l_1 \cdot \frac{M_o}{M}$ is length of third part of the riser, and angle of the deflection of the second part of the riser is:

$$\alpha_{II-part} = \frac{l_1\cdot\left(1-\frac{M_0}{M}\right)}{2R_p}$$

The sum of the last three equations will give us equation of total deflection:

$$\Delta + D - d - 2t_{pp}$$

$$= \frac{l_1^2 \cdot \left(1 - \frac{M_0}{M}\right)^2}{3 \cdot R_p} + \frac{(l_3 - l_1) \cdot l_1 \cdot \left(1 - \frac{M_0}{M}\right)}{R_p}$$

$$+ \left(\frac{l_3 - l_1}{R_p} + \frac{l_1 \cdot \left(1 - \frac{M_0}{M}\right)}{2R_p}\right) \cdot l_1 \cdot \frac{M_o}{M} + \frac{(l_3 - l_1)^2}{2 \cdot R_p}$$

By substituting equation (16) to the equation above, the following equation can be obtained:

$$\frac{\varepsilon_o \alpha (\frac{M}{M_0}) l_3^2}{d} + D - d - 2t_{pp}$$

$$= \frac{(l_3 - l_1)^2}{2 \cdot R_p} + \frac{l_1^2 \left(1 - \frac{M_0}{M}\right)^2}{3 \cdot R_p} + \frac{(l_3 - l_1) l_1 \left(1 - \frac{M_0}{M}\right)}{R_p}$$

$$+ \left(\frac{l_3 - l_1}{R_p} + \frac{l_1 \left(1 - \frac{M_0}{M}\right)}{2R_p}\right) l_1 \frac{M_o}{M}$$

The equation above can be reduced in terms of l_3^2 and takes next form:

$$l_3^2 + \frac{D - d - 2t_{pp} - \frac{l_1^2}{R_p}\left(\frac{\left(1 - \frac{M_0}{M}\right)^2}{3} - \frac{1}{2}\left(\frac{M_o}{M}\right)^2\right)}{\left(\frac{\varepsilon_o \alpha (\frac{M}{M_0})}{d} - \frac{1}{2R_p}\right)} = 0$$

Solution for this quadratic equation is:

$$l_3 = \sqrt{\frac{D - d - 2t_{pp} - \frac{l_1^2}{R_p}\left(\frac{\left(1 - \frac{M_0}{M}\right)^2}{3} - \frac{1}{2}\left(\frac{M_o}{M}\right)^2\right)}{\left(\frac{1}{2R_p} - \frac{\varepsilon_o \alpha (\frac{M}{M_0})}{d}\right)}}$$

When riser enters the straight section of the J-tube it will experience straightening, so additional force may be required. The pulling force for this case will be calculated by using

the energy method as well. As it was mentioned before the force required to pull the riser into bended section of the J-tube is:

$$F = \frac{\bar{M}}{R} = \bar{M}\left(\frac{1}{R_e} + \frac{1}{R_p}\right)$$

It can be assumed that applied energy for the riser in order to pull it into the J-tube to some incremental distance will be:

$$U_1 \sim \left(\frac{1}{R_e} + \frac{1}{R_p}\right)$$

When riser leaves the bended section of the J-tube it will experience elastic restoring, which is like spring energy tries to push riser out, and the energy to straighten it up, so the energy required to get rid of plasticity radius, so this energy can be called plasticity energy. Then equation for the energy required to take it out from the bended section of the J-tube to straight section will be:

$$U_2 \sim -\frac{1}{R_e} + \frac{1}{R_p}$$

The total energy can be calculated as sum of these energies:

$$U_2 + U_1 = \left(\frac{1}{R_e} + \frac{1}{R_p}\right) + \left(-\frac{1}{R_e} + \frac{1}{R_p}\right) = \frac{2}{R_p}$$

Consequently a force required to pull the riser into J-tube will be:

$$F = \frac{2\bar{M}}{R_p}$$

Normal force from the J-tube to the riser can be calculated by using moment equilibrium on the touch point, and calculated by the following equation:

$$N_o = \left(M - T_5(D - d)\right)\left(\frac{1}{l_3}\right)$$

Additional friction force due to additional contact of the riser to the J-tube will be:

$$F_{fric} = \left(\mu_p + \mu_{ph}\right)\left(M - T_5(D - d)\right)\left(\frac{1}{l_3}\right)$$

Total pull-in force equation in this stage can be calculated as a sum of the all friction forces between J-tube and riser including pullhead, pulling force in order to bend the riser, and the formulation for the pulling force for this stage will take following form:

$$P_5 = \frac{2M}{R_p} + F_{fric} + 2\mu_p\left(M - P_5(D-d)\right)\left(\frac{1}{l_2}\right) + T_2 + W_r$$

By substituting equation for determination normal force to the last equation, the following term can be obtained:

$$P_5 = \frac{2M}{R_p} + (\mu_{ph} + \mu_p)\left(M - P_5(D-d)\right)\left(\frac{1}{l_3}\right) + 2\mu_p\left(M - P_5(D-d)\right)\left(\frac{1}{l_2}\right) + T_2 + W_r$$

Separation terms of P_5 in one side from the equation above, gives final formulation for the pulling force in this stage.

$$P_5 = \frac{\frac{2M}{R_p} + (\mu_{ph} + \mu_p)M\left(\frac{1}{l_3}\right) + 2\mu_p(M)\left(\frac{1}{l_2}\right) + T_2 + W_r}{1 + \frac{(\mu_{ph} + \mu_p)(D-d)}{l_3} + \frac{2\mu_p(D-d)}{l_2}}$$

Whereas: Wr- is weight of the riser section in vertical section of the J-tube.

3.7.6 Pipe at topside level

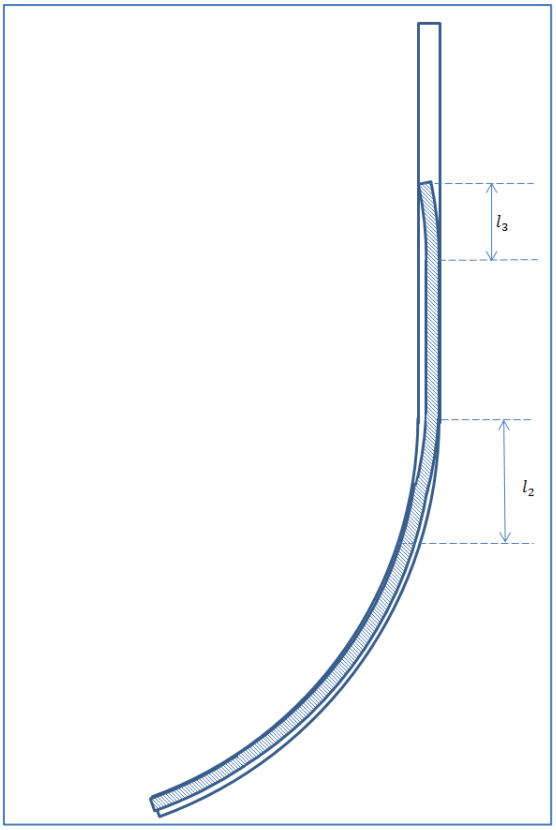

Figure 3-40 Riser at topside level

When riser goes up through straight part of the J-tube, the behavior of riser is complicated. It was assumed that riser will have long contact area with J-tube's wall and part of riser touch other side with length l3 as it is illustrated in the Figure 3-40. Because the riser will have same residual radius over the length that bending moment to straighten the riser will be same along the pipe. So the leading end of the riser will have same distance between touch points during pulling.

The formulation for total pulling force will be same as in previous stage of pulling. The only difference in the equation is the weight of the riser. The weight of the riser is higher due to length of pipeline in the vertical section of the J-tube.

$$T_6 = \frac{\frac{2M}{R_p} + (\mu_{ph} + \mu_p)M\left(\frac{1}{l_3}\right) + 2\mu_p(M)\left(\frac{1}{l_2}\right) + T_2 + W_r}{1 + \frac{(\mu_{ph} + \mu_p)(D-d)}{l_3} + \frac{2\mu_p(D-d)}{l_2}}$$

To sum up, potentially the maximum pull-in force can be experiences in three points:

- On the entrance to J-tube's bended section
- On the exit from J-tube's bended section
- On the topside of the J-tube

All the equation for these three cases has the relationship to J-tube's bending radius. By using the formulations for this stages find maximum pull-in force for the total pulling process.

3.8. Local buckling check

Integrity of riser was checked in accordance with DNV standards. Riser is checked for local buckling.

There are two methods specified in DNV-OS-F101 regarding local buckling check.

- Load controlled condition
- Displacement controlled condition

Displacement controlled condition method was selected for local buckling check because riser's response primarily defined by impacted geometrical displacement. As an example for displacement controlled condition can be pipe interaction with lay barge's stinger.

From DNV-OS-F101, pipe members subjected to bending moment, axial force and external pressure need to satisfy following criteria:

$$\left(\frac{\varepsilon_{sd}}{\frac{\varepsilon_c(t_2,0)}{\gamma_\varepsilon}}\right)^{0,8} + \frac{p_e - p_{min}}{\frac{p_c(t_2)}{\gamma_m \cdot \gamma_{sc}}} \leq 1 \qquad (33)$$

Given that following criteria satisfied

$$\frac{D}{t_2} < 45, p_{min} < p_e$$

The parameters here mainly depend on pipeline parameters, exposed media and on J-tube dimensions.

ε_{sd} is **design compressive strain** which take into account combination of functional, environmental and interferential loads. Design compressive strain can be generally expressed by the following formula (DNV, 2010).

$$\varepsilon_{sd} = \varepsilon_F \gamma_F \gamma_C + \varepsilon_E \gamma_E + \varepsilon_I \gamma_F \gamma_C + \varepsilon_A \gamma_A \gamma_C$$

Whereas:

ε_F is **functional load strain**, strain generated by axial tension on the pipe, the maximum tension on pipeline's bended segment will be right on the border with J-tube's vertical part, and can be expressed in the next format:

$$\varepsilon_F = \frac{\sigma}{E} = \frac{-T_{max}}{A_{pipe}E}$$

ε_E is **environmental load strain**, strain generated by external pressure. Pipe subjected to external pressure will experience elongation due to Poisson effect. Compressive hoop stress generated longitudinal strain on the pipe. The formulation for finding this environmental strain is given below:

$$\varepsilon_E = -\frac{v\sigma_h}{E} = \frac{v \cdot p_e \cdot d}{2 \cdot t \cdot E}$$

ε_I is **interferential load strain**, the strain generated due to pipe bending , which has tensile strain on upper part of bending and compressive strain on lower part of bending. As it was discussed on the previous chapters, the interferential strain depends on pipe's and J-tube's dimensions:

$$\varepsilon_I = \frac{d}{2R}$$

ε_A is **accidental load strain**, the strain generated due to accidental loads, as long as thesis do not consider any accidental loads, the value for the accidental strain was not taken.

$$\varepsilon_A = 0$$

γ_F , γ_E , γ_A are **load effect factors** for functional, environmental, accidental loads and γ_c is conditional load factor, which is used in order to give more safety margin for the load effect factors discussed above. The values for load effect factors are taken for local check load effect combination and for ultimate limit state from DNV-OS-F101, and condition load effect factor value is taken by considering pipe as continuously stiff supported and all this values given below.

$$\gamma_F = 1.1$$
$$\gamma_c = 0.82$$
$$\gamma_E = 1.3$$
$$\gamma_A = 0$$

p_c is **characteristic collapse pressure**, the pressure which is able to buckle pipeline. The cubic equation below is equation for determining characteristic collapse pressure (DNV, 2010).

$$(p_c(t) - p_{el}(t))\left(p_c(t)^2 - p_p(t)^2\right) = p_c(t) \cdot p_{el}(t) \cdot p_p(t) \cdot f_o \cdot \frac{d}{t}$$

Where p_{el} is **elastic collapse pressure**, pressure required collapse the pipe if the pipe deformation purely elastic. Formulation for determining elastic collapse pressure is (DNV, 2010):

$$p_{el}(t) = \frac{2 \cdot E \cdot \left(\frac{t}{d}\right)^3}{1 - \nu^2}$$

p_p is **plastic collapse pressure**, which is function of yielding stress of pipe's material and pipe's dimensions. The following formula used to calculate plastic collapse pressure (DNV, 2010):

$$p_p(t) = f_y \cdot \alpha_{fab} \cdot \frac{2 \cdot t}{d}$$

f_o is **ovality of the pipeline**, ovality is measurement of out roundness of pipeline, usually calculated as ratio of diameter difference to mean diameter:

$$f_o = \frac{d_{max} - d_{min}}{d} < 0.005$$

f_y is **characteristic material yield strength**, used to determine materials limit state criteria and can be found by the following formula (DNV, 2010):

$$f_y = (SMYS - f_{y,temp}) \cdot \alpha_u$$

$f_{y,temp}$ **is yield stress's de-rating value** due to temperature, some materials has a tendency to lose their yielding strength capacity due to temperature increase, de-rating value takes into account this changes. On the figure below is shown the relationship between de-rating value and temperature of the material.

α_u is **materials strength factor**, factor which takes into account uncertainties related to yield strength change due to temperature change. For normal cases the factor takes next value:

$$\alpha_u = 0.96$$

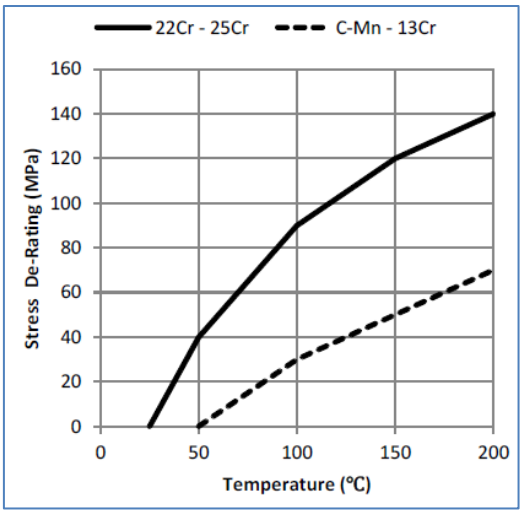

Figure 3-41 De-rating value

α_{fab} is **fabrication factor**, factor which takes into account uncertainties about tensile and yield strength reduction due to cold forming in manufacturing process. The table below was taken from DNV standard and represents fabrication factors for different pipe manufacturing types. The factor can be improved by external compression (outside cold sizing) or heat treatment can be used as well.

Maximum fabrication factor, α_{fab} (DNV, 2010)			
pipe	Seamless	UO &TRB & ERW	UOE
$\boldsymbol{\alpha_{fab}}$	1.00	0.93	0.85

Solution for the cubic equation for finding characteristic collapse pressure is presented in DNV standard and takes following format:

$$p_c = y - \frac{1}{3}b$$

Where

$$b = -p_{el}(t)$$

$$c = -\left(p_p(t)^2 + p_p(t) \cdot p_{el}(t) \cdot f_o \cdot \frac{d}{t}\right)$$

$$d = p_{el}(t) \cdot p_p(t)^2$$

$$u = \frac{1}{3}\left(-\frac{1}{3}b^2 + c\right)$$

$$v = \frac{1}{2}\left(\frac{2}{27}b^2 - \frac{1}{3}bc + d\right)$$

$$\Phi = cos^{-1}\left(\frac{-v}{\sqrt{-u^3}}\right)$$

$$y = -2\sqrt{-u}\cdot cos\left(\frac{\Phi}{3}+\frac{60\pi}{180}\right)$$

$\varepsilon_c(t_2, p_{min} - p_e)$ is **characteristic bending strain resistance**, the factor shows resistance of the pipe for bending deformation and can be calculated by using formula below (DNV, 2010).

$$\varepsilon_c(t_2, p_{min} - p_e) = 0.78\left(\frac{t}{d} - 0.01\right)\left(1 + 5.75\frac{p_{min} - p_e}{p_b(t)}\right)\alpha_h^{-1.5}\alpha_{gw}$$

$$\varepsilon_c(t_2, 0) = 0.78\left(\frac{t}{D} - 0.01\right)\alpha_h^{-1.5}\alpha_{gw}$$

The last equation is dedicated for Displacement Controlled Condition buckling check.

α_h is **minimum strain hardening**, shows increase in strength when metal deforms and goes beyond elastic range, so further deformation will require more stress. The value of strain hardening $\alpha_h = \left(\frac{R_{t0.5}}{R_m}\right)$ for duplex and 13Cr martensitic stainless steel pipelines is $\frac{R_{t0.5}}{R_m} = 0.92$ and for C-Mn steel pipes is $\frac{R_{t0.5}}{R_m} = 0.93$ was taken in DNV-OS-F101.

α_{gw} is **girth weld factor**, during buckling the strain in compressive side of bending shows high impact on girth weld. It is supposed to be due to imperfections on welding and because of that the effect is more apparent in pipes with higher diameters. Generally girth weld factor can be found by FE analysis, unless girth weld factor graph proposed in DNV-OS-F101 can be used.

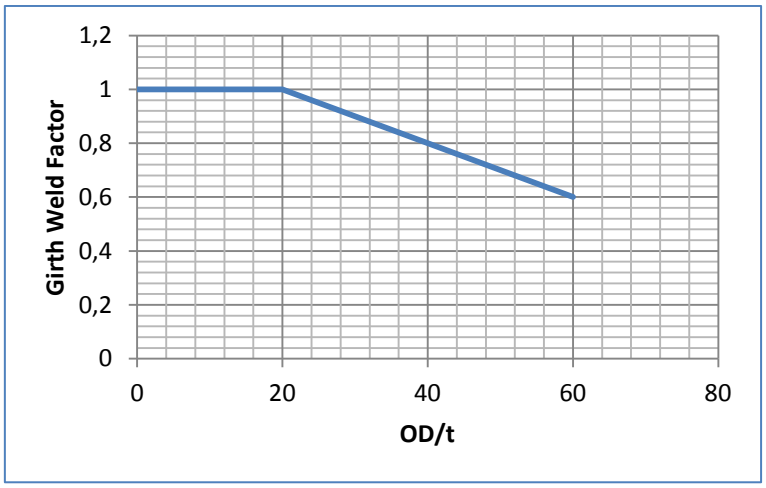

Figure 3-42 Girth weld factor

$\gamma_\varepsilon$is **resistance strain factor**, different strain factor exists regarding safety class, the installation process considered to have low safety class and that is why the factor will have next value:

$$\gamma_\varepsilon = 2$$

γ_m is **material resistance factor**, safety factor which covers resistance transformation uncertainties of a characteristic to a lower fractile. The factor depends on limit states and for ultimate limit state (ULS) the factor is:

$$\gamma_m = 1.15$$

γ_{SC} is **safety class safety factor**, safety factor which covers resistance transformation uncertainties from a lower fractile resistance to a design resistance. The factor depends on safety class and for installation phase it will take next value.

$$\gamma_{SC} = 1.04$$

In conclusion for this chapter, all the values required to get equation (33) was fitted into Excel as an input, in order to check for pipeline integrity.

4. Case Study

The chapter includes three cases with pull-in analysis. Finite Element Analysis was conducted for these cases and results were generated. The results will be compared with results from Excel calculation tool, and differences on results will be discussed. In all the cases Finite Element Analyses were conducted with software ABAQUS.

Case # 1				
Material properties	Yield Stress	σy	450	[N/mm2]
	Young's modulus	E	207000	[N/mm2]
	Density	ρ_p	7800	[kg/m3]
Riser properties	Outside diameter	OD	289,7	[mm]
	Wall thickness	WT	17,6	[mm]
	Ramberg & Osgood moment to curvature coefficient	A	0,000034	[-]
	Ramberg & Osgood moment to curvature coefficient	B	50	[-]
Coating properties	Wall thickness	WTc	6	[mm]
	Young's modulus	Ec	0	[N/mm2]
	Density	ρ_c	900	[kg/m3]
J-tube properties	Length pipe from bell mouth to upper bend	L1	12	[m]
	Length pipe from upper bend to top J-Tube	L2	100	[m]
	J-Tube inside diameter	ID	368,4	[mm]
	Angle of bend	θ	90	[degree]
	Radius bend	R	20.2	[m]
Coefficients of friction	J-tube to pipe	μp	0.15	[-]
	J-tube to cable	μc	0.15	[-]
	Pullhead to pipe up to half of bended section	μph1	1.2	[-]
	Pullhead to pipe after half of bended section	μph2	0.5	[-]
	Backtension	To	420-640	[KN]

In the case # 1, the pull-in analysis for 10” riser was conducted. the J-tube assumed to have different coefficient of bending in different sections of it. Lower part of bended section assumed to have higher coefficient of friction due to pullhead effect (scratching due to pullhead geometry).

The results obtained by FEA and analytical methods based Excel calculation tool is illustrated in the Figure 4-1. Comparison of the both result shows that in general both results have same trends, meanwhile result shown in Excel calculation tool is bit conservative but it cannot show the high pick when the riser enters the bended section of J-tube. The pullhead length or small pulling force from cable can result in high contact force between J-tube and riser. That is why FEA result has pick in pulling force when riser enters j-tube's bended section.

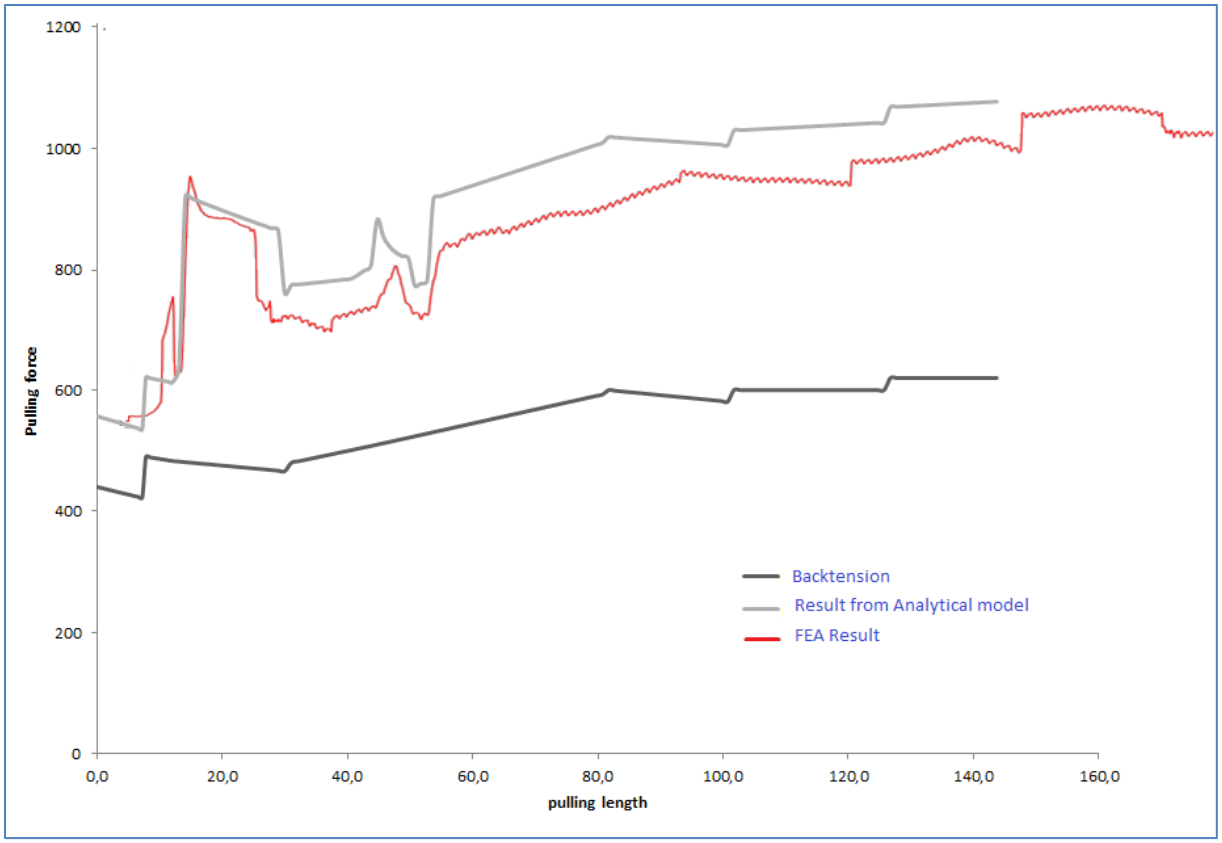

Figure 4-1 Case # 1, Illustrateation of Analytical and FEA results

In this case in Excel calculation tool the change of the backtension was taken into account. Increase of the backtension shows increase in pulling force on winch. In the figure it is clear that if the backtension maintained constant, the maximum pull-in force will occur when the riser enters J-tube's bended section.

In the case # 2 the analyses was conducted for the 14" riser. In this case backtension was taken as constant. Unlike first case, the J-tube has homogenous coefficient of friction. The coefficient of frictions between pullhead and J-tube, riser to J-tube and pulling cable to J-tube are taken as 0,3.

Case # 2				
Material properties	Yield Stress	σ_y	518	[N/mm2]
	Young's modulus	E	207000	[N/mm2]
	Density	ρ_p	7800	[kg/m3]
Riser properties	Outside diameter	OD	355.9	[mm]
	Wall thickness	WT	19.1	[mm]
	Ramberg & Osgood moment to curvature coefficient	A	0,000034	[-]
	Ramberg & Osgood moment to curvature coefficient	B	50	[-]
Coating properties	Wall thickness	WTc	6	[mm]
	Young's modulus	Ec	0	[N/mm2]
	Density	ρ_c	900	[kg/m3]
J-tube properties	Length pipe from bell mouth to upper bend	L1	12	[m]
	Length pipe from upper bend to top J-Tube	L2	100	[m]
	J-Tube inside diameter	ID	463.6	[mm]
	Angle of bend	θ	90	[degree]
	Radius bend	R	20.5	[m]
Coefficients of friction	J-tube to pipe	μp	0.3	[-]
	J-tube to cable	μc	0.3	[-]
	Pullhead to pipe up to half of bended section	$\mu ph1$	0.3	[-]
	Pullhead to pipe after half of bended section	$\mu ph2$	0.3	[-]
	Backtension	To	343	[KN]

The Figure 4-2 shows Finite Element Analysis result and Excel calculation tool results together. Like in a previous case the results have generally similar trends and result of the Excel calculation tool bit conservative except of high pick in pulling tension when risers enters bended section of J-tube. The reason for this difference can be due to pullhead effect as it was mentioned before, and getting generally bit higher result can be due to material properties. In all cases the material type was taken as elastic perfectly plastic effect of axial load was not included, the effect of axial load for bending moment reduction was done in separate Excel sheet, and it shows that in general it gives around 1-3% moment reduction what can be neglected. This may result on getting slightly higher result regarding bending pulling force in bended section of J-tube. The pulling force in the straight section of the J-tube is slightly less than FEA result. The reason for this result might be meshing effect and

material properties of the J-tube and riser behavior in straight section which was included in FEA analysis.

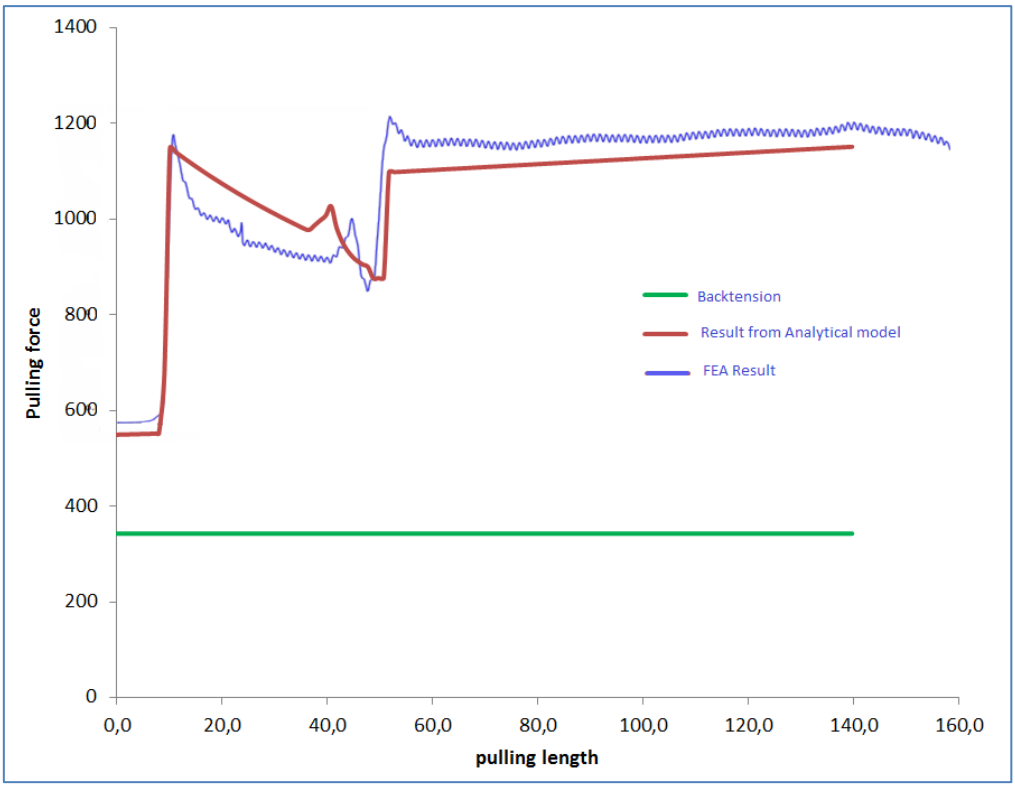

Figure 4-2 Case # 2, Illustrateation of Analytical and FEA results

In the case #3 riser was taken with similar dimensions as in first case but, without polypropylene coating. Finite Element Analysis was conducted for this case decade ago and that is why FEA result might give slightly different result from up to date software. In this case mean yield stress was taken as 475 MPa. SMYS may mislead some engineers from getting normal result. In reality the yielding stress is far more than SMYS and knowledge about mean yield stress increase accuracy in results. In the Figure 4-3 is shown Finite Element Analysis result and Excel calculation tool results together. As in previous two cases the results resembles each other. Excel tool has slightly conservative result in bended section of the J-tube , it is not clearly shown in FEA result the all length of pulling , but in initial 60 meters results corresponds each other. Again as in previous cases Excel tool lacks of peak in the beginning of riser bending, study of riser behavior in the entrance to bended section of J-tube is needed, in order to determine how much that may differ from an analytical model developed in this thesis. Suggestion about improvement of results will be mentioned in the conclusion of this project.

Case # 2				
Material properties	Yield Stress	σy	475	[N/mm2]
	Young's modulus	E	207000	[N/mm2]
	Density	ρp	7800	[kg/m3]
Riser properties	Outside diameter	OD	273	[mm]
	Wall thickness	WT	18.3	[mm]
	Ramberg & Osgood moment to curvature coefficient	A	0,000034	[-]
	Ramberg & Osgood moment to curvature coefficient	B	50	[-]
Coating properties	Wall thickness	WTc	0	[mm]
	Young's modulus	Ec	0	[N/mm2]
	Density	ρc	900	[kg/m3]
J-tube properties	Length pipe from bell mouth to upper bend	L1	9.8	[m]
	Length pipe from upper bend to top J-Tube	L2	60	[m]
	J-Tube inside diameter	ID	374.6	[mm]
	Angle of bend	θ	90	[degree]
	Radius bend	R	20.313	[m]
Coefficients of friction	J-tube to pipe	μp	0.4	[-]
	J-tube to cable	μc	0.4	[-]
	Pullhead to pipe up to half of bended section	μph1	0.4	[-]
	Pullhead to pipe after half of bended section	μph2	0.4	[-]
	Backtension	To	379	[KN]

In conclusion from the all analytical approach results, the pulling force in constant coefficient of friction will have couple of local maximums during pulling operation, and this maximums occurs in following positions.

- Riser on entrance of the J-tube's bended section.
- Riser on exit of the J-tube's bended section.
- Riser on the top-side of the J-tube.

The final maximum pull-in force can be determined as a maximum of these pull-in forces.

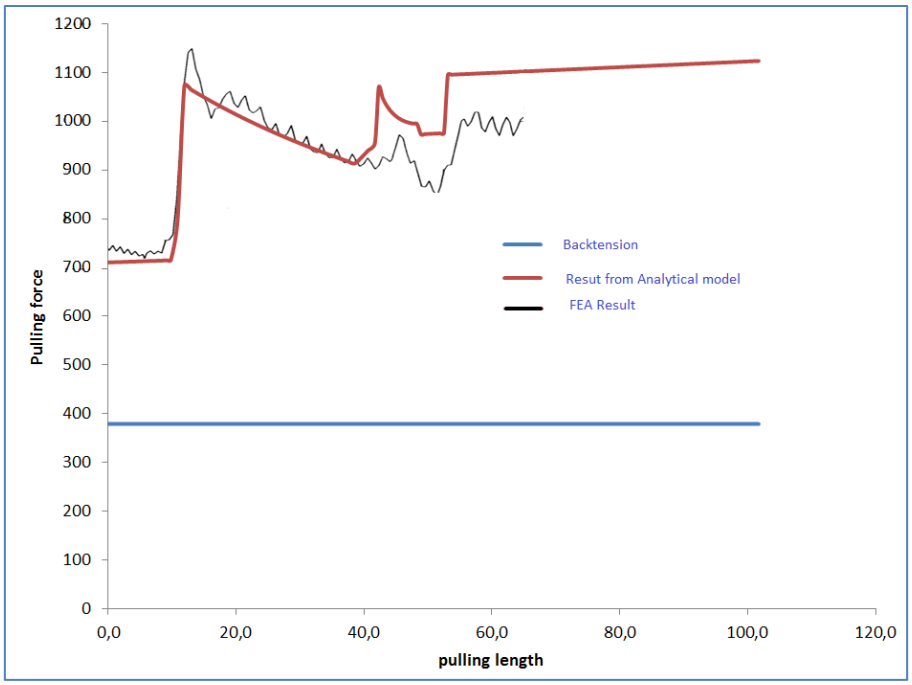

Figure 4-3 Case # 3, Illustrateation of Analytical and FEA results

5. Sensitivity analysis

Pulling force during pipeline installation can be governed by the following parameters:

- Backtension on the bellmouth.
- Dimensions of the riser.
- Geometry of the pullhead.
- Coefficients of friction between J-tube to riser, cable and pullhead.
- J-tube's geometry.
- Riser material characteristics.
- Riser coating characteristics etc.

This chapter is dedicated to present results from sensitivity analysis of the analytical model. Analysis mainly was done for determining maximum pull-in force and for local pull-in forces. Relationship pattern of pull-in force from different parameters was logged and plotted into graphs and trends for the relationships were described.

In the Figure 5-1 relationship between riser's material yield stress and pulling force is given. Results were taken for four points. Where first point indicates the pulling force when it is in J-tube's bended section entrance, second point indicates when the riser on the exit from the bended section, third point indicates second contact of pullhead with the J-tube's inner wall and the last point indicate pulling force when pullhead on J-tube's topside.

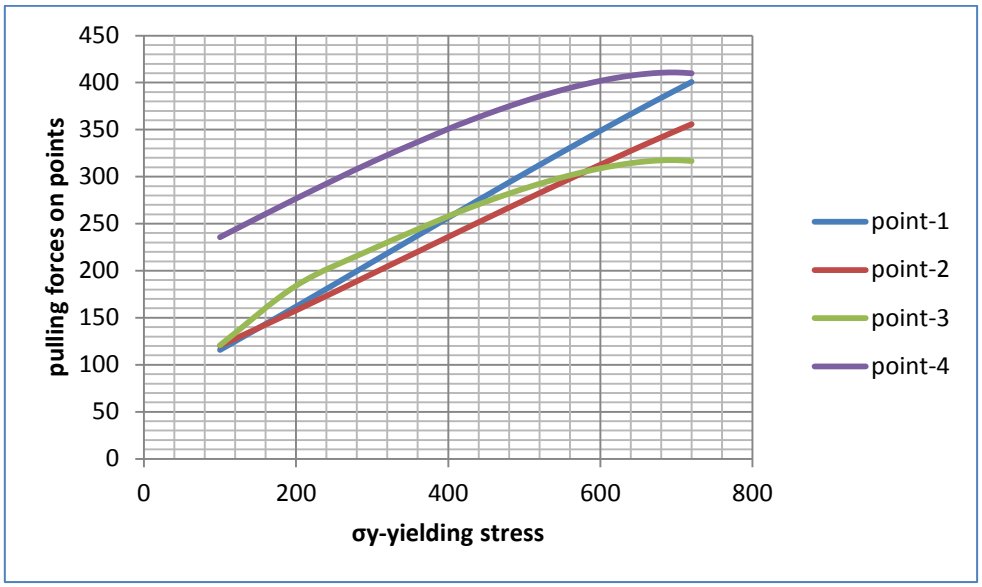

Figure 5-1 Pulling force to yield stress relationship

The relationship in the graph shows increase of yielding stress causes increase in pulling force, nevertheless pulling force in point-1 has more steep relationship than in other points. So the maximum pull-in force can be either when the riser entering the J-tube or when it is on topside depending on riser material's yielding strain.

In the Figure 5-2 relationship between pulling force and J-tube to pullhead coefficient of friction is shown. As in Figure 5-1 the pulling force in point-1 has higher rate of increase rather than point-4, that is why in higher coefficient of frictions the maximum pulling force will correspond to the point-1. The pulling force in point-4 and 3 has less gradual relationship to the coefficient friction between J-tube to pullhaed, whereas point-1 has highest rate, and this can be described because of primary bending of the riser comes to the point-1.

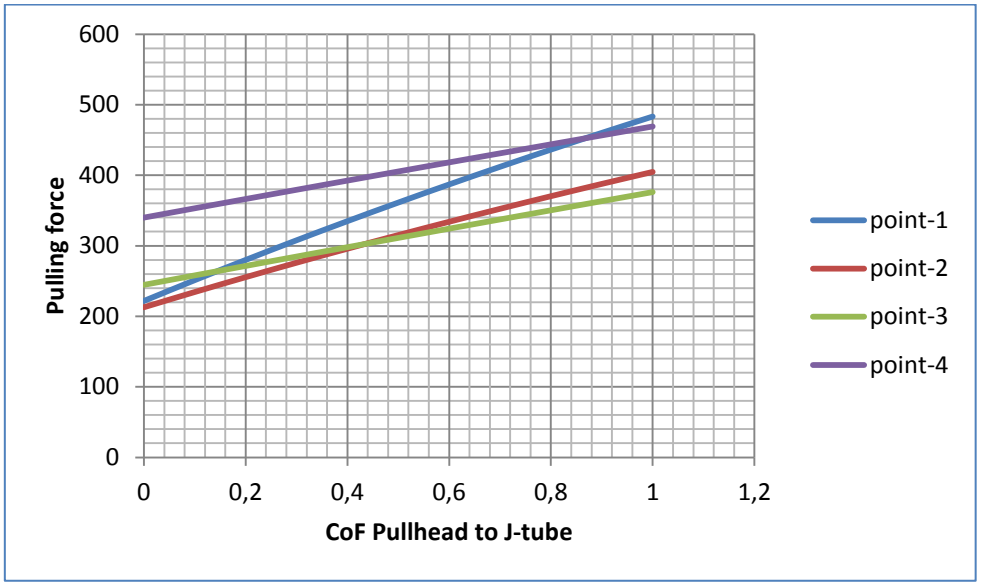

Figure 5-2 Pulling force to CoF relationship

In the Figure 5-3 the relationship between J-tube's radius of bending and pulling force is shown. Whereas pulling force has inverse relationship to the bending radius. Points 3 and 4 have steeper decline to compared points 1 and 2 , which means in J-tube's with higher radius of curvature maximum pulling force occurs on point 1. Decrease in radius of bending on the J-tube will led to sharp increase of the pulling force in point-4.

Figure 5-4 shows relationship between pull-in force and backtension. Maximum pulling force has linear dependence form backtension and all the points has almost same rate of increase from backtension, and highest backtension can be registered on the end of J-tube pulling in normal conditions.

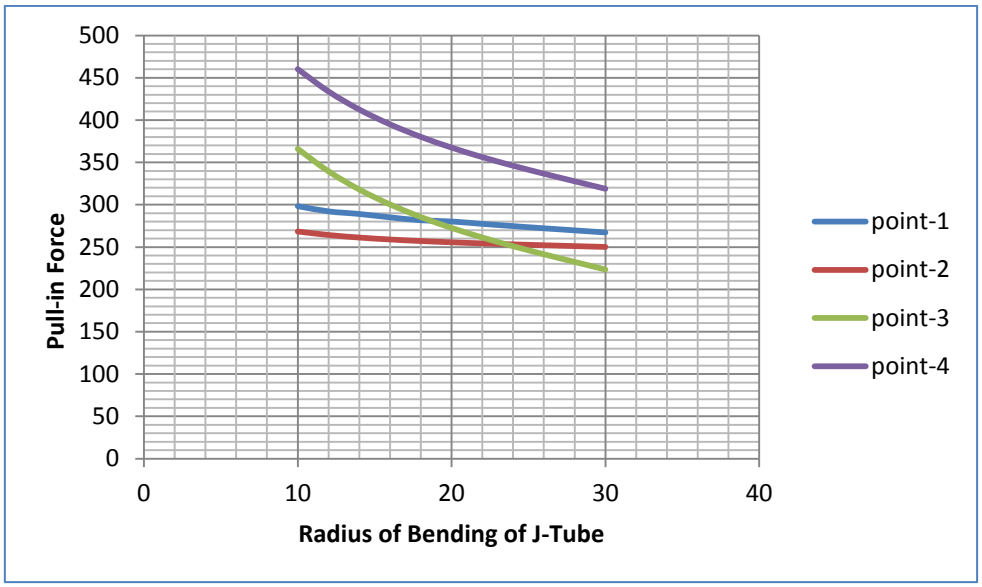

Figure 5-3 Radius of J-tube to Pulling force relationship

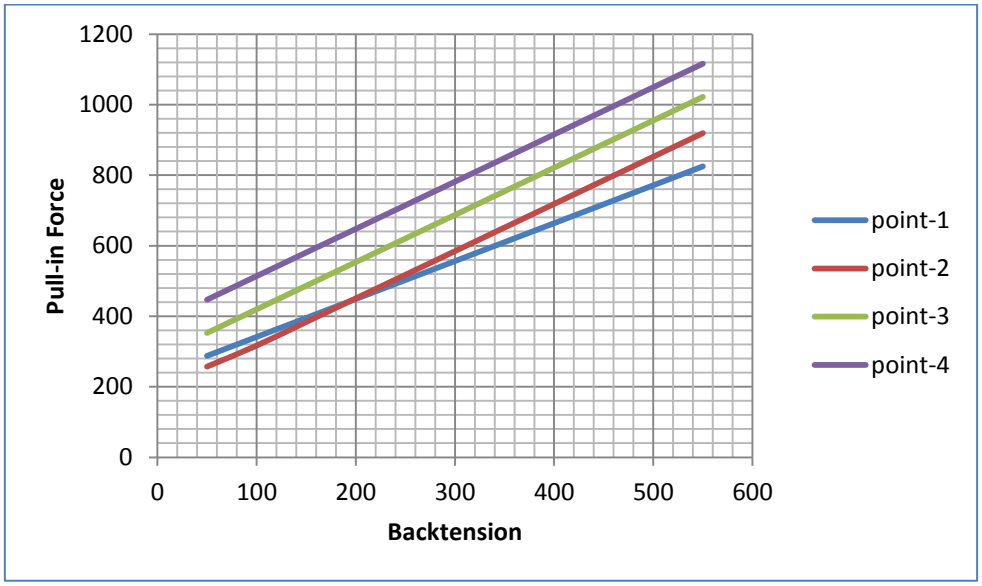

Figure 5-4 Backtension to Pull-in force relationship

In the Figure 5-5 and Figure 5-6 relationship of pulling force to the gap between riser to J-tube are shown in wall thickness profile. The Figure 5-6 clearly shows that maximum pulling force has linear relationship to the outer diameter and wall thickness of the riser. Increase of these parameters leads to increase in pull-in force. Decrease in gap between riser and J-tube will increase pulling force, this relationship is in inverse ratio, in small values of the gap decrease of the gap will led to significant increase in pulling force.

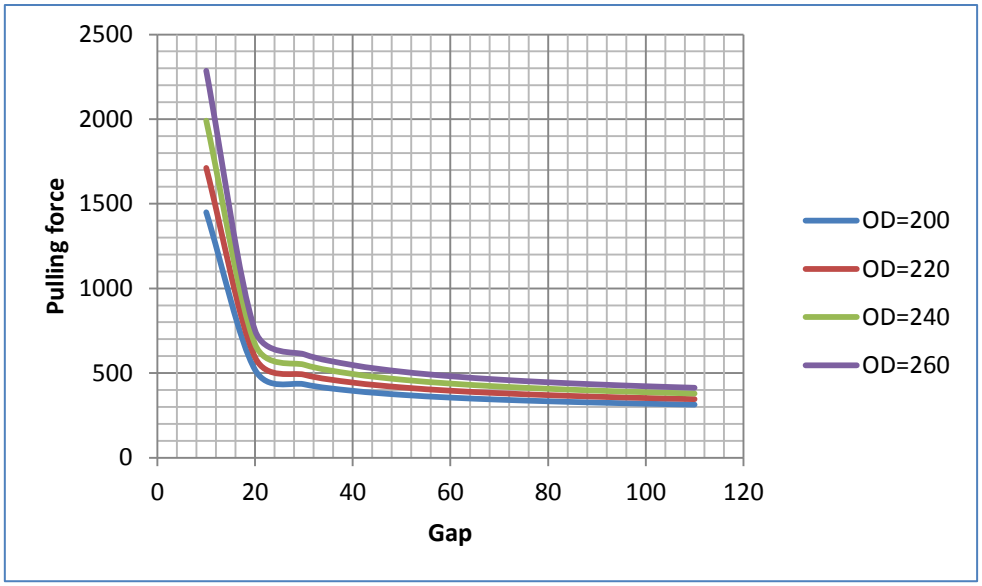

Figure 5-5 Pulling force to Gap relationship

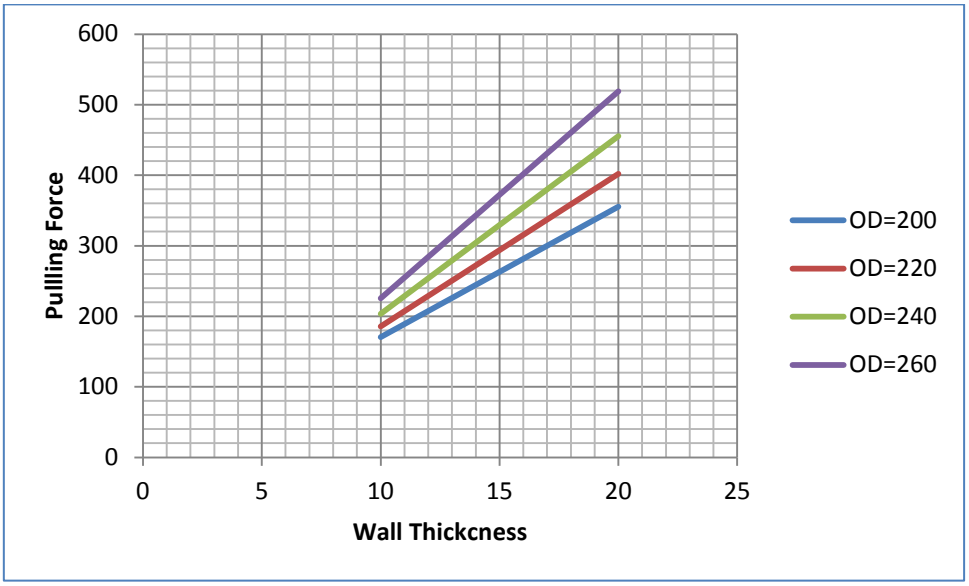

Figure 5-6 Pulling force to wall thickness relationship

Figure 5-7 shows relationship between pulling force on point-1 to coefficient of friction of the riser to J-tube in profile of coefficient of friction of the pulling cable to the J-tube's inner wall. The relationship has exponential relationship. For the total pulling force, the relationship of coefficient of friction of the riser will also have exponential relationship. To summing up the increase of the coefficient of friction between cable and J-tube does not have any effect on maximum pull-in force, unless it is less than certain value, because when pipe in vertical section the pulling wire is assumed to not to have any contact, that is why it is more prudent to decrease the friction between J-tube to riser.

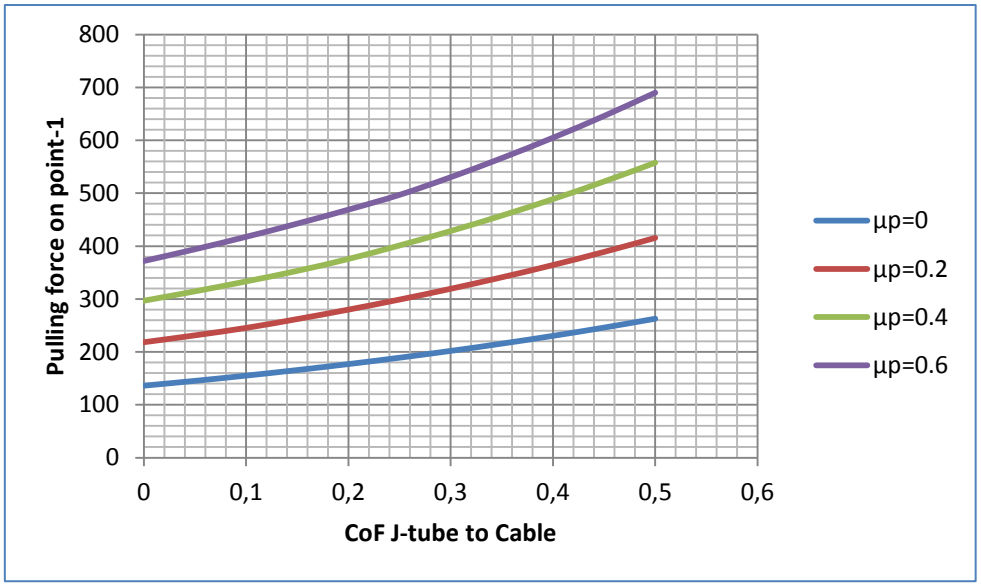

Figure 5-7 CoF to pulling force at point-1 relationship

In conclusion for the sensitivity analysis has been done above, most affecting parameters for the maximum pull-in force are:

- Gap between riser and J-tube: reduction of the gap between riser and J-tube leads to dramatic increase in maximum pulling force.
- Backtension on riser: Backtension has linear dependence with maximum pulling force so basically decrease of the backtension and coefficient of friction between riser and J-tube leads to reduction of the total pulling force.
- Wall thickness of the pipe: increase of wall thickness has significant effect on increase of bending moment of the pipe consequently it leads to increase in maximum pulling in force.

Despite the fact that other values have lower effect than three mentioned before, they must be also included and taken into consideration during designing.

Conclusion and recommendation for further study

In this paper an analytical model for J-tube Pull-in method was developed. Developed equations were introduced into Excel as a calculation tool and were checked against FEA results. Riser integrity check formulations were inserted into same excel sheet, which allows finding not only minimum required winch capacity, but also pipe dimensions for the installation. The results obtained by the analytical method fairly similar results to FEA results. In order to improve accuracy of the analytical method the following areas can be studied in more detail:

- Riser's behavior on vertical part of J-tube
- Riser's behavior and mechanics on entrance J-tube's bended section
- Effect of riser's entering angle on pulling force
- Deflection of J-tube due to contact with the riser
- More study can be done regarding riser integrity (rupture and accumulative plastic strain etc.)

Despite some limitations, the project meets all the objectives established in the beginning of work. Unlike previously developed analytical approaches, the new approach includes:

- Effect of coating on riser.
- Effect of ovality on riser's bending moment.
- Effect of pullhead's geometry on changing coefficient of friction.
- Effect of axial tension on riser's bending moment.
- Realistic strain-stress relationship can be implemented.
- Contact force between pullhead and J-tube can be calculated.
- Shows pulling force change through the installation.

Accuracy of the developed tool is in the acceptable region and was checked with around 15 cases and showed accuracy around 5-10% with FEA results. It is author hopes that the paper can be implemented in activities related to j-tube pull-in method in oil and gas industry, and be good guideline for other studies in other industries. The thesis enclosed with Excel calculation tool, so reader able to assess it.

References

A.C Walker, P. D., 1983. A Design Basis for the J-Tube Method of Riser Installation.. *Journal of Energy Resources Technology,* Issue 105, pp. 263-270.

Allsea, 2013. *Pipeline installation.* [Online]
Available at: http://www.allseas.com/uk/33/company/activities/pipeline-installation.html
[Accessed 2 May 2013].

Arthur P, B. R. J. S., 2003. *Advanced Mechanics of Material.* 6th ed. USA: John Wiley & Sons, inc..

Assitant, O., 2013. *RO User Manual.* [Online]
Available at: http://www.oeassistant.com/download/Ramberg-Osgood%20Convertor%20User%20Manual%201.0.2.pdf
[Accessed 10 May 2013].

Boyun Guo, S. S. J. C. A. G., 2005. *Offshore Pipelines.* Oxford: Elsevier.

Bruton D.A.S, M. D. M. P., 1989. *DiverlessFlowlineTie-InTechniquesfor the DISPSProject.* Houston, OTC.

DNV, 2010. *Submarine pipeline systems,* Oslo: DET NORSKE VERITAS.

Eriksen G, J. O. S. S., 1989. *Design and Installation of the Oseberg Fowline Bundles.* Houston, Offshore Technology Conference.

FMC, 2012. *Universal Connection Systems.* [Online]
Available at: http://www.fmctechnologies.com/en/SubseaSystems/Technologies/SubseaProductionSystems/TieInAndFlowlines/VerticalAndHorizontalTieInSystems/HorizontalTieIn/UCON.aspx
[Accessed 3 May 2013].

Gjertveit, L. S. a. E., 2013. *Constructing the World's Longest Subsea Pipeline, Langeled Gas Export.* Houston, Offshore Technology Conference.

Hauch Søren, Y. B., 2000. *Bending Moment Capacity of Groove Corroded Pipes.* Houston, ISOPE.

Huisman, 2008. *Reel-Lay.* [Online]
Available at: http://www.huismanequipment.com/en/products/pipelay/reel_lay
[Accessed 2 May 2013].

ISOVER, 2012. *Marine insulations.* [Online]
Available at: http://www.isover-technical-insulation.com/MARINE-INSULATION/Applications/Subsea/SeaLine
[Accessed 2 May 2013].

Jirsa .J.O, F.-H. L. W. J. M. J. R. U., 1972. *Oval ng of Pipe I I nes Under Pure Bend i ng.* Dallas, Offshore Technology Conference.

Kazimi, S. M. A., 2006. *Solid Mechanics.* I ed. New Delhi: TheMcGraw Hill Companies.

Larson, R. & Edwards, B. H., 2010. *Calculus of a single variable.* Cole: Cengage Learning.

MacGregor, 2013. *Offshore winches.* [Online]
Available at: http://www.cargotec.com/en-global/macgregor/products/offshore-load-handling-solutions/offshore-winches/Pages/default.aspx
[Accessed 6 May 2012].

Mikael W.B, J. B. A. L. W. A. M. B. C. J. C. N.-J. R. N., 2005. *Design and installation of marine pipelines.* 1st ed. Oxford: Blackwell Science.

Mousselli, A., 1979. *Analysis of Deepwater Pipeline Riser Installation by J-tube Pull Method.* Houston, Offshore Technology Conference.

Peter Lindenfeld, S. W. B., 2011. *Physics - The First Science.* New Jersey: Rutgers University Press.

Ramberg W, W. R. O., 1943. Description of Stress-Strain Curves by Three. *National Advisory Comm. Aeronaut..*

S. S. Bhavikatti, K. G. R., 1998. *Engineering Mechanics.* II ed. New Delhi: New Age International.

Shane E. Flores, M. G. P. F. W. Z., 2008. Scratching of Elastic/Plastic Materials With Hard Spherical Indenters. *Journal of Applied Mechanics,* Volume 75.

Stelios K, E. C., 2007. *Mechanics of Offshore Pipelines.* 1st ed. Oxford: Elsevier.

Tan H, K., 1981. *Investigation of the Mechanics of Pipeline Installation by J-tube Pull Method,* Guildford: University of Surrey.

Titus, P. E., 1992. *Reduced J-tube Riser Pull Force.* US/Texas, Patent No. 5,145,289.

Wisnom, M., 1994. The effect of fibre rotation in ±45° tension tests on measured shear properties. *Composites,* pp. 25-32.

Young Bai, Q. B., 2005. *Subsea Pipelines and Risers.* I ed. Oxford: Elsevier.

Young Bai, Q. B., 2010. *Subsea Engineering Handbook.* Oxford: Elsevier.

Appendix

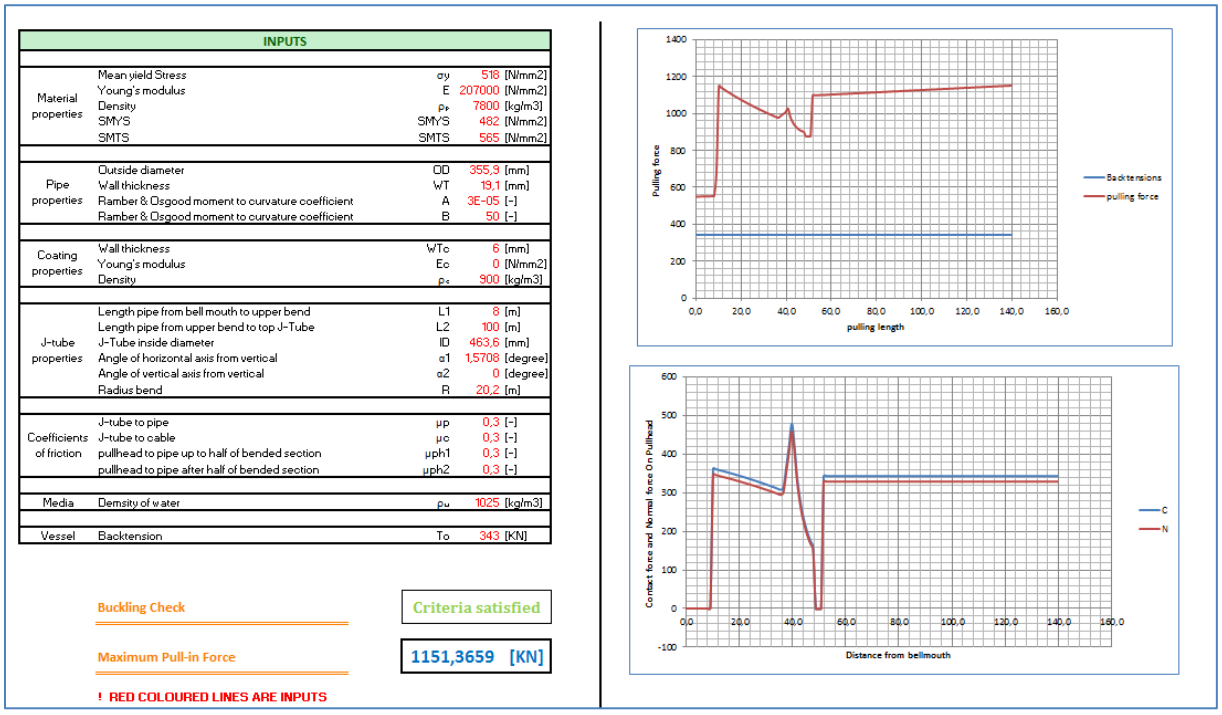

INPUTS				
Material properties	Mean yield Stress	σy	518	[N/mm2]
	Young's modulus	E	207000	[N/mm2]
	Density	ρs	7800	[kg/m3]
	SMYS	SMYS	482	[N/mm2]
	SMTS	SMTS	565	[N/mm2]
Pipe properties	Outside diameter	OD	355,9	[mm]
	Wall thickness	WT	19,1	[mm]
	Ramber & Osgood moment to curvature coefficient	A	3E-05	[-]
	Ramber & Osgood moment to curvature coefficient	B	50	[-]
Coating properties	Wall thickness	WTc	6	[mm]
	Young's modulus	Ec	0	[N/mm2]
	Density	ρc	900	[kg/m3]
J-tube properties	Length pipe from bell mouth to upper bend	L1	8	[m]
	Length pipe from upper bend to top J-Tube	L2	100	[m]
	J-Tube inside diameter	ID	463,6	[mm]
	Angle of horizontal axis from vertical	α1	1,5708	[degree]
	Angle of vertical axis from vertical	α2	0	[degree]
	Radius bend	R	20,2	[m]
Coefficients of friction	J-tube to pipe	μp	0,3	[-]
	J-tube to cable	μc	0,3	[-]
	pullhead to pipe up to half of bended section	μph1	0,3	[-]
	pullhead to pipe after half of bended section	μph2	0,3	[-]
Media	Demsity of water	ρw	1025	[kg/m3]
Vessel	Backtension	To	343	[KN]

Buckling Check — Criteria satisfied

Maximum Pull-in Force — 1151,3659 [KN]

! RED COLOURED LINES ARE INPUTS

Front screen of the Excel calculation tool

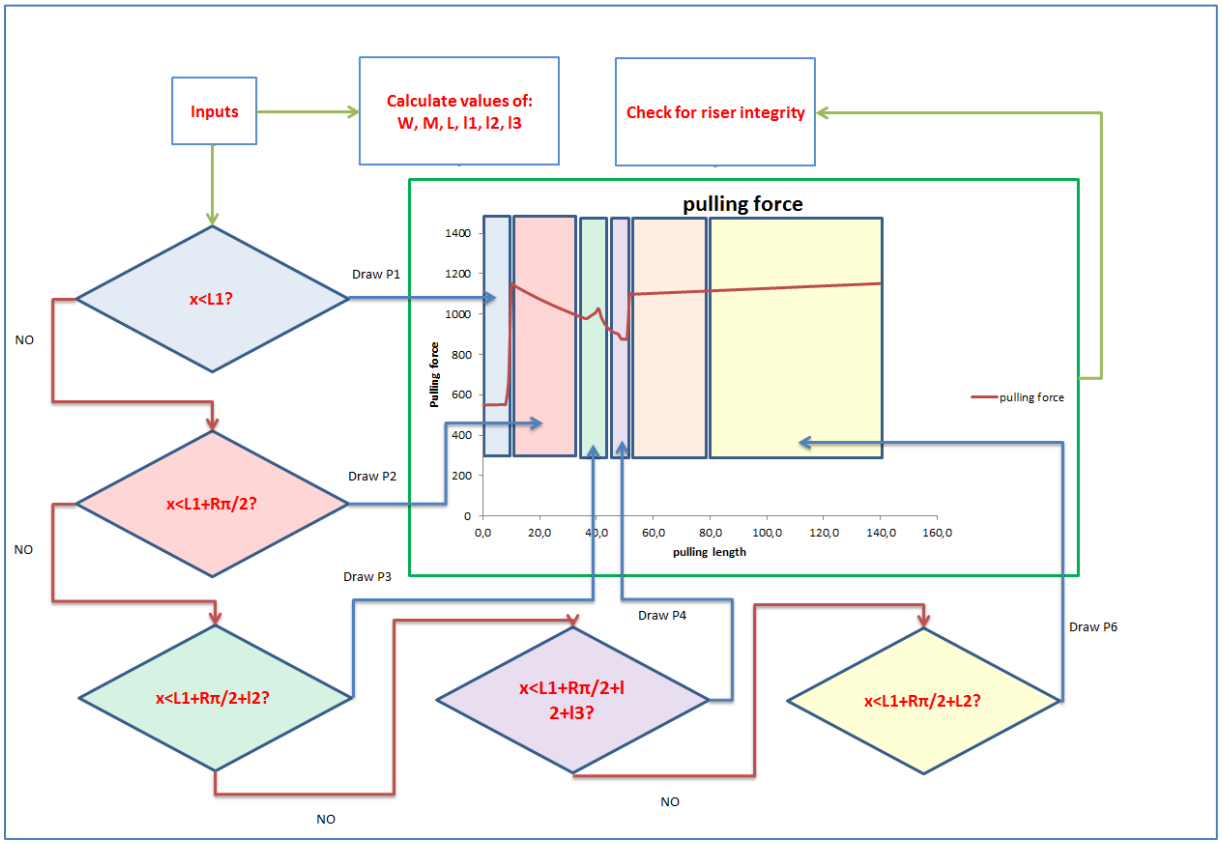

Algorithm of the Excel calculation tool